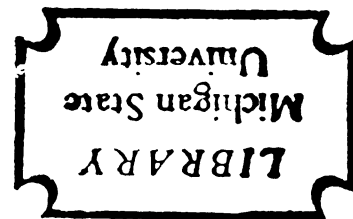


A SPECIFIC HEAT STUDY OF $\text{Cs}_2 \text{MnCl}_4 \cdot 2\text{H}_2\text{O}$
IN A MAGNETIC FIELD

Thesis for the Degree of Ph. D.
MICHIGAN STATE UNIVERSITY
NORMAN DUANE LOVE
1967



This is to certify that the
thesis entitled
A Specific Heat Study of
 $\text{Cs}_2\text{MnCl}_4 \cdot 2\text{H}_2\text{O}$ in a Magnetic Field
presented by
Norman Duane Love

has been accepted towards fulfillment
of the requirements for

Ph.D. degree in Physics

Harold Forest
Major professor

Date May 15, 1967

ABSTRACT

A SPECIFIC HEAT STUDY OF $\text{Cs}_2\text{MnCl}_4 \cdot 2\text{H}_2\text{O}$ IN A MAGNETIC FIELD

by Norman Duane Love

Adiabatic calorimeters for studies at He^4 and He^3 temperatures, and the measuring electronics have been described. Specific heat studies of single crystals of $\text{Cs}_2\text{MnCl}_4 \cdot 2\text{H}_2\text{O}$ have been made in zero and non-zero magnetic fields. The zero field specific heat study: 1) compares well with the calculated specific heat from the magnetic susceptibility, 2) gives the Néel temperature as $1.84^\circ \pm 0.01^\circ\text{K}$, 3) indicates that 25 percent of the entropy is recovered above the Néel temperature due to short range ordering, and 4) gives a sublattice magnetization curve as a function of reduced temperature which agrees with the measured magnetization curve from an nmr study and with the curve computed for a f.c.c. lattice using a three dimensional Ising model.

Specific heat studies for several external magnetic fields in each of three orientation A, B, and C which are approximately the $(0 \bar{1} \bar{1})$, $(1 \bar{1} \bar{1})$, and $(\bar{1} \bar{1} \bar{1})$ directions respectively, have been made. They show that the transition temperature are reduced, in agreement with the calculations

A SPECIFIC HEAT STUDY OF
 $\text{Cs}_2\text{MnCl}_4 \cdot 2\text{H}_2\text{O}$
IN A MAGNETIC FIELD

By

Norman Duane Love

A THESIS

Submitted to
Michigan State University
in partial fulfillment of the requirements
for the degree of

DOCTOR OF PHILOSOPHY

Department of Physics

1967

246120
4-27-61

ACKNOWLEDGMENTS

I would like to express my appreciation to all of those people who have made this study possible, to my thesis advisor Dr. H. Forstat for his time, assistance and many fruitful discussions, to Dr. J. A. Cowen who allowed me to use two of his single crystals of $\text{Cs}_2\text{MnCl}_4 \cdot 2\text{H}_2\text{O}$ and his unpublished susceptibility results, to Dr. R. D. Spence and Mr. John A. Casey for the use of their unpublished nmr results and their assistance in determining the crystal orientation, and to Mr. James N. McElearney whose programming made for accurate and fast data reduction by the computer and whose assistance with the experiments was invaluable. Acknowledgment is also made to the U.S. Air Force Office of Scientific Research for their support of this study.

TABLE OF CONTENTS

	Page
ACKNOWLEDGMENTS	ii
I. INTRODUCTION	1
II. THEORY	3
A. Thermodynamics of Specific Heats	3
B. Magnetism	7
C. Magnetic Susceptibility for Antiferromagnetism	16
D. Transition Temperature	22
E. Spin-flop	25
III. EXPERIMENTAL APPARATUS AND PROCEDURE	28
A. Helium Dewar	28
B. He ⁴ Calorimeter	30
C. He ³ Calorimeter	35
D. Electrical Measurement Apparatus	38
E. Preparation of Sample	42
F. Experimental Procedure	45
1. Pre-cooling	45
2. Adding Exchange Gas	48
3. Liquid-Helium Transfer	48
4. The Calibration of Sample Thermometer	50
5. Specific Heat Measurements	51
6. Voltage-Calibration Data	54
7. Shut-down	55
G. Data Reduction	55
1. Calibration of Thermometer	55
2. Voltage-Calbration	56
3. Specific-Heat Data	61
IV. RESULTS AND DISCUSSIONS	63
A. Description of Crystal	63
B. Zero-Field Results	63

	Page
C. Magnetic-Field Results	69
D. Phase Diagram.	82
E. Conclusion	90
REFERENCES	95
APPENDIX I	97
APPENDIX II	100

LIST OF TABLES

TABLE		Page
1.	Temperature-Calibration-Curve Parameters from an Experiment made January 13, 1967.	56
2.	One-Millivolt-Voltage Calibration-Curve Parameters for an Experiment made January 13, 1967.	59
3.	The Specific Heat of $\text{Cs}_2\text{MnCl}_4 \cdot 2\text{H}_2\text{O}$ for Sample 1, Run 2, September 16, 1966, Zero Field.	100
4.	The Specific Heat of $\text{Cs}_2\text{MnCl}_4 \cdot 2\text{H}_2\text{O}$ for Sample 1, Run 3, September 21, 1966, Zero Field.	102
5.	The Specific Heat of $\text{Cs}_2\text{MnCl}_4 \cdot 2\text{H}_2\text{O}$ for Sample 2, Run 1, October 5, 1966, Zero Field.	104
6.	The Specific Heat of $\text{Cs}_2\text{MnCl}_4 \cdot 2\text{H}_2\text{O}$ for Sample 2, Run 2, October 17, 1966, Zero Field.	106
7.	The Specific Heat of $\text{Cs}_2\text{MnCl}_4 \cdot 2\text{H}_2\text{O}$ for Sample 1, Run 5, December 23, 1966, 8150 Gauss, Orientation A.	107
8.	The Specific Heat of $\text{Cs}_2\text{MnCl}_4 \cdot 2\text{H}_2\text{O}$ for Sample 1, Run 6, January 12, 1967, 8150 Gauss, Orientation A.	108
9.	The Specific Heat of $\text{Cs}_2\text{MnCl}_4 \cdot 2\text{H}_2\text{O}$ for Sample 1, Run 7, January 13, 1967, 5150 Gauss, Orientation A.	110

Table		Page
10.	The Specific Heat of $\text{Cs}_2\text{MnCl}_4 \cdot 2\text{H}_2\text{O}$ for Sample 1, Run 8, January 18, 1967, 5150 Gauss, Orientation A.	111
11.	The Specific Heat of $\text{Cs}_2\text{MnCl}_4 \cdot 2\text{H}_2\text{O}$ for Sample 1, Run 9, January 20, 1967, 3500 Gauss, Orientation A.	112
12.	The Specific Heat of $\text{Cs}_2\text{MnCl}_4 \cdot 2\text{H}_2\text{O}$ for Sample 1, Run 10, January 23, 1967, 3500 Gauss, Orientation A.	114
13.	The Specific Heat of $\text{Cs}_2\text{MnCl}_4 \cdot 2\text{H}_2\text{O}$ for Sample 1, Run 12, February 11, 1967, 8400 Gauss, Orientation B.	116
14.	The Specific Heat of $\text{Cs}_2\text{MnCl}_4 \cdot 2\text{H}_2\text{O}$ for Sample 1, Run 13, February 13, 1967, 8400 Gauss, Orientation B.	118
15.	The Specific Heat of $\text{Cs}_2\text{MnCl}_4 \cdot 2\text{H}_2\text{O}$ for Sample 1, Run 14, February 16, 1967, 6050 Gauss, Orientation B.	120
16.	The Specific Heat of $\text{Cs}_2\text{MnCl}_4 \cdot 2\text{H}_2\text{O}$ for Sample 1, Run 15, February 16, 1967, 6050 Gauss, Orientation B.	122
17.	The Specific Heat of $\text{Cs}_2\text{MnCl}_4 \cdot 2\text{H}_2\text{O}$ for Sample 1, Run 16, March 1, 1967, 8400 Gauss, Orientation C.	124
18.	The Specific Heat of $\text{Cs}_2\text{MnCl}_4 \cdot 2\text{H}_2\text{O}$ for Sample 1, Run 17, March 3, 1967, 8400 Gauss, Orientation C.	126
19.	The Specific Heat of $\text{Cs}_2\text{MnCl}_4 \cdot 2\text{H}_2\text{O}$ for Sample 1, Run 18, March 18, 1967, 6050 Gauss, Orientation C.	127
20.	The Specific Heat of $\text{Cs}_2\text{MnCl}_4 \cdot 2\text{H}_2\text{O}$ for Sample 1, Run 19, March 10, 1967, 9830 Gauss, Orientation C.	128

Table	Page
21. The Specific Heat of $\text{Cs}_2\text{MnCl}_4 \cdot 2\text{H}_2\text{O}$ for Sample 1, Run 20, March 14, 1967, 6050 Gauss, Orientation C.	129
22. The Specific Heat of $\text{Cs}_2\text{MnCl}_4 \cdot 2\text{H}_2\text{O}$ for Sample 1, Run 21, March 22, 1967, 8900 Gauss, Orientation C.	131
23. The Specific Heat of $\text{Cs}_2\text{MnCl}_4 \cdot 2\text{H}_2\text{O}$ for Sample 1, Run 22, April 5, 1967, 9830 Gauss, Orientation C.	132
24. The Specific Heat of $\text{Cs}_2\text{MnCl}_4 \cdot 2\text{H}_2\text{O}$ for Sample 1, Run 23, April 5, 1967, 3500 Gauss, Orientation C.	133
25. The Specific Heat of $\text{Cs}_2\text{MnCl}_4 \cdot 2\text{H}_2\text{O}$ for Sample 1, Run 24, April 5, 1967, 8900 Gauss, Orientation C.	134
26. The Specific Heat of $\text{Cs}_2\text{MnCl}_4 \cdot 2\text{H}_2\text{O}$ for Sample 1, Run 25, April 7, 1967, 3500 Gauss, Orientation C.	135
27. The Temperature Changes from an Adiabatic Magnetization Experiment on Sample 1, Orientation C, April 21, 1967.	136

LIST OF FIGURES

FIGURE		Page
1a.	Magnetization Curve Calculated from the Molecular-Field Theory.	15
1b.	Shape of Specific Heat Curve Calculated from the Molecular-Field Theory	15
2.	The Susceptibility of an Antiferromagnetic Material as a Function of Temperature in Reduced Units	21
3.	A Magnetic Dewar.	29
4.	Scale Drawing of Lower Portion of He ⁴ Calorimeter	31
5.	Front and Side View of Top of He ⁴ Calorimeter	32
6.	Photograph of Unassembled Calorimeter	33
7.	The Needle Valve.	36
8.	Schematic of He ³ Calorimeter.	37
9.	Electrical-Measurement Circuit Diagrams	39
10.	A Photograph of Total System.	46
11.	Schematic Diagram of Top of Dewar	47
12.	Sample Recorder Chart	52
13.	A Cross-Sectional View of Cs ₂ MnCl ₄ ·2H ₂ O Perpendicular to the Elongated Axis with an Arrow Indicating the Direction of Easy Magnetization	64
14.	Specific Heat Curve in Zero Magnetic Field.	65

Figure	Page
15. Sublattice Magnetization Curves	70
16. Specific Heat Curve for Orientation A and 3500 Gauss.	72
17. Specific Heat Curve for Orientation A and 5150 Gauss.	73
18. Specific Heat Curve for Orientation A and 8150 Gauss.	74
19. Specific Heat Curve for Orientation B and 6050 Gauss.	75
20. Specific Heat Curve for Orientation B and 8400 Gauss.	76
21. Specific Heat Curve for Orientation C and 3500 Gauss.	77
22. Specific Heat Curve for Orientation C and 6050 Gauss.	78
23. Specific Heat Curve for Orientation C and 8400 Gauss.	79
24. Specific Heat Curve for Orientation C and 8900 Gauss.	80
25. Specific Heat Curve for Orientation C and 9830 Gauss.	81
26. Entropy Curves for Orientation A.	83
27. Entropy Curves for Orientation B.	84
28. Entropy Curves for Orientation C.	85
29. Entropy, Field, and Temperature Surface for Orientation A.	86
30. Entropy, Field, and Temperature Surface for Orientation B	87
31. Entropy, Field, and Temperature Surface for Orientation C	88

Figure		Page
32.	Phase Diagram for Orientations A, B, and C.	89
33.	Temperature vs. Angle from Easy Direction for an Adiabatic Rotation of a Constant External Magnetic Field of 8000 Gauss . . .	92
34.	Circuit Diagram for a Simple Potentiometer.	98

LIST OF APPENDICES

	Page
APPENDIX I	97
APPENDIX II.	100

I. INTRODUCTION

Some nmr studies by Spence¹ and susceptibility measurements by Cowen² indicated an antiferromagnetic-paramagnetic transition at about 1.8°K in $\text{Cs}_2\text{MnCl}_4 \cdot 2\text{H}_2\text{O}$. Since 1.8°K is easily attained by He^4 calorimetry, a measure of its specific heat in a zero magnetic field would be of interest and would provide a check on the transition temperature, and a comparison with the molecular-field theory for the sublattice magnetization and magnetic susceptibility. After the zero-field study was completed, studies in an external magnetic field were begun. These studies show that the transition temperatures are reduced as the external magnetic field is increased, in agreement with the molecular-field theory. The magnetic phase diagram indicated which of the three crystal orientations is sufficiently close to having its sublattice magnetization direction parallel to the external magnetic-field direction.

This study has three purposes: 1) to construct He^4 and He^3 calorimeters for use in specific heat measurements for the temperature range 0.4°-4.2°K, 2) to report the results of the specific heat study on $\text{Cs}_2\text{MnCl}_4 \cdot 2\text{H}_2\text{O}$ in both zero and non-zero external fields, 3) to search for a possible spin-flop magnetic region by a calorimetric method.

The study is divided into three sections. The first section describes the theories pertinent to the present study. Section two describes the apparatus and the step-by-step procedures for measuring the specific heat. The last section discusses the results, using the theories and equations developed in section one.

It is hoped that the present study may provide sufficient information concerning the magnetic transition in $\text{Cs}_2\text{MnCl}_4 \cdot 2\text{H}_2\text{O}$, that additional problems which have been raised from these experiments may be pursued fruitfully.

II. THEORY

A. Thermodynamics of Specific Heats^{3,4}

When energy, as heat, is absorbed by a substance, a temperature change will be observed except for first-order phase transitions. The function which related this temperature change to the amount of heat absorbed by the substance is called heat capacity or specific heat, if divided by the mass of the material. This can formally be written as

$$d'Q = C_x dT \quad (1)$$

where $d'Q$ is an increment of heat measured in calories, dT is the change in temperature measured in Kelvin degrees, and C_x is the heat capacity measured in calories/degree.

The First Law of Thermodynamics, more commonly known as the conservation of energy, can be written for a reversible process as

$$dU = d'Q - d'W. \quad (2)$$

The function U is the internal energy and dU is an exact differential, the reason for the absence of the apostrophe. $d'Q$ has already been defined and $d'W$ is

$$d'W = PdV - HdM + \text{other forms of work} \quad (3)$$

where P is pressure, V is volume, M is magnetization, and H is the magnetic field. This study deals with solids at

low temperatures, and dV will be essentially zero for all of the measurements.

The Second Law of Thermodynamics defines another function with an exact differential, called entropy, which can be used as a measure of a material's disorder. $d'Q$ may now be written for a reversible process as

$$d'Q = TdS \quad (4)$$

Now the First Law becomes

$$TdS = dU - HdM. \quad (5)$$

Consider S and U functions of T and M only and write

$$dS = \left. \frac{\partial S}{\partial T} \right|_M dT + \left. \frac{\partial S}{\partial M} \right|_T dM \quad (6)$$

and

$$dU = \left. \frac{\partial U}{\partial T} \right|_M dT + \left. \frac{\partial U}{\partial M} \right|_T dM \quad (7)$$

Substituting into equation (5),

$$T \left. \frac{\partial S}{\partial T} \right|_M dT + T \left. \frac{\partial S}{\partial M} \right|_T dM = \left. \frac{\partial U}{\partial T} \right|_M dT + \left[\left. \frac{\partial U}{\partial M} \right|_T - H \right] dM \quad (8)$$

But

$$T \left. \frac{\partial S}{\partial T} \right|_M = C_M. \quad (9)$$

Therefore

$$C_M = \left. \frac{\partial U}{\partial T} \right|_M, \quad (10)$$

and

$$T \left. \frac{\partial S}{\partial M} \right|_T = \left[\left. \frac{\partial U}{\partial M} \right|_T - H \right]. \quad (11)$$

Now consider S and M functions of H and T, and U a function of M and T. Using the results (10) and (11) write,

$$T \left. \frac{\partial S}{\partial T} \right|_H dT + T \left. \frac{\partial S}{\partial H} \right|_T dH = C_M dT + T \left. \frac{\partial S}{\partial M} \right|_T \left[\left. \frac{\partial M}{\partial T} \right|_H dT + \left. \frac{\partial M}{\partial H} \right|_T dH \right] \quad (12)$$

But

$$T \left. \frac{\partial S}{\partial M} \right|_H = C_H \quad (13)$$

then

$$C_H - C_M = T \left. \frac{\partial S}{\partial M} \right|_T \left. \frac{\partial M}{\partial T} \right|_H. \quad (14)$$

Using Maxwell's equation,

$$\left. \frac{\partial H}{\partial T} \right|_M = - \left. \frac{\partial S}{\partial M} \right|_T, \quad (15)$$

write

$$C_H - C_M = -T \left. \frac{\partial H}{\partial T} \right|_M \left. \frac{\partial M}{\partial T} \right|_H. \quad (16)$$

It follows that for low temperatures, $C_H \approx C_M$. From equations (10) and (13), one may write,

$$S(T_1) - S(T_2) = \int_{T_1}^{T_2} C_x/T dt \quad (17)$$

where x is either M or H. Statistical mechanics defines entropy⁵ as the natural logarithm of the volume of phase space or of the total number of states available. If a mole of substance has a quantum number J then there are

$2J + 1$ states and

$$\Delta S = R \ln (2J + 1) \quad (18)$$

where

$$\Delta S = \int_0^{\infty} C_X/T dt. \quad (19)$$

Energy may be absorbed by a solid in a variety of ways,⁶ such as, through an increase in the oscillations of the atoms about their lattice sites (U_L); an increase in the kinetic energy of the free electrons (U_e); by the presence of a magnetic exchange energy (U_H); by the excitation of atoms (U_S) and nuclei (U_n) to higher energy levels. The internal energy can thus be written as a sum of terms,

$$U_T = U_L + U_H + U_n + \dots \quad (20)$$

Therefore the specific heat of the solid may be written as,

$$C_T = \left. \frac{\partial U_L}{\partial T} \right) + \left. \frac{\partial U_N}{\partial T} \right) + \left. \frac{\partial U_H}{\partial T} \right) + \dots \quad (21)$$

where the appropriate variables are kept fixed during the process. Consequently,

$$C_T = C_L + C_H + C_n + \dots \quad (22)$$

can be written and specific heats are additive. C_L and C_n need only be measured or calculated and subtracted from C_T to give C_H .

B. Magnetism

Magnetism has been a curiosity for centuries, as it revealed itself in the form of magnets called lodestones or magnetite. The formal study of magnetism did not begin until the beginning of the 17th century by Gilbert. It was not until the advent of quantum mechanics that a reasonable explanation for the origin of magnetism was forthcoming. It was first thought that magnetic effects could be explained on the basis that different paramagnetic ions coupled together through a magnetic dipole-dipole interaction. For most substances this interaction is too weak to account for high internal fields observed, 100 gauss calculated, compared to 10,000 gauss measured.

Heisenberg⁷ suggested a quantum mechanical exchange interaction (between electrons of different paramagnetic ions) which gave internal fields of the order of those measured.

Two atoms each with one unpaired electron in similar potentials are considered. They are labeled "1" and "2" with coordinates r_1 and r_2 . The Hamiltonian⁸ can be written as,

$$H(1,2) = -(\hbar^2/2M) \nabla_1^2 - (\hbar^2/2M) \nabla_2^2 + V_T(r_1, r_2, r_{12}) \quad (23)$$

where

$$V_T(r_1, r_2, r_{12}) = V_1(r_1) + V_2(r_2) + V(r_{12}) \quad (24)$$

and r_{12} is the radius vector between the electrons. Assume

the electrons to be independent, then $V(r_{12}) = 0$, and

$$H\psi(r_1, r_2) = E_T \psi(r_1, r_2) \quad (25)$$

Equation (23) is then separable into,

$$-(\hbar/2M)\nabla_1^2 \psi_\alpha(r_1) + V_1(r_1) \psi_\alpha(r_1) = E_\alpha \psi_\alpha(r_1) \quad (26)$$

$$-(\hbar/2M)\nabla_2^2 \psi_\beta(r_2) + V_2(r_2) \psi_\beta(r_2) = E_\beta \psi_\beta(r_2) \quad (27)$$

where ψ_α and ψ_β are the normalized wave functions of the separated equations and α and β designate the energy state. Thus there exist two possible solutions

$$\psi(r_1, r_2) = \psi_\alpha(r_1) \psi_\beta(r_2) \quad (28)$$

or

$$\psi(r_1, r_2) = \psi_\alpha(r_2) \psi_\beta(r_1) \quad (29)$$

to equation (25) with the same energy $E_T = E_\alpha + E_\beta$. To keep the identical electrons indistinguishable when considering probability densities, two linear combinations, a symmetric ψ_S and an anti-symmetric ψ_A , of the above solutions must be used,

$$\psi_S(r_1, r_2) = \frac{1}{\sqrt{2}} \left[\psi_\alpha(r_1) \psi_\beta(r_2) + \psi_\alpha(r_2) \psi_\beta(r_1) \right] \quad (30)$$

$$\psi_A(r_1, r_2) = \frac{1}{\sqrt{2}} \left[\psi_\alpha(r_1) \psi_\beta(r_2) - \psi_\alpha(r_2) \psi_\beta(r_1) \right] \quad (31)$$

Spins have so far not been considered. All electrons have spin angular momentum $\pm \hbar/2$. Thus a magnetic field

applied along the z-direction would orient the magnetic moment μ_z , with magnitude of one Bohr magneton, either parallel or antiparallel to this field. The Pauli principle limits the total wave function for the electrons to be only anti-symmetric. Thus the two total wave functions including the spin wave functions (χ) may be written as,

$$\psi_I = B_I \psi_S \left[\chi_\alpha(1) \chi_\beta(2) - \chi_\alpha(2) \chi_\beta(1) \right] \quad (32)$$

$$\psi_{II} = B_{II} \psi_A \chi_\alpha(1) \left\{ \begin{array}{l} \chi_\alpha(1) \chi_\beta(2) \\ \chi_\beta(2) + \chi_\alpha(2) \chi_\beta(1) \\ \chi_\alpha(2) \chi_\beta(1) \end{array} \right\} \quad (33)$$

where ψ_I represents the singlet state and ψ_{II} represents the triplet state, and where B_I and B_{II} are the normalization factors.

Adding the interaction between the electrons $V(r_{12})$ and applying first order perturbation theory the energies are,

$$E_I = B_I^2 (A_{12} + J_{12}) \quad (34)$$

and

$$E_{II} = B_{II}^2 (A_{12} - J_{12}) \quad (35)$$

where

$$A_{12} = \int \psi_\alpha^*(r_1) \psi_\beta^*(r_2) V(r_{12}) \psi_\alpha(r_1) \psi_\beta(r_2) d\tau_1 d\tau_2 \quad (36)$$

and

$$J_{12} = \int \psi_{\alpha}^*(r_1) \psi_{\beta}^*(r_2) V(r_{12}) \psi_{\alpha}(r_2) \psi_{\beta}(r_1) d\tau_1 d\tau_2 \quad (37)$$

A_{12} is the average value of $V(r_{12})$, and J_{12} is called the exchange intergal.

If J_{12} is positive the ground state is E_{II} and the spins are parallel; but if J_{12} is negative, E_I is the ground state and the spins are antiparallel. If this process is applied to an assembly of electrons in a solid, such as the 3d electrons in a transition element, and J_{12} is positive, the internal magnetic moments add and may be detected externally as a magnetic field. J_{12} being positive results in a mechanism for ferromagnetism. If J_{12} is negative, the spins are coupled antiparallel, and there is no external field possible; this is called antiferromagnetism. Néel⁹ and Van Vleck,^{10,11,12} using two interpenetrating sublattices and the molecular field theory, calculated some properties that characterized an antiferromagnet. It was not until the development of neutron diffraction techniques that antiferromagnetism was directly verified, completing the exchange interaction picture.

In the above discussion on exchange, the interaction potential is assumed spin independent. But the spins are coupled with a scalar potential proportional to $\vec{s}_1 \cdot \vec{s}_2$. Keeping only the spin-dependent part, the exchange energy may be written as,

$$E_{\text{ex}} = -2J_{12} \vec{s}_1 \cdot \vec{s}_2. \quad (38)$$

Considering two atoms which have more than one unpaired electron the exchange energy becomes,

$$E_{\text{ex}} = -2J_{12} \vec{S}_1 \cdot \vec{S}_2 \quad (39)$$

where \vec{S} is the total spin of the atom. All electrons are assumed to have the same exchange integral. If the exchange integral is assumed isotropic (J_e) and is negligible except for nearest neighbors, then for all of the atoms in a crystal the exchange energy is

$$E_{\text{ex}} = -2J_e \sum'_{i,j} \vec{S}_i \cdot \vec{S}_j \quad (40)$$

The summation is taken over all of the atoms in the crystal. The prime means $i = j$ is not included.

Solving this Hamiltonian should give the properties of magnetism. This has not been possible without making further assumptions. The Bethe-Peierls-Weiss^{13,14,15} method assumes a model where a central atom and its interaction with its nearest neighbors is calculated from (40) but the nearest neighbors are assumed to interact with an internal field due to their neighbors.

Instead, if the assumption is made that the interaction $2J_e(S_{xi}S_{xj} + S_{yi}S_{yj})$ may be neglected, where S_x , S_y , and S_z are the components of S , the exchange energy is then written as,

$$E_{\text{ex}} = -2J_e \sum'_{i,j} S_{zi} \cdot S_{zj} \quad (41)$$

The above assumption amounts to replacing the instantaneous

spin values with their time averages and is called the Ising¹⁶ model. There is an extensive literature on the calculations made with the Ising model,^{17,18} but these will not be discussed here.

Following Van Vleck,¹⁰ the quantum mechanical justification will be made for the Weiss¹⁹ molecular-field approximation. Since the interactions are only for the z nearest neighbors,

$$E_{\text{ex}} = -2J_e \sum_i S_{zi} \cdot \sum_{n=1}^z \bar{S}_{zn} \quad (42)$$

$$E_{\text{ex}} = -g\beta \sum_i S_{zi} \cdot (2J_e/g\beta) \sum_{n=1}^z \bar{S}_{zn} \quad (43)$$

where g is the gyromagnetic ratio, β is the Bohr magneton, and \bar{S}_{zn} is the average of the neighboring spin. An internal field H_i may be defined,

$$H_i = (2J_e/g\beta) \sum_{n=1}^z \bar{S}_{zn} \quad (44)$$

Then,

$$E_{\text{ex}} = -g\beta \sum_i S_{zi} \cdot H_i \quad (45)$$

The magnetization of a specimen with N atoms is

$$M = Ng\beta\bar{S} \quad (46)$$

Thus

$$H_i = (2J_e z / Ng^2 \beta^2) M = \lambda M \quad (47)$$

where λ is Weiss' molecular-field constant.

The problem of magnetism has now been reduced to solving for the case of N independent atoms with a permanent moment ($g\beta S$) in an applied magnetic field H . According to statistical mechanics the magnetization is,

$$M = N \frac{\sum_{-S}^S g\beta S e^{-g\beta SH/kT}}{\sum_{-S}^S e^{-g\beta SH/kT}} \quad (48)$$

where k is Boltzmann's constant, and S is the spin. Let $x = g\beta H/kT$ and using the formula for the sum of the geometric progression, the reduced equation becomes,

$$M = Ng\beta S B_S(y) \quad (49)$$

where

$$B_S(y) = \left[\frac{2S+1}{2S} \text{Coth}\left(\frac{2S+1}{2S}y\right) - \frac{1}{2S} \text{Coth}\left(\frac{1}{2S}y\right) \right] \quad (50)$$

and is called the Brillouin function, and

$$y = (g\beta S/kT)H \quad (51)$$

Substituting H_i for H in (49), (50), and (51) gives the solution for the magnetization of a ferromagnet.

The sublattice magnetization for an antiferromagnet is found in a similar matter. Divide the lattice into two interpenetrating sublattices such that the next nearest neighbors of an atom in sublattice, a , all lie in sublattice, b , and vice versa. The molecular field acting on an atom at site, a , is

$$H_{ia} = \gamma M_b \quad (52)$$

and the molecular field acting on an atom at site, b, is

$$H_{ib} = \gamma M_a \quad (53)$$

where γ corresponds to the Weiss molecular-field constant and is assumed to be the same for both sublattices; but a distinction is made with λ for the ferromagnetic case, since now only one-half of the atoms contribute to each of the molecular fields.

If $|M_a| = |M_b| = |M_o|$ and $M_a = -M_b$ then,

$$M_o = M_s B_s(y) \quad (54)$$

and

$$y = (g\beta S/kT)\gamma M_o \quad (55)$$

where $M_s = \frac{1}{2}Ng\beta S$. The $\frac{1}{2}$ appears because each sublattice contains only half the atoms. The solution for M_o is found by solving equations (54) and (55) graphically. The curve in Figure 1a shows the reduced magnetization M_o/M_s as a function of the reduced temperature T/T_n for $S = 5/2$ and T_n is the Néel temperature about which more will be said later.

Since,

$$E_{ex} = -g\beta \sum_i S_{zi} \cdot \gamma M_o \quad (56)$$

then

$$E_{ex} = -2\gamma M_o^2 \quad (57)$$

where $M_o = \frac{1}{2}Ng\beta \bar{S}$ and \bar{S} is the average spin.

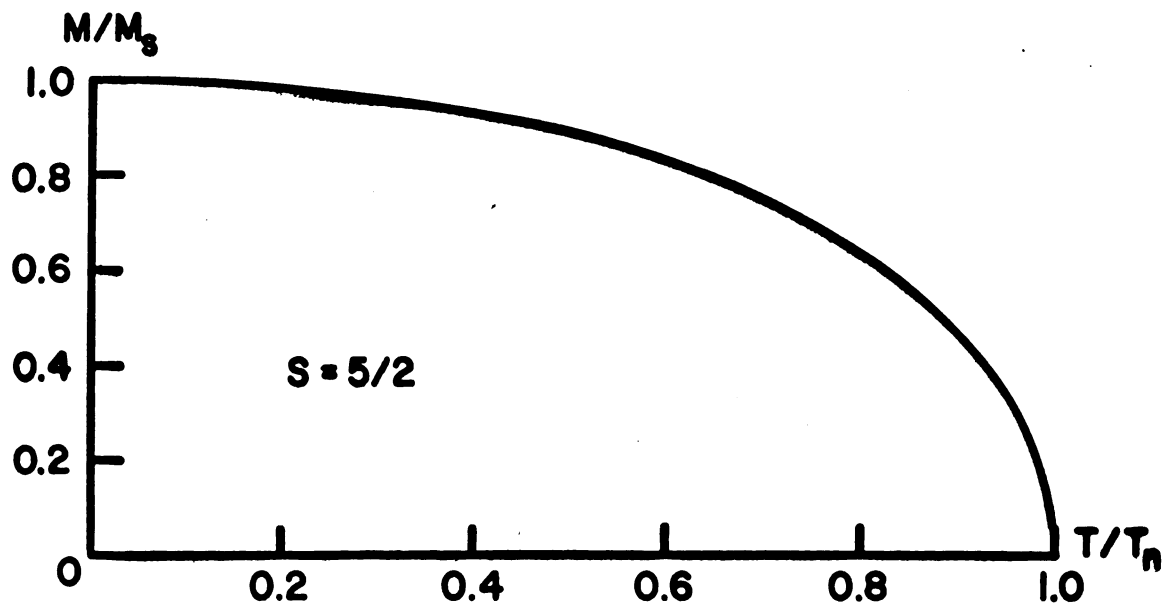


Fig. 1a. Magnetization Curve Calculated from the Molecular-Field Theory.

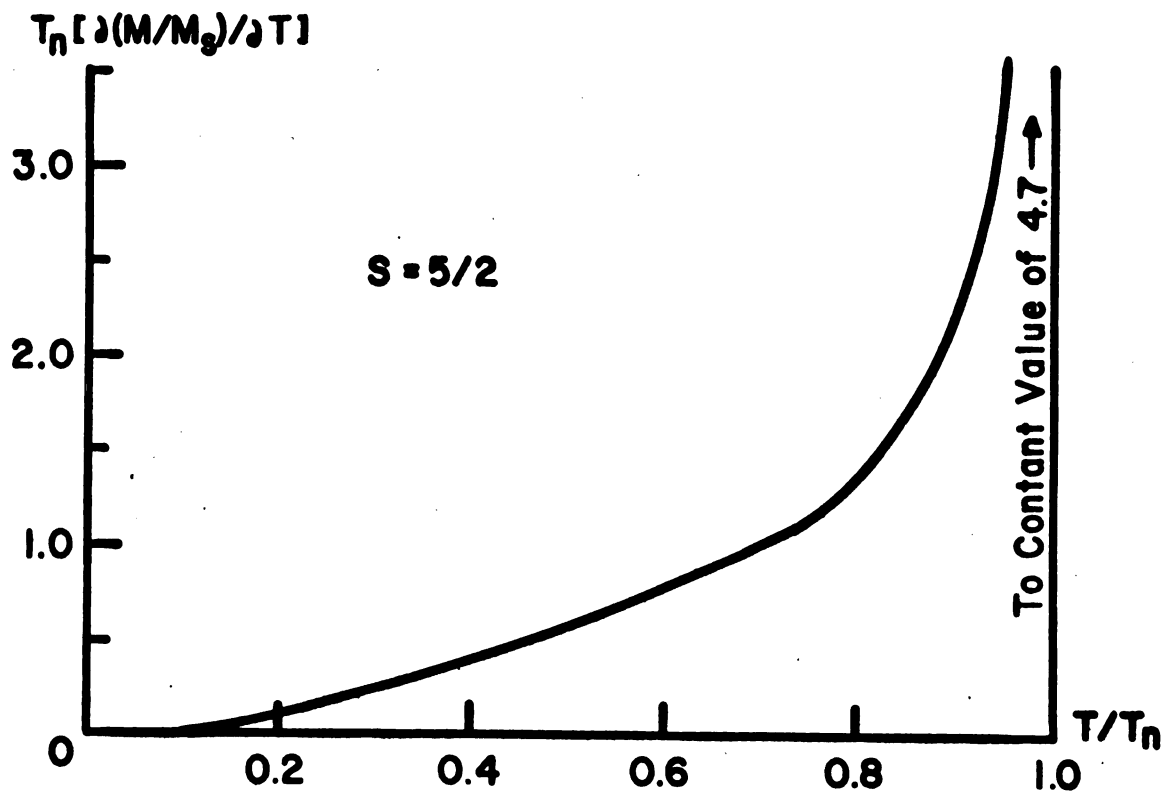


Fig. 1b. Shape of Specific Heat Curve Calculated from the Molecular-Field Theory.

Now,

$$C_H = \left. \frac{\partial E_{ex}}{\partial T} \right)_H \sim M_0 \frac{\partial M_0}{\partial T} \quad (58)$$

where C_H is the magnetic specific heat. Since M_0 was determined graphically, equation (58) will have to be solved numerically. Figure 1b shows the curve which is proportional to the specific heat calculated from equation (58) using points on Figure 1a.

C. Magnetic Susceptibility for Antiferromagnetism

The susceptibility curve is separated into parts by the Néel temperature, i.e. the region above the Néel temperature which is the normal paramagnetic state, and the region below the Néel temperature which is the antiferromagnetic state. All the calculations are based on the molecular-field theory and follow the method outlined in the text by Morrish.²⁰

For temperature well above the Néel temperature there are no exchange forces and thus no molecular-field. If a small external field is applied at high enough temperatures, only the first term in the expansion of the Brillouin function need be considered for the calculation of the susceptibility. The expansion of the Brillouin function is,

$$B_S(y) = \frac{1}{3} \left(\frac{S+1}{S} \right) y + \frac{1}{6} B_S'''(0) y^3 + \dots \quad (59)$$

where

$$B_S'''(0) = -6(S+1)[(S+1)^2 + S^2]/90S^3 \quad (60)$$

Now,

$$y = (g\beta S/kT)H_{\text{ex}} \quad (61)$$

where H_{ex} is the external field instead of the internal molecular-field. M may be written using the first term of (59),

$$M = Ng\beta S \left[\frac{1}{3} \frac{S+1}{S} \left(\frac{g\beta S}{kT} \right) H_{\text{ex}} \right] \quad (62)$$

Then

$$\chi = M/H_{\text{ex}} = \frac{Ng^2\beta^2 S(S+1)}{3k} \left(\frac{1}{T} \right) = \frac{C}{T} \quad (63)$$

where C is the Curie constant. Equation (63) is called the Curie Law. For temperatures near the Néel temperature M_a and M_b must be considered since there is usually some short range ordering.

Now,

$$H_{\text{Ta}} = H_{\text{ex}} - \gamma M_a \quad (64)$$

and

$$H_{\text{Tb}} = H_{\text{ex}} - \gamma M_b \quad (65)$$

and notice that the magnetization vectors are both in the direction of the applied field because of the absence of the long range exchange forces. Again using the first term of the expansion of the Brillouin function and the total magnetization M , as the sum of the two sublattices magnetizations, write,

$$M = \frac{Ng\beta S}{2} \left(\frac{S+1}{3S} \right) \frac{g\beta S}{kT} \left[2 H_{\text{ex}} - \gamma (M_a + M_b) \right] \quad (66)$$

$$M = \frac{1}{2} C/T (2 H_{\text{ex}} - \gamma M) \quad (67)$$

$$M \left(1 + \frac{C\gamma}{2T} \right) = \left(\frac{C H_{\text{ex}}}{T} \right) \quad (68)$$

$$\chi = \frac{C}{T + \theta} \quad (69)$$

where

$$\theta = \frac{1}{2} C\gamma \quad (70)$$

Equation (69) is the Curie-Weiss Law and θ will turn out to be the Néel temperature.

Below the Néel temperature two cases must be considered, the case with external field parallel to the sublattice magnetization and the case with the external field perpendicular to the sublattice magnetization. Consider the parallel case first. Now the internal field will include the external and molecular fields; and,

$$y_a = (g\beta S/kT)(H + \gamma M_b) \quad (71)$$

and

$$y_b = (g\beta S/kT)(-H + \gamma M_a) \quad (72)$$

At $H = 0$, $M_a = -M_b = M_0$, and $y_a = -y_b = y_0$. Now expand the Brillouin function about y_0 and keep only first order terms,

$$B_S(y_a) = B_S(y_0) + B'_S(y_0) \left[H + \gamma(M_b - M_0) \right] \frac{g\beta S}{kT} \quad (73)$$

and

$$\left. \begin{aligned} B_S(y_b) &= B_S(y_0) - B'_S(y_0) \left[H + \gamma(M_0 - M_a) \right] \frac{g\beta S}{kT} \\ B_S(y_a) &= B_S(y_0) - B'_S(y_0) \left[-H - \gamma(M_b - M_0) \right] \frac{g\beta S}{kT} \end{aligned} \right\} \quad (74)$$

where $B'_S(y_0)$ is the derivative of the Brillouin function with respect to its argument. Now M_a and M_b are computed from equation (54) and M the total magnetization is

$$M = M_a - M_b \quad (75)$$

Thus,

$$M = M_S \left[B'_S(y_0) \left\{ \left[H + \gamma(M_b - M_0) \right] + \left[H + \gamma(M_0 - M_a) \right] \right\} \frac{g\beta S}{kT} \right] \quad (76)$$

$$M = \frac{1}{2} \frac{Ng^2\beta^2 S^2}{kT} B'_S(y_0) [2H - \gamma M] \quad (77)$$

$$\chi_{//} = \frac{Ng^2\beta^2 S^2 B'_S(y_0)}{kT + \frac{1}{2}Ng^2\beta^2 S^2 B'_S(y_0)\gamma} \quad (78)$$

Now $B'_S(y_0)$ goes to zero exponentially as T goes to 0; and since

$$\chi_{//} = \frac{Ng^2\beta^2 S^2}{\frac{1}{2}Ng^2\beta^2 S^2\gamma + \frac{kT}{B'_S(y_0)}}, \quad (79)$$

then $\chi_{//}$ goes to zero as T goes to zero.

The applied field when perpendicular to the sublattice magnetization will cause each of the magnetization vectors to rotate through a small angle ϕ . At equilibrium the torque on the sublattice magnetization must be zero, therefore,

$$|\vec{M}_a \times (\vec{H}_{ex} + \gamma\vec{M}_b)| = 0 \quad (80)$$

or

$$M_a H \cos \phi - \gamma M_a M_b \sin 2\phi = 0 \quad (81)$$

$$2M_b \sin \phi = H/\gamma \quad (82)$$

and since $M_a = M_b$ then

$$M = (M_a + M_b) \sin \phi = 2M_b \sin \phi \quad (83)$$

Thus,

$$\chi_{\perp} = 1/\gamma \quad (84)$$

Figure 2 shows the qualitative plot of the susceptibility for an antiferromagnetic material.

Fisher²¹ has also worked out a relationship between the parallel susceptibility and the specific heat. He calculates,

$$C_M(T) \approx 2R f \left(1 - \frac{2}{3}\alpha \right) \frac{\partial}{\partial \theta} \left[(TX_{//}) / (TX_{//})_{\infty} \right] \quad (85)$$

where f is a slowly varying function of T and is equated to 1, α is a measure of the anisotropy of the interaction (equal to zero for pure isotropic interactions), θ is T/T_n , and $(TX_{//})_{\infty}$ is the value of $(TX_{//})$ extrapolated to high temperatures. Assuming an isotropic interaction,

$$C_M = 2R \frac{T_n}{(TX_{//})_{\infty}} \frac{\partial (TX_{//})}{\partial T} \quad (86)$$

is the form of Fisher's equation which may be used to compare the zero field specific heat with the parallel susceptibility.

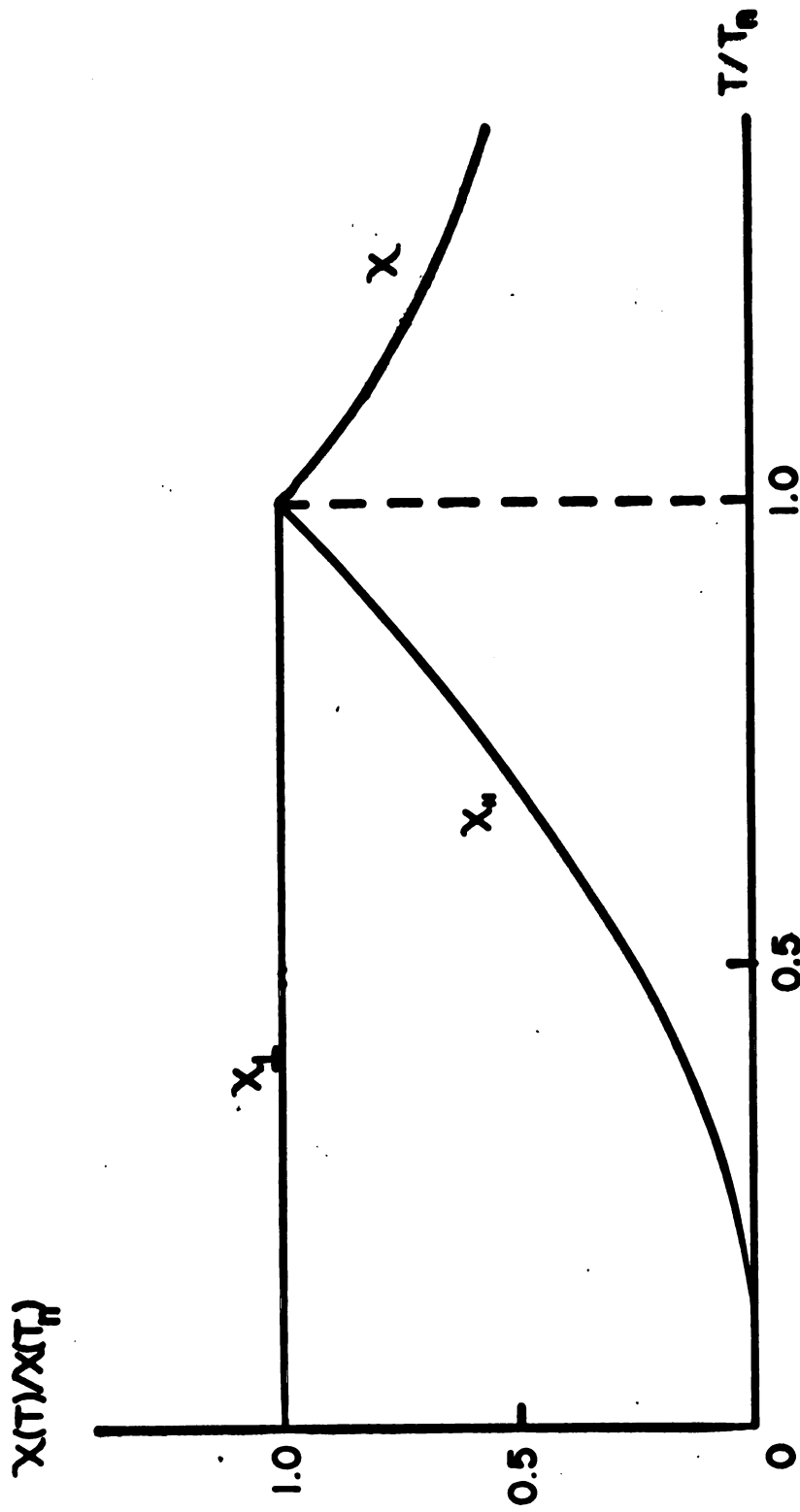


Fig. 2. The Susceptibility of an Antiferromagnetic Material as a Function of Temperature in Reduced Units.

D. Transition Temperatures

As Figure 1a shows, the sublattice magnetization drops to zero at some transition temperature T_n , commonly called the Néel temperature to distinguish it from the Curie temperature for a ferromagnet. This value of T_n can be calculated by expanding $B_s(y)$ in powers of y , equation (59); then allowing M_0 to approach zero, which means that T goes to T_n and y becomes small, so that in the first approximation one may write,

$$M_0/M_s = \frac{1}{3} \left(\frac{S+1}{S} \right) y \quad (87)$$

Now combining equations (55), (87), and the definition for M_s , one obtains,

$$T_n = \frac{1}{2} \frac{Ng^2\beta^2 S(S+1)}{3k} \gamma = \frac{1}{2} C\gamma \quad (88)$$

This result neglects any external field. Comparing the calculated specific heat curve in Figure 1b with the zero field measured curve in Figure 14 indicates that the molecular-field theory can only give qualitative results.

The following discussion will consider the case for $H \neq 0$, and its effect on the transition temperature. The method of Kubo¹² will be used, although several calculations, using other methods, have been performed. These have been, (1) calculations of the phase diagram by Gorter,²² who used the molecular-field theory to find the Gibb's energy, (2) the calculations by Garrett²³ who obtained a graphical solution for the field parallel to the magnetization using

using the molecular-field theory, (3) the method used by Temperley²⁴ to calculate a phase diagram for pure dipole interactions, and (4) the technique of Callen²⁵ to calculate the phase diagram using spin waves with a Green's function method.

The transition temperature for the case of the applied field, parallel to the magnetization direction will be calculated first. To do this, one starts with,

$$M_a = M_s B_s(y_a), \quad (89)$$

$$M_b = M_s B_s(y_b), \quad (90)$$

$$y_a = (g\beta S/kT)(H - \gamma M_b), \quad (91)$$

and
$$y_b = (g\beta S/kT)(H + \gamma M_a) \quad (92)$$

where the field is the total field and M_a is parallel and M_b is antiparallel to the applied field H . As the temperature is raised M_b first decreases in magnitude, becoming zero, then it becomes parallel to H and finally coincides with M_a . The temperature at which this occurs will be denoted by $T_n(H)$. Now writing from (92),

$$\left(\frac{\partial M_a}{\partial y_b}\right)_H = (kT/g\beta S)\gamma \quad (93)$$

and from (89),

$$\left(\frac{\partial M_a}{\partial y_a}\right)_H = M_s \frac{\partial}{\partial y_a} [B_s(y_a)] \quad (94)$$

The slopes in (93) and (94) become equal as T approaches $T_n(H)$ in (93) and as $M_b \rightarrow M_a$ which become zero as T goes to $T_n(0)$ in (94). Now expanding the Brillouin function, neglecting all terms of γM_a and powers of H/T greater than 3, the combination of (93) and (94) may be written as,

$$\frac{k T_n(H)}{\gamma g \beta S} = M_s \left[\frac{1}{3} \left(\frac{S+1}{S} \right) + \frac{3}{6} B_s''''(0) \frac{g^2 \beta^2 S^2}{k^2} \left(\frac{H^2}{T_n^2(0)} \right) \right] \quad (95)$$

Now,

$$T_n(H) = \frac{1}{2} \frac{N g^2 \beta^2 S^2 \gamma}{k} \left[\frac{1}{3} \left(\frac{S+1}{S} \right) + \frac{1}{2} B_s''''(0) \frac{g^2 \beta^2 S^2}{k^2} \left(\frac{H}{T_n(0)} \right)^2 \right] \quad (96)$$

Applying the definition of C, equation (63), (96) reduces to,

$$T_n(H) = \frac{1}{2} C \gamma + \frac{1}{4} B_s''''(0) \frac{N g^4 \beta^4 S^4}{k^3} \left(\frac{H}{T_n(0)} \right)^2 \quad (97)$$

Multiplying and dividing the last term on the right by C^3 one gets,

$$T_n(H) = \frac{1}{2} C \gamma + \frac{1}{4} B_s''''(0) \frac{3^3 C^3 S \gamma}{(S+1)^3 N^2 g^2 \beta^2} \left(\frac{H}{T_n(0)} \right)^2 \quad (98)$$

$$= \frac{1}{2} C \gamma + \frac{1}{4} B_s''''(0) \left(\frac{3S}{S+1} \right)^3 \frac{\gamma C^3}{N^2 g^2 \beta^2 S^2} \left(\frac{H}{T_n(0)} \right)^2 \quad (99)$$

$$= \frac{1}{2} C \gamma + \frac{1}{4} B_s''''(0) \left(\frac{3S}{S+1} \right)^3 \frac{\left(\frac{\gamma C}{2} \right)^3 2^3}{4 M_s^2 \gamma^2} \left(\frac{H}{T_n(0)} \right)^2 \quad (100)$$

Applying the definition of $T_n(0)$ and χ_{\perp} the final result is

$$\frac{T_n(H) - T_n(0)}{T_n(0)} = \frac{1}{2} B_s''''(0) \left(\frac{3S}{S+1} \right)^3 \frac{\chi_{\perp}^2 H^2}{M_s^2} \quad (101)$$

Kubo goes on to do a calculation for the case of the field perpendicular to the direction of magnetization. He gets results similar to those for the parallel case (101),

$$\frac{T_n(H) - T_n(0)}{T_n(0)} = -kH^2$$

where k is a function of S , g , β , etc. and is smaller than the constant terms on the right side of equation (101).

Note that both (101) and (102) predict that $T_n(H) < T_n(0)$ since $B_s''''(0)$ is negative [see equation (60)].

E. Spin-Flop

If a large enough external field is applied parallel to the direction of the sublattice magnetization at sufficiently low temperatures, a phenomenon called spin-flop^{12,22,25,26} may occur.

Consider the crystalline anisotropy energy for a uniaxial antiferromagnetic crystal.

$$F_K = \frac{1}{2} K (\sin^2 \theta_a + \sin^2 \theta_b) \quad (103)$$

where θ_a and θ_b are the angles between the sublattice magnetization M_a and M_b and the easy direction, the direction in which the magnetization lies with no external forces. K is the anisotropy coefficient and is assumed the same for

both lattices. Now making the further assumptions that $\theta_a = \theta_b = \theta$ and $M_a = M_b = M_o$, equation (103) may be written as,

$$F_K = K \sin^2 \theta \quad (104)$$

Let H_K be a magnetic field associated with the anisotropy energy, and let it be the same for both M_a and M_b . Then,

$$F_K = -2H_K M_o \cos \theta \quad (105)$$

Now for an arbitrary variation.

$$\delta F_K = 2H_K M_o \sin \theta \delta \theta \quad (106)$$

$$\delta F_K = 2K \sin \theta \cos \theta \delta \theta \quad (107)$$

Therefore,

$$H_K = (K \cos \theta) / M_o \quad (108)$$

Now apply an external field parallel to the easy direction. The change in energy per unit volume is,

$$\Delta E = - \int H dM \quad (109)$$

but $dM = \chi dH$ (110)

and $\Delta E_{//} = -\chi_{//} H^2 / 2$ (111)

Suppose the magnetization is perpendicular to this direction then,

$$\Delta E_{\perp} = -H_K M_o \cos (\pi/2) + H_K M_o \cos (0) - \chi_{\perp} H^2 / 2 \quad (112)$$

$$\Delta E_{\perp} = K - \chi_{\perp} H^2/2 \quad (113)$$

Now let H_f be some external-field value such that $\Delta E_{\perp} = \Delta E_{//}$ then,

$$-\chi_{//} H_f^2/2 = K - \chi_{\perp} H_f^2/2 \quad (114)$$

and

$$H_f = \left[\frac{2K}{\chi_{\perp} - \chi_{//}} \right]^{1/2} \quad (115)$$

For antiferromagnetic materials, $\chi_{\perp} > \chi_{//}$ when $T < T_n$, and there may exist a magnetic field H_f such that the magnetization will flop from the easy direction to a direction normal to the easy direction.

This phenomenon was first observed²⁷ in $\text{CuCl}_2 \cdot 2\text{H}_2\text{O}$ with $T_n = 4.3^\circ\text{K}$. Maximum fields were applied in the present study to see if such an effect could be observed.

III. EXPERIMENTAL APPARATUS AND PROCEDURE

A. Helium Dewar

Before any low-temperature work can be performed, a container which will hold the cryogenic fluid for a reasonable period of time is necessary. Figure 3 shows one such container. It is made from pyrex glass and essentially consists of two dewars with separate silvered vacuum jackets for insulation. A slit in the silver allows the interior to be seen. The bottom has a smaller diameter so that narrower pole gaps may be used in conjunction with an electromagnet thus providing higher, more homogeneous fields for magnetic measurements.

The outer dewar holds about three liters of inexpensive (relatively speaking) liquid nitrogen. The nitrogen acts as a pre-coolant and a radiation shield for the inner dewar. The liquid nitrogen needs replenishing at the rate of approximately one liter per hour. This is done automatically. Occasionally, about 1000 microns of dry nitrogen gas is admitted into the vacuum jacket of the inner dewar by means of the stopcock to facilitate pre-cooling. This gas will condense, producing a good vacuum insulation when the liquid helium is transferred into the inner dewar. The vacuum jacket of the inner dewar is evacuated periodically since

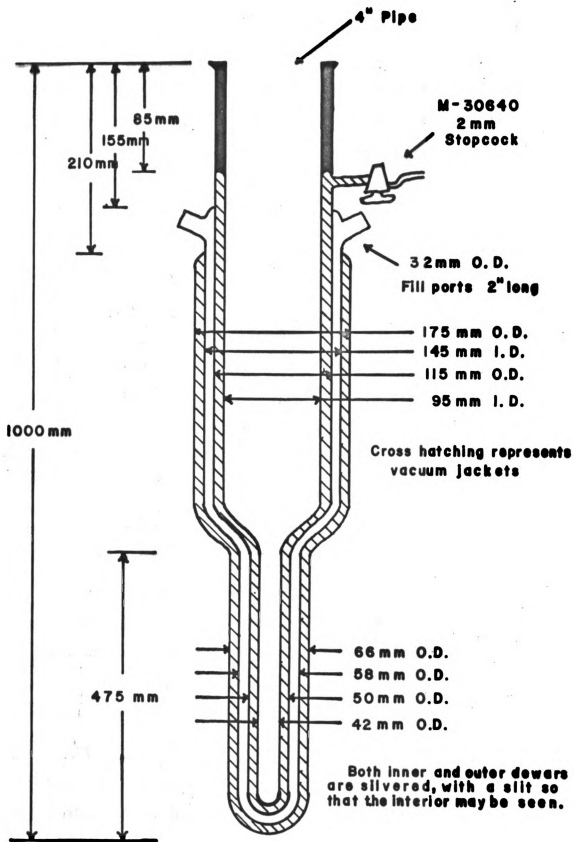


Fig. 3. A Magnetic Dewar.

pyrex is porous to helium at room temperature. The inner dewar is designed to be connected to a vacuum system which allows the vapor pressure of the liquid helium to be lowered, thus making it possible to reduce and control the temperature. For the calorimeter described below, a six-liter transfer will maintain good experimental conditions for about six hours.

B. He⁴ Calorimeter

Figures 4 and 5 are drawn to scale and show the calorimeter used for all of the experiments in the liquid He⁴ temperature region. Figure 6 is a photograph of the assembled calorimeter. This calorimeter is mounted in the previously described dewar which contains the liquid helium. The top and flanges of the calorimeter are machined from brass. The outer can, the inner liquid helium container, and the elbows are made from copper. The calorimeter can is made from brass. All copper-to-copper tubing joints are hard silver soldered where strength is necessary. The remaining joints are soft soldered. All evacuation lines or tubes are low-thermal-conducting alloys such as german silver or stainless steel. Not shown in the diagrams is a bellows which was installed in the outer can evacuation line. This was necessary after several soft-solder joints failed from thermal stresses due to cooling. The calorimeter can and the bottom of the outer can, which must be removable, are soldered in place with the low-melting Cerrolow 117 alloy solder using a liquid non-acid flux (Superior #30).

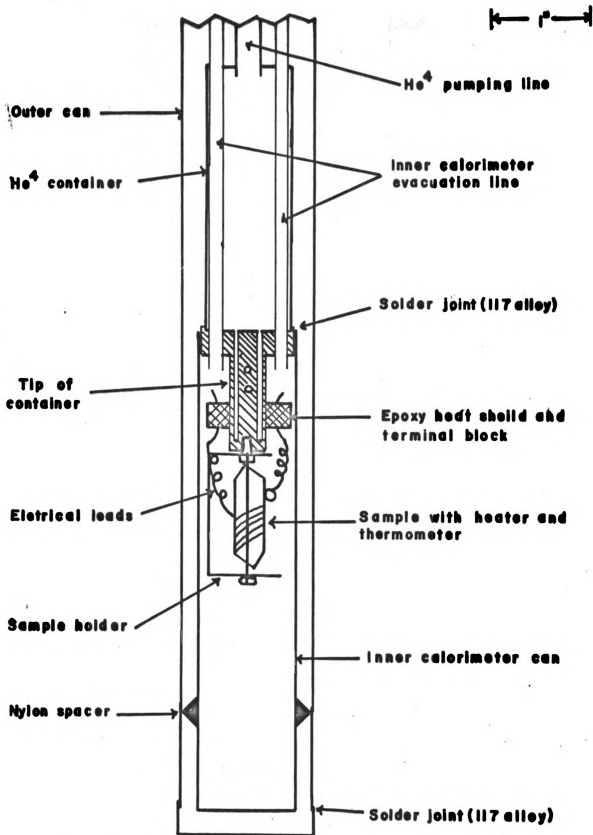


Fig. 4. Scale Drawing of Lower Portion of He⁴

Calorimeter.

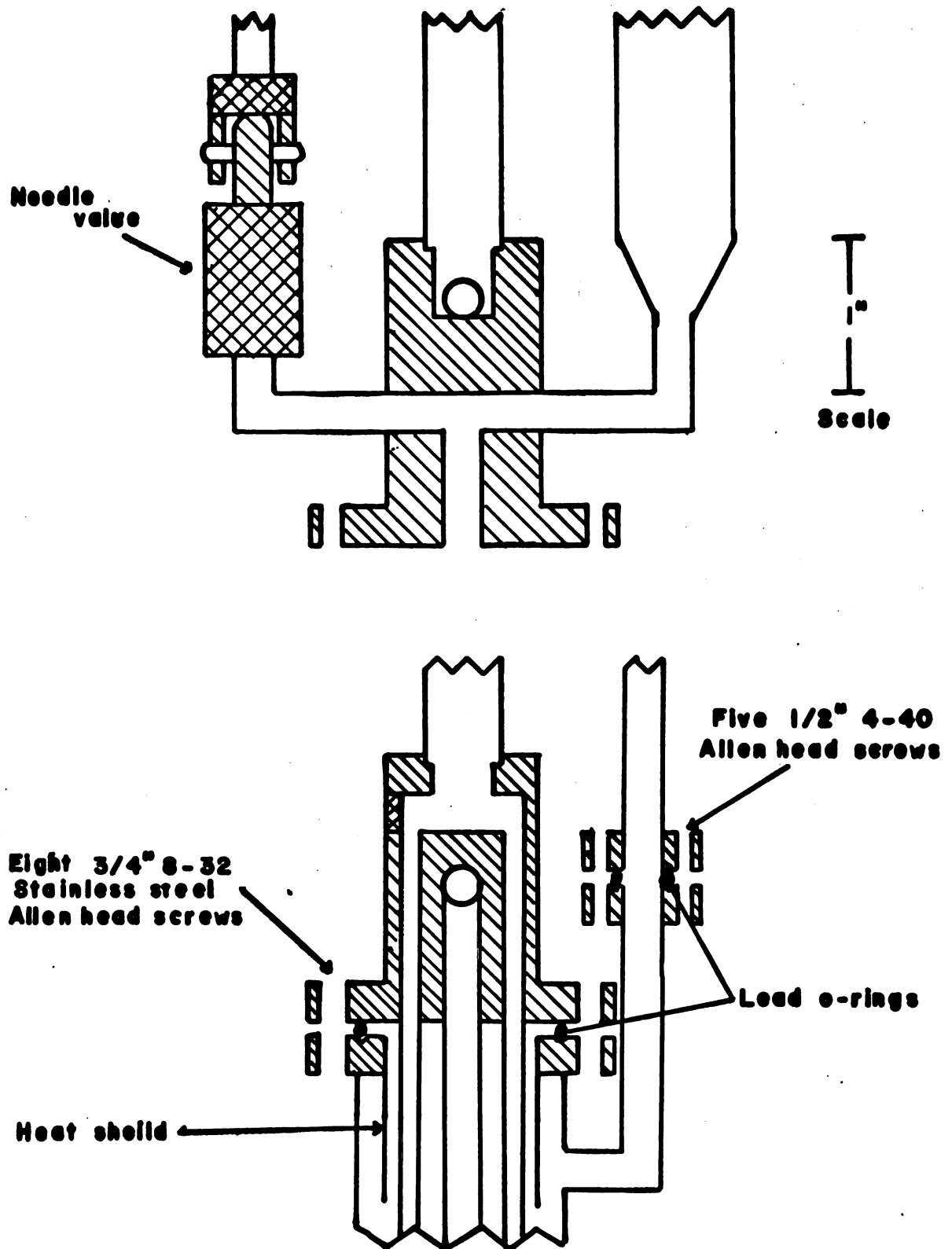


Fig. 5. Front and Side View of Top of He⁴ Calorimeter.

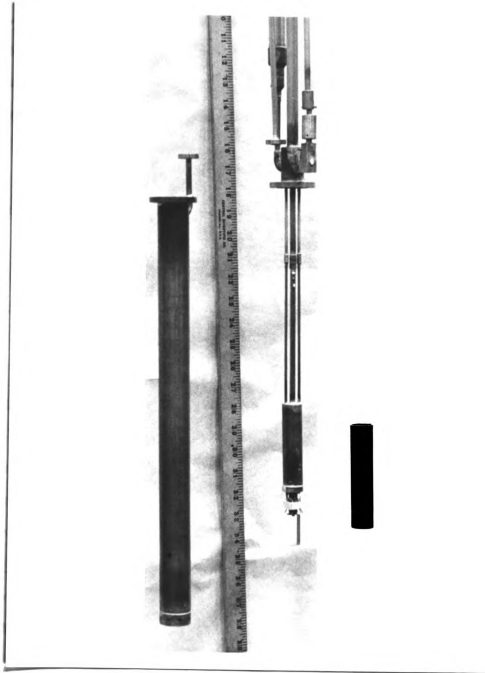


Fig. 6.--Photograph of Unassembled Calorimeter.

All evacuation lines in contact with room temperature must have some means of trapping the radiation flowing down them. This was achieved by having the lines turn right angle corners in the outer liquid helium bath where the radiation is absorbed. Any reflected radiation is reduced by radiation shields at the mouth of the outer can evacuation line, and the calorimeter can evacuation line.

The bottom of the outer can is removable to allow the calorimeter can to be centered while it is being soldered into place. Once this has been determined the outer can is tightened, the nylon spacer is positioned, and the bottom is soldered into place.

The outer can and its evacuation line are sealed by lead o-rings. Care must be taken to tighten the o-rings uniformly. When the o-ring grooves, which are little more than a scratch, were machined, a deeper groove of the same diameter was cut into a die. A three ampere Buss Fuse Wire is laid in the groove on the die and is cut to fill the groove. A low flame of an oxygen-gas torch is passed over the junction of the ends until they fuse to make an o-ring. A proficiency of nearly 70 percent in making good o-rings can be achieved with practice.

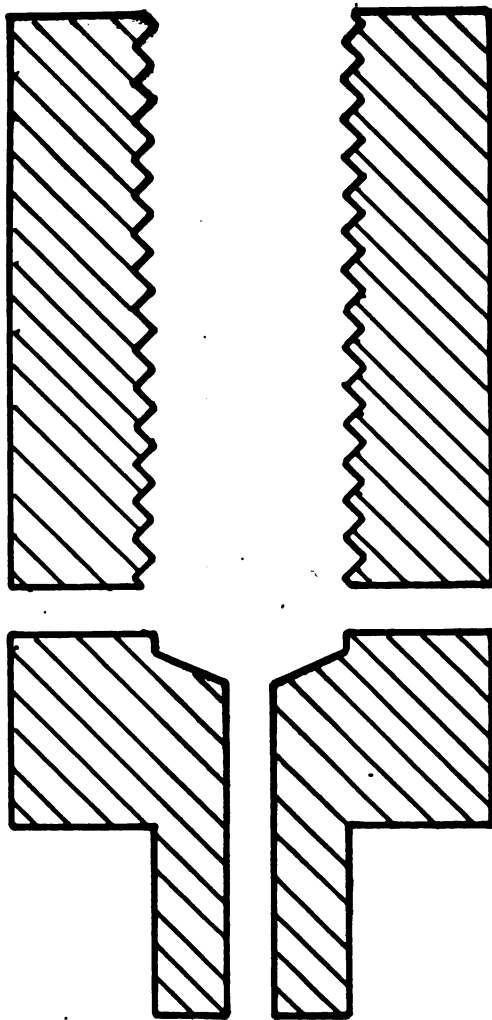
The fourteen formex coated 0.0031-inch diameter manganin electrical leads enter by means of kovar seals mounted in flanges sealed by rubber o-rings at the top of the system. They extend down the calorimeter evacuation line inside a length of teflon spaghetti, and make a twist around the tip

of the He^4 container. A small amount of G. E. #1202 varnish is applied to hold them in place and to make good thermal contact with this temperature. Eight of the leads go to one side of the epoxy thermal block. Four leads go to the 56 ohm, 1/10 watt Allen-Bradley resistor used as a bath thermometer. The resistor is glued into a hole cut in the tip of the He^4 container with G. E. #1202 varnish. The remaining two leads go to the 120 ohm, 1/10 watt Allen-Bradley resistor used as the bath heater which is glued into a similar hole.

Since the needle valve is a critical part of the system, Figure 7 shows the working parts. It allows liquid helium to be drawn into the inner He^4 container. The needle valve must be closed, isolating the inner He^4 container from the outer dewar. The smallest leak through this valve increases the lowest temperature that could be attained.

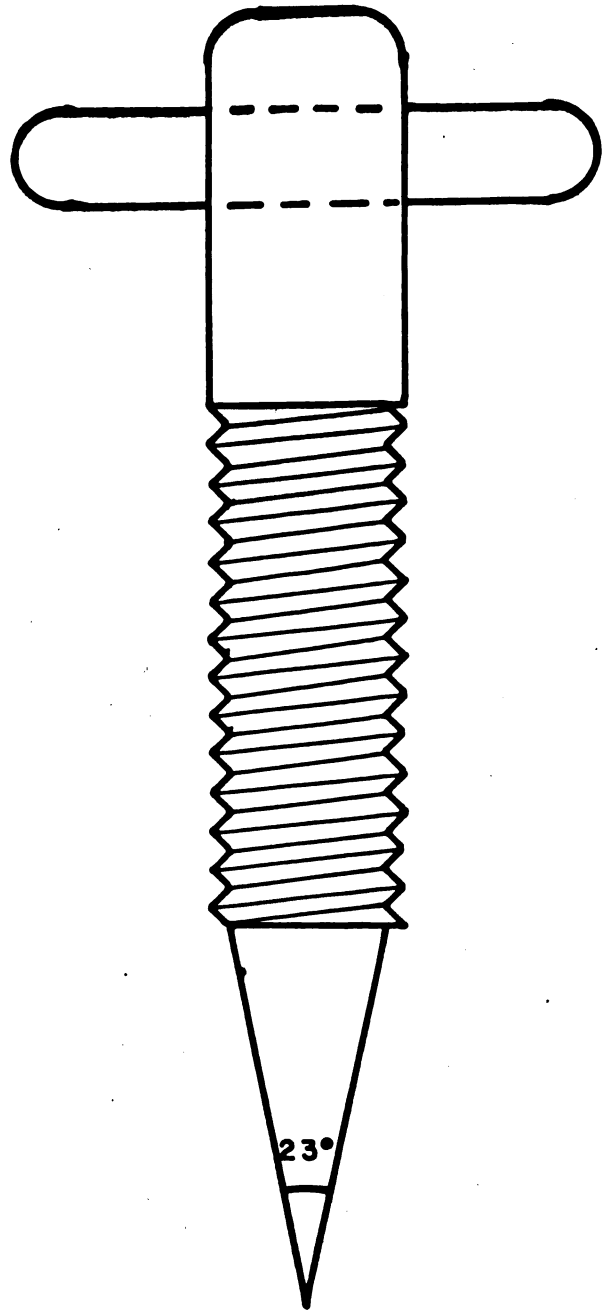
C. He^3 Calorimeter

The advantage of using liquid He^3 is that temperatures as low as 0.4°K can easily be attained as compared to 1°K for He^4 . Figure 8 shows a schematic of a He^3 calorimeter used for one of the zero field experiments. It is similar to the He^4 calorimeter except that the He^3 section is completely isolated from the He^4 . It also has an additional line for measuring the He^3 vapor pressure. All removable cans are soldered using Cerrolow 117 alloy. The electrical leads enter the system at the top by means of a kovar seal, reaching the interior of the outer can by means of its



Brass

← 1/4" →
Scale



Stainless
Steel

Fig. 7. The Needle Valve.

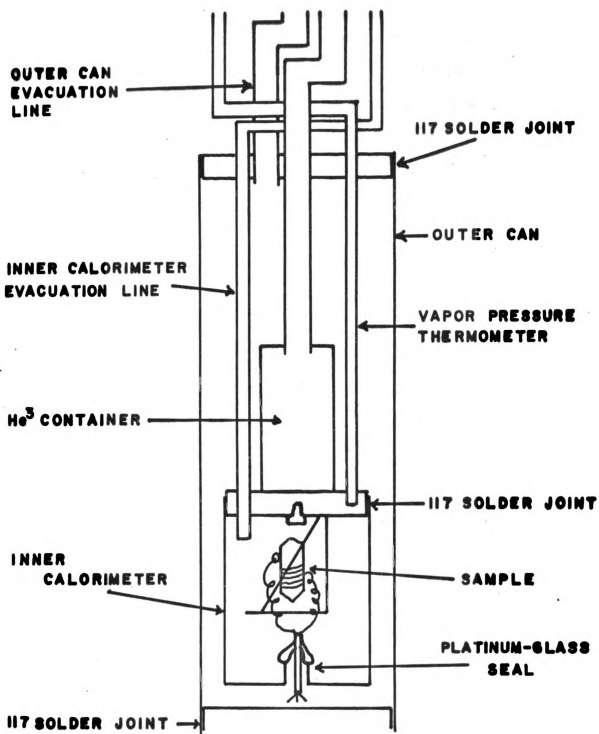


Fig. 8. Schematic of He^3 Calorimeter.

evacuation line. Any thermal conduction down these leads is minimized by having the leads make good thermal contact to the liquid He⁴ bath, and then to the liquid He³ bath. The leads enter the calorimeter through the bottom by means of a platinum-glass seal.

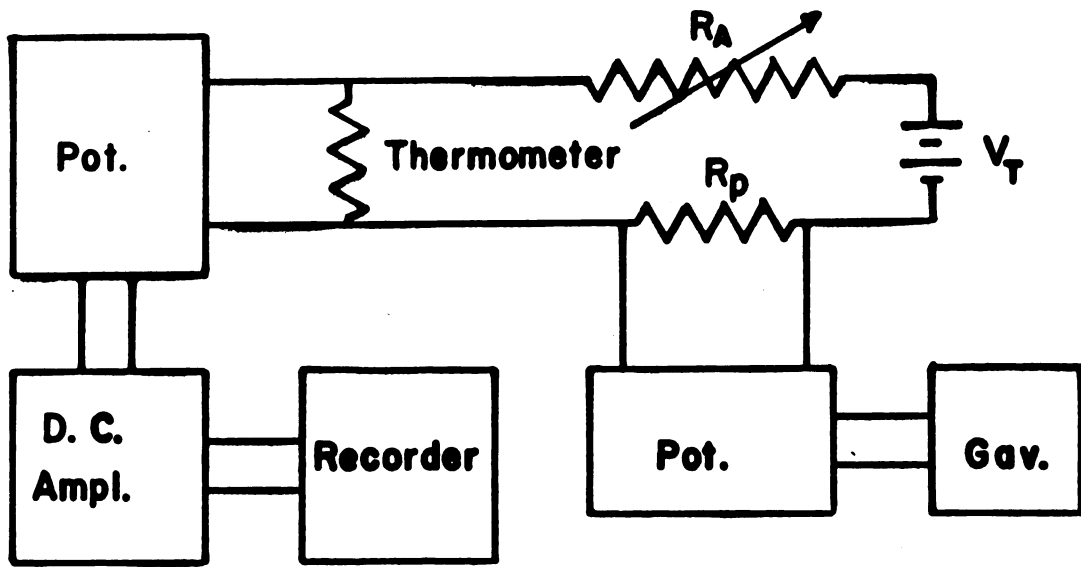
These seals are made from ten 0.010-inch diameter platinum wires about six inches long, a $\frac{1}{4}$ -inch diameter tubing, and soft-glass tubing. The platinum tube has one end feathered, i.e. a very sharply ground edge. The feathered end of the platinum tube is fused to the soft glass tubing. Each platinum wire is individually fused inside two inches of glass capillary tubing, and the ten are fused together. This bundle is fused inside the glass of the glass-platinum tube. If constructed properly with the proper glass, these seals are He II tight. Any well equipped glass blower can produce these seals. It has later been discovered that Wheatley's²⁸ method of sealing manganin wires inside metallic tubing using epoxy is also satisfactory at He II temperatures.

D. Electrical Measurement Apparatus

The four separate circuits which are used to make the specific heat measurements are the bath heater, the bath thermometer, the sample thermometer, and the sample heater. The sample thermometer and sample heater circuits are diagrammed in Figure 9. There are three boxes labeled "Pot." Two of them are Leeds and Northrup K-3 potentiometers, and the one across R_p is a Leeds and Northrup K-2 potentiometer.



THERMOMETER CIRCUIT



HEATER CIRCUIT

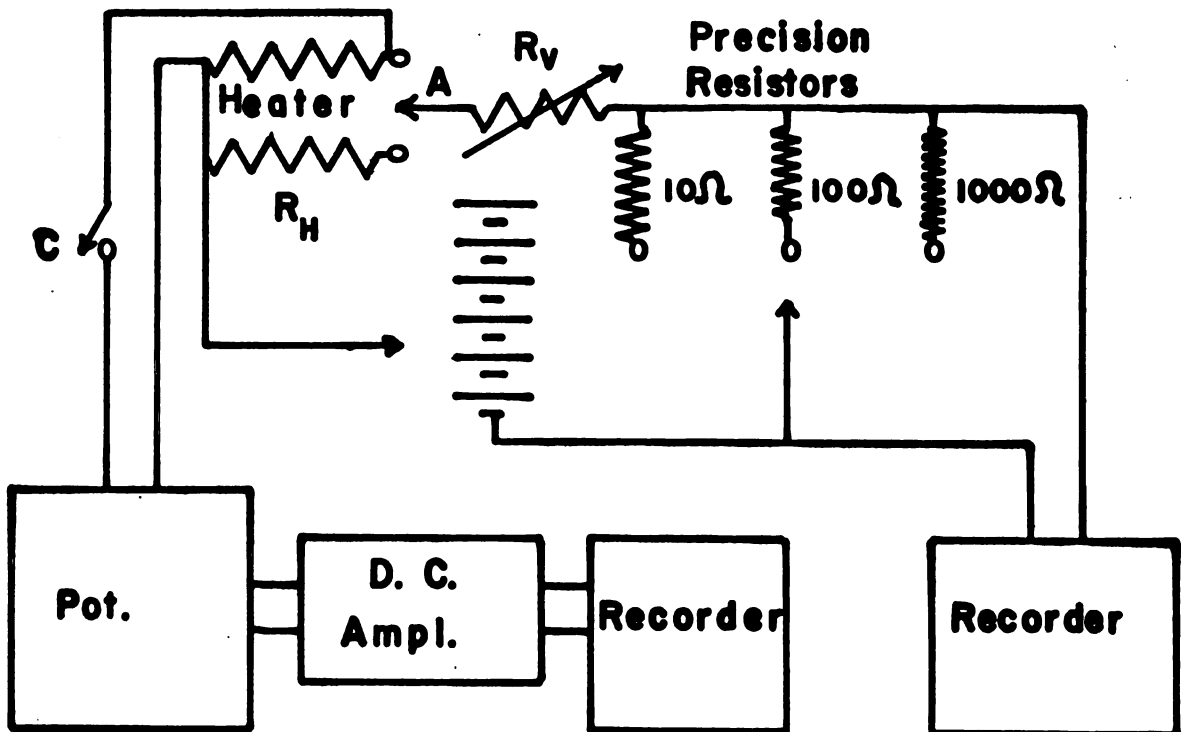


Fig. 9. Electrical-Measurement Circuit Diagrams.

The "D. C. Ampl." boxes are Leeds and Northrup D. C. Voltage Amplifiers. The two boxes marked "Recorders" which connect to the D. C. amplifiers represent a single variable range card, Leeds and Northrup 2-pen Speedomax G recorder. The remaining recorder is a Leeds and Northrup single pen Speedomax G recorder. "Gav." is a Leeds and Northrup box type galvanometer. The precision resistors are all manufactured by General Radio.

The bath heater is the simplest of the four circuits. It consists of a 120 ohm, 1/10 watt Allen-Bradley resistor in series with a 10,000 ohm rheostat. These are across a 0-115 volt Variac. The a. c. heater current is controlled by both the rheostat and the Variac.

The voltage measurement across the bath thermometer is identical to the one shown in Figure 9. Since the bath thermometer is used only for control, the precise temperature is not required and the tolerances on the current supply need not be so stringent. A transistorized constant current supply is used and will not be discussed since it is not pertinent to the experiment. The bath thermometer, supplied with a current of ten microamperes, gives adequate sensitivity for a 56 ohm, 1/10 watt Allen-Bradley resistor.

In the sample thermometer circuit V_T is a pair of Mallory 28 volt mercury batteries connected in series, R_A is a 50 megohm resistor in series with a 10 megohm variable resistor for adjusting the current, and R_p is a 0.1 megohm precision resistor with a tolerance of 0.01 percent. The galvanometer will read null when the potentiometer across

R_p is set for 0.1 volt and R_A is adjusted to allow one microampere of current to flow through the circuit. The current is monitored continually and can be kept constant manually. However, adjustments were found unnecessary because the thermometer resistance changes were small compared to R_A .

The multiplying scale factor of the D. C. amplifier, the range of the recorder, and the thermometer current all determine the sensitivity of the recorder in measuring the emf across the thermometer. The range of each pen in the 2-pen recorder can be changed to 10, 5, or 1 millivolt full scale with zero left by using different range cards. The thermometer current cannot be adjusted freely since the greater the current the more power dissipated by the thermometer. It is set to give the maximum tolerable power, and any further sensitivity increases must be attained electronically.

The heater voltage is measured by the same techniques applied to determine the thermometer voltage. A recorder measures the voltage across a precision resistor which determines the heater current. Several different precision resistors are available to keep the voltage within the range of the recorder. The heater current is controlled by varying a resistor in series with the heater (R_V in Figure 9) and by adjusting the voltage through the number of cells selected from the battery supply. When switch A makes contact to the right, current is bypassed through R_H , the substitute heater which has the same resistance as the heater.

The current is allowed to pass through the heater when switch A makes contact to the left. At the same time switch C is closed allowing the potentiometer to monitor the heater voltage. A timer operates both switches and measures the time that current flows through the heater for energy measurements. The timer can be programmed either to shut off after a predetermined time or to be stopped manually. The use of the substitute heater for balancing purposes is to eliminate a pulse of unknown current in the heater due to the unbalance of the measuring recorder. The heater circuit potentiometer is also used, by appropriate switching, to measure the bath thermometer voltage, voltage across a precision resistor in either the bath circuit or in the heater circuit, or across any external potential.

E. Preparation of Sample

There are six steps in the preparation of a sample for an experimental run: 1) the selection of a single crystal of adequate size, 2) deciding on the proper resistor to be used for the thermometer, 3) connecting manganin leads to the thermometer and the heater, 4) gluing the heater and the thermometer to the crystal, 5) mounting the sample in its holder, and 6) orientating the crystal in the field.

$\text{Cs}_2\text{MnCl}_4 \cdot 2\text{H}_2\text{O}$ crystals were grown from an aqueous solution at room temperature of a mixture of CsCl_2 and $\text{MnCl}_2 \cdot 2\text{H}_2\text{O}$.^{*} Two crystals about one inch long and 0.25 cm.² in cross section area weighing about one gram each were used.

^{*}Crystals were kindly supplied by Professor J. Cowen.

The resistance thermometer selected will depend upon the temperature range to be covered. A 10 ohm, 1/10 watt carbon Ohmite resistor gives the best results for He³ temperatures and a 56 ohm, 1/10 watt carbon Allen-Bradley resistor works best for He⁴ temperatures. The plastic coating on these resistors were not removed, since no problems with thermal equilibrium were noticed previously and the carbon would have to be recoated to prevent the absorption of gas.

The sample heater consists of twelve inches (about 450 ohms) of enamel coated Evenohm* wire 0.0014 inch in diameter. About one-half inch of the insulation is stripped from both ends of the heater and the ends are tinned using regular solder with a resin core. Eight formex coated manganin wires about six inches long (approximately 15 ohms) and 0.0031 inch in diameter are used as leads. They also have their ends stripped and tinned. Two manganin leads are joined to each side of the heater and two leads are soldered as close as physically possible to each side of the thermometer resistor. The excess terminal wire on the thermometer is cut off. The pairs of leads on each side of the heater and the thermometer are wound around a nail to form a coil of about one-quarter inch in diameter. On both the heater and the thermometer two leads provide current flow and two leads allow the voltage to be measured.

After the surfaces have been coated with G. E. varnish #1202, the twelve inches of heater wire are wound as

*Trade name for wire supplied by Wilber B. Driver Co., Newark, N.J.

non-inductively as possible around the crystal. The thermometer is tied to a smooth face of the crystal by means of a nylon thread and is covered by a drop of varnish for better thermal contact.

A C-shaped holder (see Figure 4) is made from one-quarter inch german-silver tubing pressed into a metal strip. A nylon thread is looped through two small holes at the top and at the bottom, so that there are two parallel lines across the opening of the holder. The crystal is placed between these threads and held in place by an application of varnish. The tip of a small brass tack wedged between the loop of thread and the bottom of the holder pulls the sample rigid. A larger hole is drilled in the top to mount the holder to the tip of the inner helium container. The holder can be rotated about the mounting screw and all orientations of the crystal around this axis of rotation are possible.

The crystal is now orientated with respect to the field. The calorimeter system without the outer or inner calorimeter cans is positioned in the dewar. By use of a flashlight and the slit in the dewar, one of the previously placed marks on the epoxy terminal block is chosen to be normal to the magnetic field. The calorimeter system is then removed from the dewar and the chosen fiducial mark is then used to place two other similar indices on the epoxy, such that a line drawn through them is parallel to the field. The orientation of the crystal is made using these two latter

indices. It is estimated that there is an error of approximately 5° in this orientation technique.

After the above steps have been completed, the leads are soldered to the terminal block, which in turn connect them to the outside through the kovar seals at the top of the system.

F. Experimental Procedure

After the system has been prepared, the following is the step-by-step procedure necessary for taking data. Figure 10 shows a photograph of the total assembled system. For the name of pumps and valves etc. refer to Figure 11.

1. Pre-Cooling.--At least six hours before the transfer of liquid helium the outer dewar should be filled, and kept filled with liquid nitrogen. In preparation for this, evacuate the vacuum jacket of the inner dewar for about twenty minutes. In the meantime valve C is closed and the needle valve is opened. Just before the transfer of liquid nitrogen the inside of the dewar is evacuated with the large two inch Kinney pump (pump Y). The inner container is then flushed with helium gas and re-evacuated but care must be taken since pyrex glass is porous to helium gas at room temperature. With pump Y still pumping on the inner dewar, liquid nitrogen is added to the outer container.

Shortly after the liquid nitrogen has been transferred, pump Y is closed off and helium gas is added to the inner dewar to act as an exchange gas. This helium gas also keeps liquid oxygen from condensing and frost from clouding the

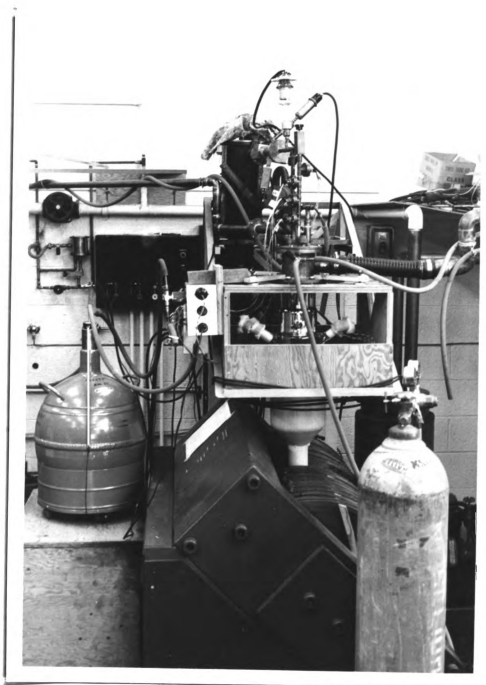


Fig. 10.--A Photograph of Total System.



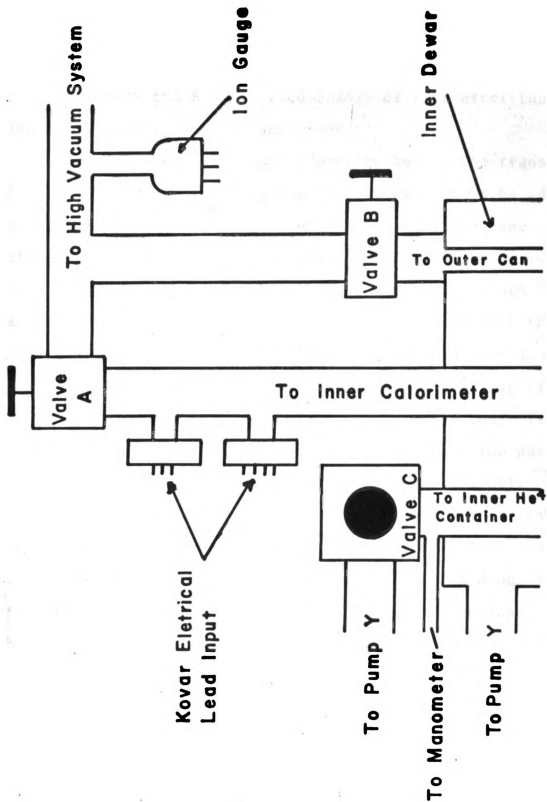


Fig. 11. Schematic Diagram of Top of Dewar.

inner dewar. The largest decrease in pressure of the helium gas due to its cooling occurs during the first hour after it has been added. From then on a three pound per square inch over-pressure will last twelve hours or longer.

Valves A and B are closed before or soon after the liquid nitrogen has been transferred.

2. Adding Exchange Gas.--Sometime before the transfer of liquid helium, helium gas for heat exchange must be added to the calorimeter and outer cans. This should be done after the six-hour pre-cooling period, since the calorimeter will be evacuated and if the crystal is not cold enough it may be damaged. Valves A and B are opened to evacuate the cans. After twenty minutes the ion gauge should read about 5×10^{-4} millimeters of mercury; if not, a possibility of leaks in the seals or solder joints may be suspected. If there are no leaks, valves A and B are closed and the pumping line is flushed and filled with helium gas slightly above one millimeter of mercury. The pressure should read one millimeter of mercury after the opening of valves A and B. If the pressure is too high carefully pump it down, if it is too low add more helium gas in the same manner as above.

Once the desired pressure is obtained valves A and B are closed and the pumping line is evacuated. The system is now ready for the transfer of the liquid helium.

3. Liquid-Helium Transfer.--The needle valve is closed and the vent of the liquid helium dewar is connected to the

recovery system by means of a hose. A rubber hose through which there is a slight flow of helium gas is connected to the pressurizing port of the transfer tube. The liquid helium storage container is moved into position and the transfer tube is lowered simultaneously into the storage container and dewar. The transfer tube is sealed from the atmosphere and pressure is applied to the surface of the liquid helium in the storage container by means of helium gas through the transfer tube's pressurizing port. Liquid helium will be forced over into the dewar and any vapor from the boiling due to the "warm" system is vented and recovered.

The liquid level is watched for, using the observation slit and a flashlight. When the level reaches the desired height the pressurizing gas is shut off and the transfer tube is removed. The container is sealed. If the system has been pre-cooled sufficiently a transfer of about six to seven liters will result.

The bath thermometer is watched and when its resistance has come to equilibrium at a value about ten times its room temperature resistance open the needle valve filling the inner He⁴ container. Valve B is opened to evacuate the outer can of exchange gas allowing the isolation of the inner He⁴ container thermally from the outer bath.

The electromagnet is turned on and the field is adjusted to the desired value. When the sample thermometer comes to equilibrium the first temperature calibration point is taken.

4. The Calibration of Sample Thermometer.--The thermometer resistance is calibrated against the helium vapor pressure whose temperatures are listed in the T_{58} liquid helium vapor pressure table.²⁹ After the thermometer has come to equilibrium the thermometer resistance, the mercury manometer readings, room temperatures, and height of liquid helium above the sample's position are recorded. The room temperature reading and height of liquid helium are unnecessary below the λ -point.

The needle valve is closed and valve C is opened. Immediately begin to slowly pump on the inner He^4 container with pump Y. The pumping speed is manually adjusted by opening and closing a valve, not shown, in the pumping line of Y. The vapor pressure is reduced ten centimeters on the mercury manometer and is manually held at this pressure by watching the bath thermometer and the manometer. This pressure is kept constant until the sample thermometer achieves an equilibrium resistance. This takes several minutes at the beginning and up to three quarters of an hour for the final calibration points. The thermometer equilibrium resistance and the vapor pressure are recorded. Continue to lower the pressure in ten centimeter steps until four centimeters pressure remain. This calibration point is recorded and then the oil manometer is connected to the system. This manometer is subsequently used for observing the pressure as the pumping valve is adjusted. Below 2.5 centimeters of mercury, the vapor pressure is read from the McLeod gauge. Continue to pump down in steps of ten centimeters

on the oil manometer. This procedure is maintained until all valves are open to pump Y and the lowest possible pressure is attained. This will give a temperature of approximately 1°K.

Since carbon resistors are used for the thermometers a temperature calibration must be made every time a resistor has had its temperature changed by approximately 20°K. Although it has been discovered that a magnetic field as high as 10,000 gauss does not change the temperature calibration within the tolerances of this study.

5. Specific Heat Measurements.--After recording the final temperature calibration point, the bath thermometer is turned off, valve B is closed, and valve A is opened evacuating the calorimeter of exchange gas and thermally isolating the sample. After five minutes the ion gauge should read approximately 10^{-5} millimeters of mercury and specific heat data can be taken. The sample can never be completely isolated from its surroundings for there are always heat leaks due to radiation, and to thermal conduction along electrical leads and nylon threads. These heat leaks constitute the "background."

Since it is not always possible to eliminate the background, some means must be established to measure it or subtract off its heat.

A method of subtracting off the background heat is described using the lettered points in Figure 12. The figure shows how a portion of a recorder chart would appear. The

lines AB and CD represent the change in resistance due to the background heating. The slopes of these lines can be altered by changing the pumping speed of the bath or by supplying power to the bath heater which changes the temperature surrounding the sample. The slope of line BC is due to the background heat and the power added to the crystal by the sample heater. The resistance change resulting from the background heat while the sample heater was on can be eliminated in the following manner. Line EF is constructed midway between points B and C. Lines AB and CD are extended to cross EF. D_s and D_e represent the resistance change due only to the power put into the sample by this heater. The line segment $B'D_s$ represents the resistance change from the background on first half of heating cycle and D_eC' is the resistance change from the background of final half of heating cycle. If the change in the temperature of the sample during the heating cycle is small compared to the temperature difference between the sample and its surroundings then $B'D_s$ and D_eC' are equal. This is usually the case and it is preferred since no assumption is made as to where the background slope changed.

These lines are drawn and D_s , D_e , heater current, heater voltage, and the time that the current flowed through the heater are recorded for each point as the experiment progresses. A specially constructed apron for the recorder, facilitates the drawing of the lines.

Before any specific heat data are taken the background heating of the sample is adjusted. When at the desired level

the potentiometer setting is changed to move the pen of the recorder to the extreme left. Here the resistance is recorded. This resistance corresponds to the thermometer resistance at the null position. This resistance is noted whenever the pen is moved from the extreme right to the extreme left of the recorder chart. This process is continued until the highest temperature desired is attained.

Since the specific heat of the sample may change, the difference between D_s and D_e will change. To obtain minimum scatter in specific heat points the heater current should be adjusted to maintain this difference greater than ten chart divisions in 20 to 30 seconds of heating.

6. Voltage-Calibration Data. - - Voltage calibration data are also taken while the specific heat points are being recorded. When the pen of the recorder reaches the right of the chart (D_r) due to the increase in temperature, the potentiometer setting is changed and the recorder pen moves back to the left (D_l), see Figure 12. Two potentiometer settings, in terms of resistances, and the pen position, in chart divisions are recorded. Since neither the change in potentiometer setting nor the pen's movement can be instantaneous the slopes of the background heating are extrapolated to give the positions of the pen for an instantaneous movement across the chart. Continue taking this data until the last specific heat point has been recorded. The pen is moved to the left and the final voltage calibration point is taken.

7. Shut-down.--By the time the final point has been recorded pump Y may have been closed off and the system vented. To begin shut down, pump Y is opened to both outer and inner helium baths by opening the needle valve. Valve B is reopened and the diffusion pump on the high vacuum system is turned off allowing the cooling water and forepump to run. All electrical measuring equipment is switched off. Liquid nitrogen is maintained in the outer dewar until it is certain all of the liquid helium has been evaporated. When there is no more liquid helium in the inner dewar, pump Y is shut off, and the outer can, inner calorimeter can, and inner dewar are vented with dry nitrogen gas. When the diffusion pump is cold the forepump and cooling water are turned off.

G. Data Reduction

1. Calibration of Thermometer.--The T_{58} liquid helium vapor-pressure table lists all of the vapor pressures in microns of mercury at 0°C . The mercury-manometer reading must be normalized from room temperature to 0°C . This correction is unnecessary for the McLeod gauge.

The vapor pressure must be corrected for the height of liquid helium above the level of the sample. Below the λ -point this correction becomes unnecessary, because He II has a very high thermal conductivity and the temperature is uniform throughout the liquid.

The calibration temperatures and their corresponding resistances are fitted to the two parameter Clement-Quinnell³⁰ equation,

$$\left[\frac{\log R}{T} \right]^{1/2} = a + b \log R \quad (116)$$

by the method of least squares. The relative deviations from this curve are then fitted by the method of least squares to a sixth-degree polynomial,

$$\frac{\left[\frac{\log R}{T} \right]_{\text{meas.}}^{1/2} - \left[\frac{\log R}{T} \right]_{\text{calc.}}^{1/2}}{\left(\frac{\log R}{T} \right)_{\text{meas.}}^{1/2}} = \sum_{n=0}^6 C_n (\log R)^n \quad (117)$$

where the C_n 's are arbitrary constants. The temperature is calculated from the resistance by combining the parameters of these two fitted equations into the following,

$$T = \log R \left[\frac{a + b \log R}{1 - \sum_{n=0}^6 C_n (\log R)^n} \right]^{-2} \quad (118)$$

Table 1 shows the temperature calibration, curve fitting results for an experiment made January 13, 1967. The maximum deviation is about ten millidegrees at the higher temperatures. This deviation becomes smaller for lower temperatures. Temperature changes of the order of one millidegree or less can be detected but the actual temperature is known only to ten millidegrees.

2. Voltage-Calibration.--The voltage calibration or the volts-per-division data is needed to calculate the thermometer resistance (R_t) from the potentiometer reading, when the recorder pen is not at the null position. When the

Table 1. Temperature-Calibration-Curve Parameters from an Experiment made
January 13, 1967.

$$a = 1.813236, b = 0.470429,$$

$$C_0 = -3.570883, C_1 = 1.687682, C_2 = -0.2906558, C_3 = 0.02152158, C_4 = -0.0005747483$$

Measured Resistance (ohm)	Measured Temperature (°K)	Calculated Temperature (°K)	Difference (milli-°K)	Percent Difference
663.0	4.18660	4.17754	9.06	0.2163
709.5	4.00930	4.01017	-0.77	-0.0193
764.0	3.83500	3.84114	-6.14	-0.1601
840.0	3.63890	3.64348	-4.58	-0.1258
946.2	3.41760	3.42127	-3.67	-0.1075
1,145.0	3.11810	3.11498	3.12	0.1001
1,538.0	2.73760	2.73287	4.73	0.1727
3,513.9	2.01490	2.01643	-1.53	-0.0759
4,308.4	1.88740	1.88764	-0.24	-0.0129
5,955.0	1.70620	1.70700	-0.80	-0.0467
10,010.2	1.46320	1.46210	1.10	0.0749
20,600.0	1.18470	1.18490	-0.20	-0.0170

thermometer is replaced by a variable resistor, R_t can be calculated from the equation,

$$R_t = \frac{R_0 - C_1 D}{1 + C_2 D} \quad (119)$$

where R_0 is the potentiometer reading divided by the thermometer current. D is the distance from the pen position to the null position on the recorder chart. This is taken as positive if the pen position is to the right of the null position and negative if it is to the left. C_1 and C_2 are obtained from a least-squares fit of the voltage-calibration data to the equation,

$$\frac{R_{01} - R_{02}}{D_1 - D_2} = C_1 + C_2 \left(\frac{R_{01} + R_{02}}{2} \right)$$

or

$$\Delta R / \Delta D = C_1 + C_2 \bar{R} \quad (121)$$

For the derivation of these equations see Appendix I.

When the variable resistor is replaced by the thermometer, the plot of $\Delta R / \Delta D$ vs \bar{R} is fitted best by a third-degree polynomial instead of (121). Table II gives the results of this fit. The necessity for such an analysis for the voltage-calibration curve is due to the off-balance readings of the potentiometer. Since such off-balance readings introduce an error current in the thermometer, the proper correction is necessary. Inserting an amplifier with a high-impedance input would reduce the error current, and

Table 2. One-Millivolt-Voltage Calibration-Curve Parameters for an Experiment made January 13, 1967.

$$\Delta R/\Delta D = C_1 + C_2 \bar{R} + C_3 \bar{R}^2 + C_4 \bar{R}^3$$

$$C_1 = 1.99669 \times 10^{-1}, \quad C_2 = 5.004588 \times 10^{-4}, \quad C_3 = -2.694505 \times 10^{-9}, \quad C_4 = 1.059814 \times 10^{-13}$$

R_0 (ohms $\times 10^3$)	Measured $\Delta R/\Delta D$ (ohms/div.)	Calculated $\Delta R/\Delta D$ (ohms/div.)	Difference (ohms/div.)	Percent Difference
17.5809	8.7829	8.7413	0.0417	0.47
14.8228	7.3024	7.3710	-0.0686	-0.94
12.4671	6.0976	6.2255	-0.1279	-2.10
10.4346	5.4798	5.2488	0.2311	4.22
8.6217	4.4023	4.3821	0.0203	0.46
7.2512	3.6675	3.7273	-0.0599	-1.63
6.0750	3.1250	3.1643	-0.0393	-1.26
5.3227	2.8409	2.8031	0.0378	1.33
4.5363	2.3713	2.4244	-0.0531	-2.24
3.7382	2.0559	2.0383	0.0176	0.85

Table 2. (Continued)

R_0 (ohms $\times 10^3$)	Measured $\Delta R/\Delta D$ (ohms/div.)	Calculated $\Delta R/\Delta D$ (ohms/div.)	Difference (ohms/div.)	Percent Difference
3.2126	1.7801	1.7831	-0.0031	-0.17
2.6603	1.5133	1.5140	-0.0006	-0.04
2.3076	1.2976	1.3416	-0.0439	-3.38
1.9633	1.1667	1.1726	-0.0060	-0.51
1.5956	1.0081	0.9918	0.0163	1.62
1.3010	0.8538	0.8464	0.0074	0.87
1.0797	0.7511	0.7370	0.0141	1.87
0.8645	0.6466	0.6304	0.0162	2.50

it has been tried with several amplifiers, but the noise level was increased beyond a tolerable level.

An empirical formula which gives R_t , using the cubic fit, R_0 , and D has been derived by trial and error. This is,

$$R_t = \frac{R_0 - [C_1 - C_2R - 2C_3R^2 - 3C_4R^3]D}{1 + [C_2 + 2C_3R + 3C_4R^2]D} \quad (122)$$

where the C 's are the coefficients of the third-degree polynomial fit, and R_t in the first approximation, is calculated using $R = R_0$. The calculation is iterated using $R = R_t$ until the previous calculated value differs by 0.1 percent from the final value.

3. Specific Heat Data.--The specific heat of the point ABCD in Figure 12 can now be calculated. The resistance at D_s and D_e are determined using the voltage-calibration data and the empirical formula. The temperature for these resistances are computed using the thermometer calibration equation. The heater current (I_h), heater voltage (V_h), the time of heating (t), and the mass of the sample in moles (M) have all been measured. Therefore C_m may be written as,

$$C_m = \frac{I_h \times V_h \times t}{(T_e - T_s)M} \quad (123)$$

The specific heat (C_m) curve is the plot of C_m versus \bar{T} where $\bar{T} = \frac{1}{2}(T_e + T_s)$, the average of the temperatures calculated from D_e and D_s .

There are several possible sources of errors, but the largest is reading distances on the chart. The scatter caused by this error, as mentioned before, is kept to a minimum by keeping the difference between D_e and D_s greater than ten small divisions, where the chart is divided into 100 of these divisions. Another source of error is the additional heat capacities of the thermometer, heater wire, and varnish. This error is largest at 4°K and the calculation indicates that it contributes approximately 2.8 percent of the total specific heat at that temperature.

IV. RESULTS AND DISCUSSION

A. Description of Crystal

The samples each consisting of a single crystal of $\text{Cs}_2\text{MnCl}_4 \cdot 2\text{H}_2\text{O}$ were studied. They both are about one inch long with a cross sectional area of 0.25 cm^2 . The mass of sample 1 is 1.353 grams or 0.00272 mole, and the mass of sample 2 is 0.905 gram or 0.00181 mole, using 498.63 grams/mole as the molecular weight. S. J. Jensen³⁰ has made an x-ray study of $\text{Cs}_2\text{MnCl}_4 \cdot 2\text{H}_2\text{O}$. The crystals are triclinic, of space group $\text{P}\bar{1}$ with one formula unit per unit cell. The parameters are:

$$\begin{array}{ll} a = 5.75\text{\AA} & \alpha = 67.0^\circ \\ b = 6.66\text{\AA} & \beta = 87.8^\circ \\ c = 7.27\text{\AA} & \gamma = 84.3^\circ \end{array}$$

Figure 13 shows a cross section of the crystal and identifies several faces.

B. Zero Field Results

Four separate specific heat studies were made in a zero magnetic field. Two studies were made on sample 1 in the He^4 calorimeter between $1.4^\circ - 5.0^\circ\text{K}$. Sample 2 was studied first in the He^4 calorimeter, and then secondly in the He^3 calorimeter between 0.6° and 3.0°K . Figure 14 shows these results plotted as a function of temperature, and

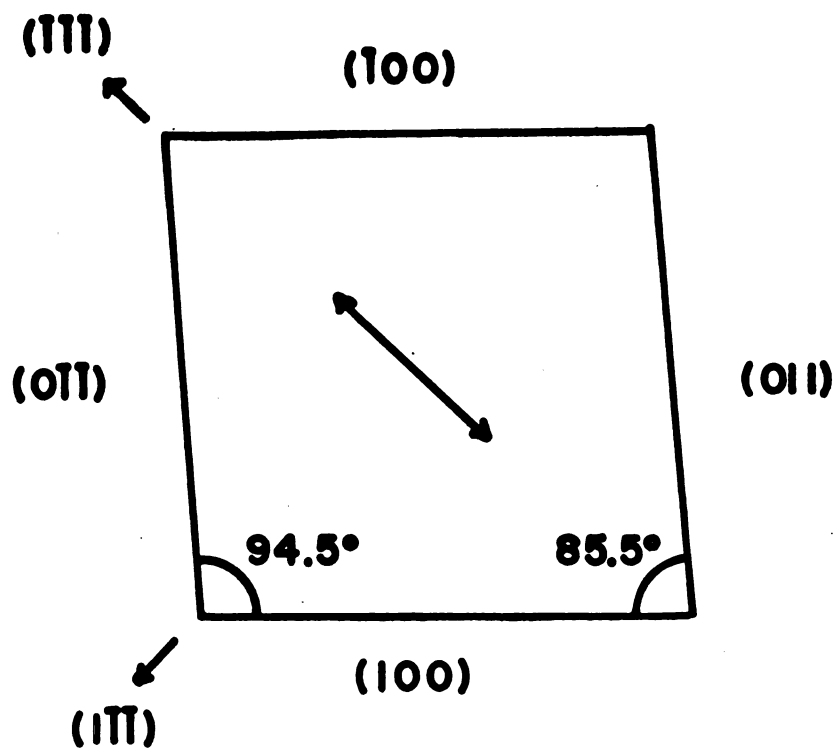


Fig. 13. A Cross Sectional View of $\text{Cs}_2\text{MnCl}_4 \cdot 2\text{H}_2\text{O}$ Perpendicular to the Elongated Axis with an Arrow Indicating the Direction of Easy Magnetization.

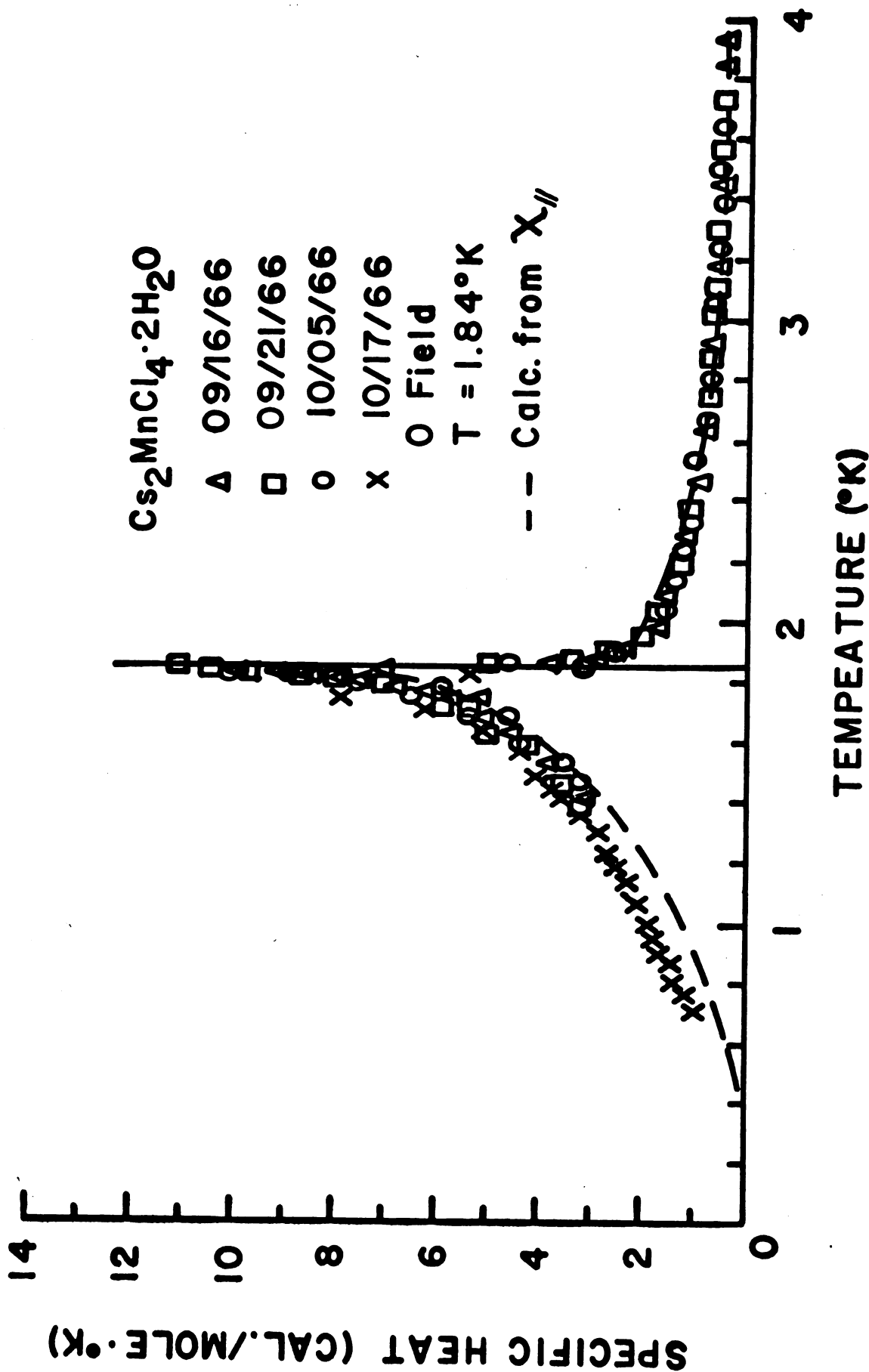


Fig. 14. Specific Heat Curve in Zero Magnetic Field.

Appendix II, Tables 3, 4, 5, and 6 list the experimental values. The transition temperature is $1.84^\circ \pm 0.01^\circ\text{K}$.

The specific heat curve shown in Figure 14 is the total specific heat. This includes the lattice specific heat, the specific heat due to the nuclear-spin interaction, and that due to the spin-spin exchange interaction. The electronic specific heat will be negligible since the samples are non-metals. The specific heat measurements of MnF_2 made by Cooke and Edmond³¹ suggest that the nuclear-spin interaction contributes less than 2 percent at 0.6°K . Since this interaction tails off as $1/T^2$, it will contribute even less at higher temperature.

To calculate the lattice contribution the well known Debye³² function is used,

$$C_L = 9Nk \left(\frac{T}{\theta} \right)^3 \int_0^{\theta/T} \frac{x^4}{(e^x - 1)(1 - e^{-x})} dx \quad (124)$$

where θ is a constant and called the Debye theta, and x is given by $\hbar\omega/kT$. For low temperature the integral can be approximated by a constant, so that,

$$C_L = DT^3 \quad (125)$$

Van Vleck has indicated that the specific heat above the Néel temperature, i.e. in the paramagnetic state, may be written as,

$$C_m = A/T^2 + B/T^3 + C/T^4 \quad (126)$$

where A, B, and C are arbitrary. Combining (125) and (126) the total specific heat above T_n is,

$$C_T = A/T^2 + B/T^3 + C/T^4 + DT^3 \quad (127)$$

Fitting (127) by the method of least squares, to the specific heat data above 2.2°K gives A = 8.24, B = -14.95, C = 22.39, and D = 0.00118. The Debye theta calculated from D is found to be 73°K. C_L represents 14 percent of C_T at 4.0°K but the area under the C_L curve is just 1 percent of the total area under the curve in Figure 14. Therefore the curve in Figure 14 may be considered the specific heat for the exchange interaction only. The dashed curve in Figure 14 represents the specific heat, calculated from the parallel susceptibility results, equation (86), where $(TX_{//})_{\infty}$ was found to be 3.01°K·cc/mole. The agreement is remarkably good in the light of the approximation made for equation (86).

If the total change in entropy is calculated graphically, using (17), between 0° and 2.2°K, and mathematically, using (126) between 2.2°K and ∞ , it is found to be 3.75 cal./mole·°K. (The extrapolated value from 0° - 0.6°K amounts to 0.13 cal./mole·°K.) This value compares favorably with the theoretical value, 3.56 cal./mole·°K, computed from equation (18) using $J = 5/2$. Some short range ordering above the transition temperature is indicated since 25 percent of the measured entropy is recovered above the Néel temperature.

The exchange energy, evaluated by computing the area under the magnetic specific heat curve, is equal to 7.25

cal./mole. Using this energy value, together with $S = 5/2$, and the expression for E_{ex} , equation (57), T_n can be calculated. The calculated value of 3.4°K is almost twice the measured value of 1.84°K for the transition temperature. This would indicate that the molecular-field theory does not give exact agreement as far as details are concerned, although it appears to predict the qualitative features.

In the temperature region $0.6^\circ - 1.6^\circ\text{K}$, C_m is found to fit a curve of the form,

$$C_m = 0.94T^{3.22} \quad (128)$$

Now from equation (58), this may be written as,

$$\int C_m dT = k \int M dM \quad (129)$$

where k is just a constant of proportionality. Then,

$$aT^{4.22} = (k/2)M^2 + p \quad (130)$$

where $a = 0.94/4.22$ and p is the constant of integration.

At $T = T_n$, $M = 0$ thus,

$$p = aT_n^{4.22}, \quad (131)$$

but at $T = 0$, $M = M_s$ and,

$$p = -(k/2)M_s^2 \quad (132)$$

Divide by p and write,

$$(T/T_n)^{4.22} = -(M/M_s)^2 + 1 \quad (133)$$

Solving for M/M_S one obtains,

$$M/M_S = \left[1 - (T/T_n)^{4.22} \right]^{1/2} \quad (134)$$

Burley,³³ using a three dimensional Ising model and, by expanding the partition function and extrapolating to T_n predicts that near T_n ,

$$M/M_S \sim (1 - T/T_n)^m \quad (135)$$

where m is between 0.25 and 0.50. Plotting $\log (M/M_S)$ as measuring in (134) against $\log (1 - T/T_n)$ the slope of the best straight line will be m . Using only points close to T_n , m is found to be 0.27. Figure 15 shows M/M_S plotted as a function of reduced temperature for the specific heat results, for the calculation of Burley's f.c.c. model, and for the calculation based on the molecular-field theory with $S = 5/2$. Figure 15 also show the sublattice magnetization as measured by nmr. The specific heat results agree fairly well with the nmr data, and appear to be better represented by the Burley calculation than by the molecular-field theory. Again, the molecular-field theory appears to represent the experimental results in a qualitative way.

C. Magnetic-Field Results

Using the zero field transition temperature for $\text{Cs}_2\text{MnCl}_4 \cdot 2\text{H}_2\text{O}$ an order of magnitude of the critical field (H_c), the value of the field needed to break the exchange forces at 0°K , can be calculated from the expression

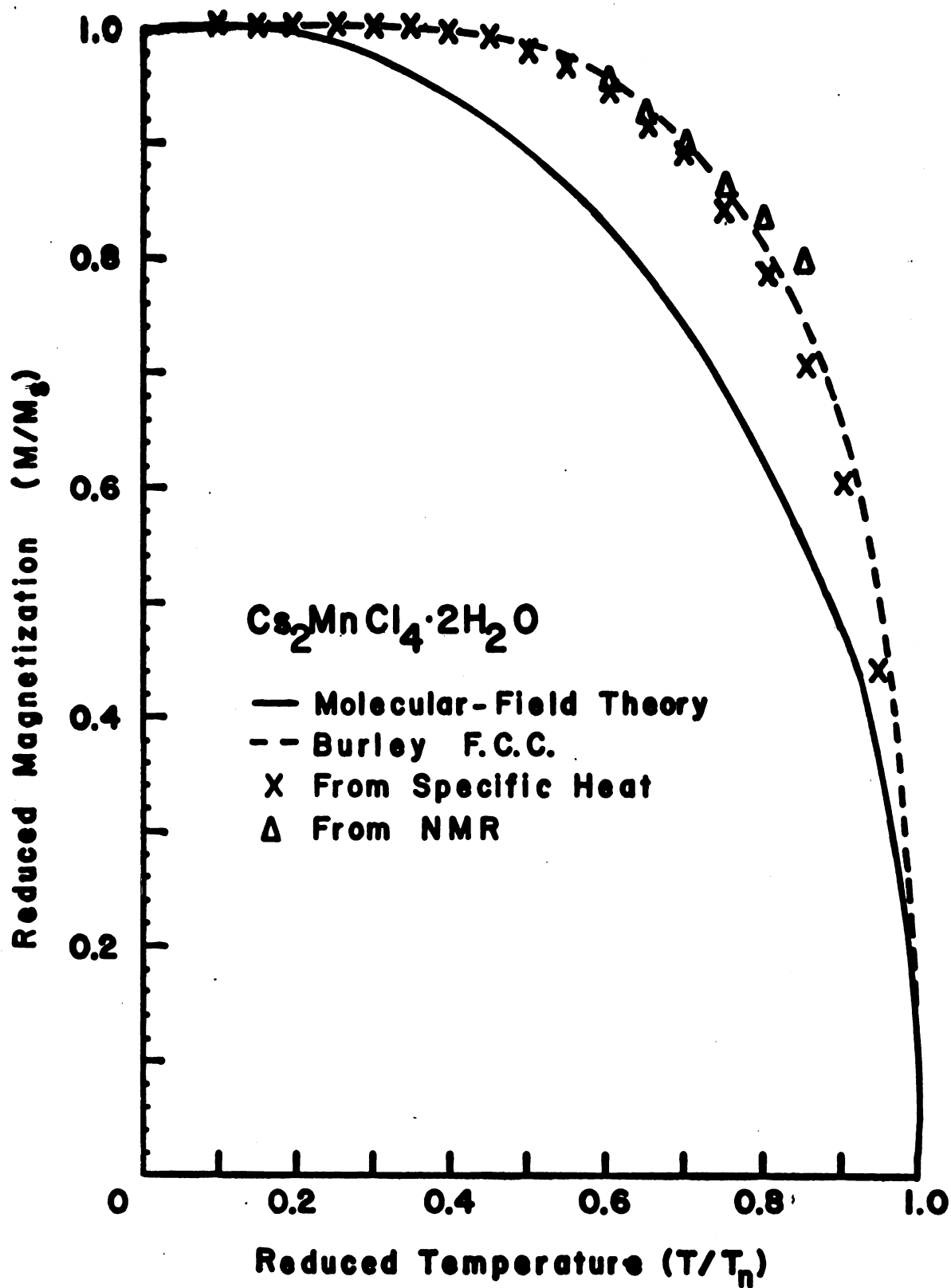


Fig. 15. Sublattice Magnetization Curves.

$g\beta SH_C/kT_n = 1.23$ This gives $H_C = 5500$ gauss. Since fields of almost 10,000 gauss are available, the specific heat measured in a magnetic field should show an observable difference from the similar study in a zero field.

The specific heat of sample 1 has been measured in several applied magnetic fields for each of three different orientations of the crystal. Two separate runs were made for each field and orientation. The three orientations are A, B, and C in the directions $(0 \bar{1} \bar{1})$, $(1 \bar{1} \bar{1})$, and $(\bar{1} \bar{1} \bar{1})$ respectively, as shown in Figure 13. Figure 16, 17, and 18 show the results of the specific heat measurements for three different fields for orientation A, and Appendix II, Tables 7-12 list the results. Figure 19 and 20 show the results for orientation B and two applied fields, and Appendix II, Tables 13-16 list the results. Figures 21, 22, 23, 24, and 25 show the specific heat results for orientation C for five applied fields, and Appendix II, Tables 17-26 list the experimental values.

It should be noted that the transition temperature decreases with increasing magnetic field for all three orientations, and that the lowest transition temperature occurred for orientations C in an applied field of 9830 gauss. This phenomenon is predicted from the theory and will be discussed in Section D. (Phase Diagram). Qualitatively, one can also see that, in general, the specific heat peaks become sharper as the field is increased and this is reflected in the entropy curves.

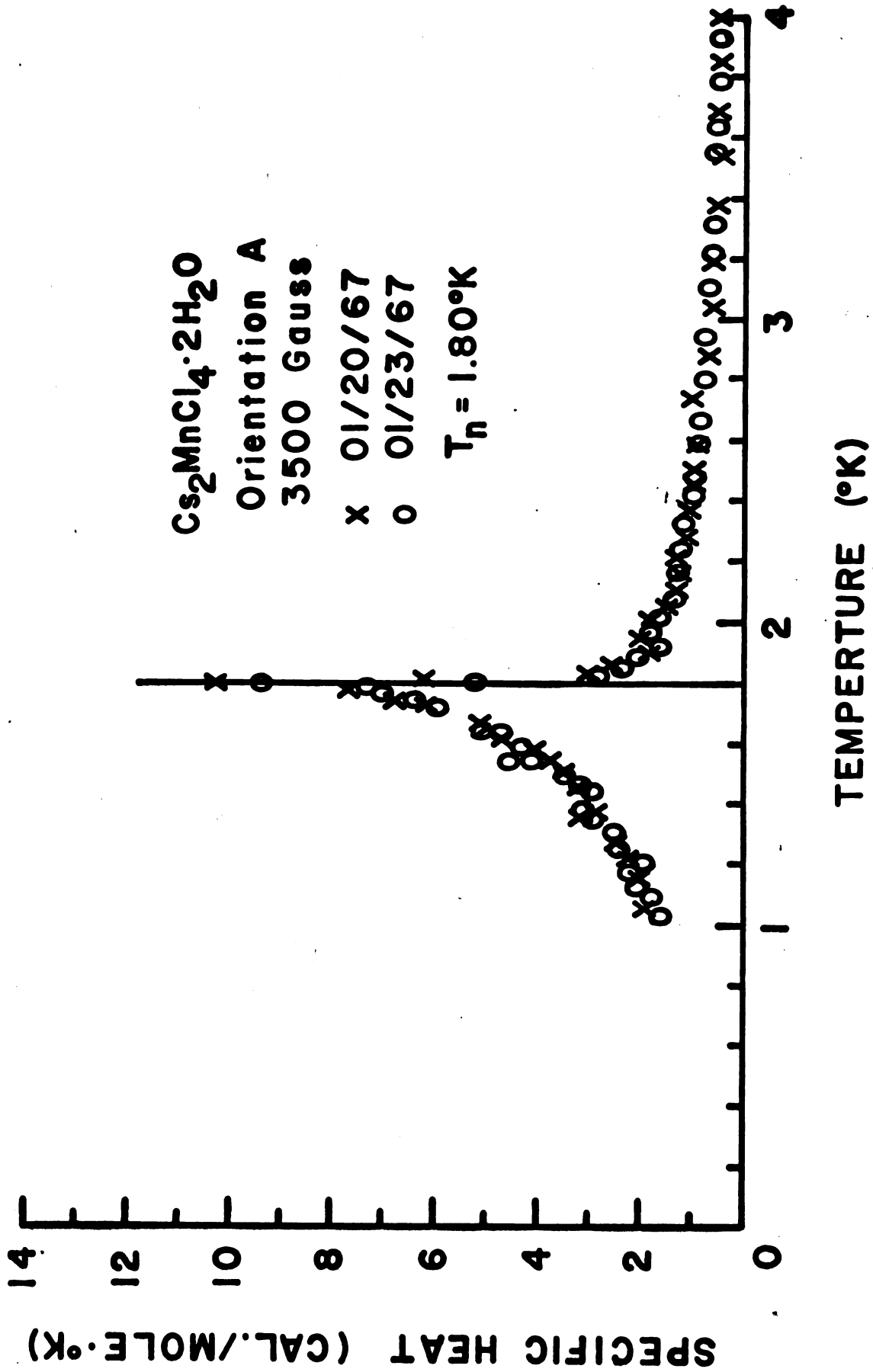


Fig. 16. Specific Heat Curve for Orientation A and 3500 Gauss.

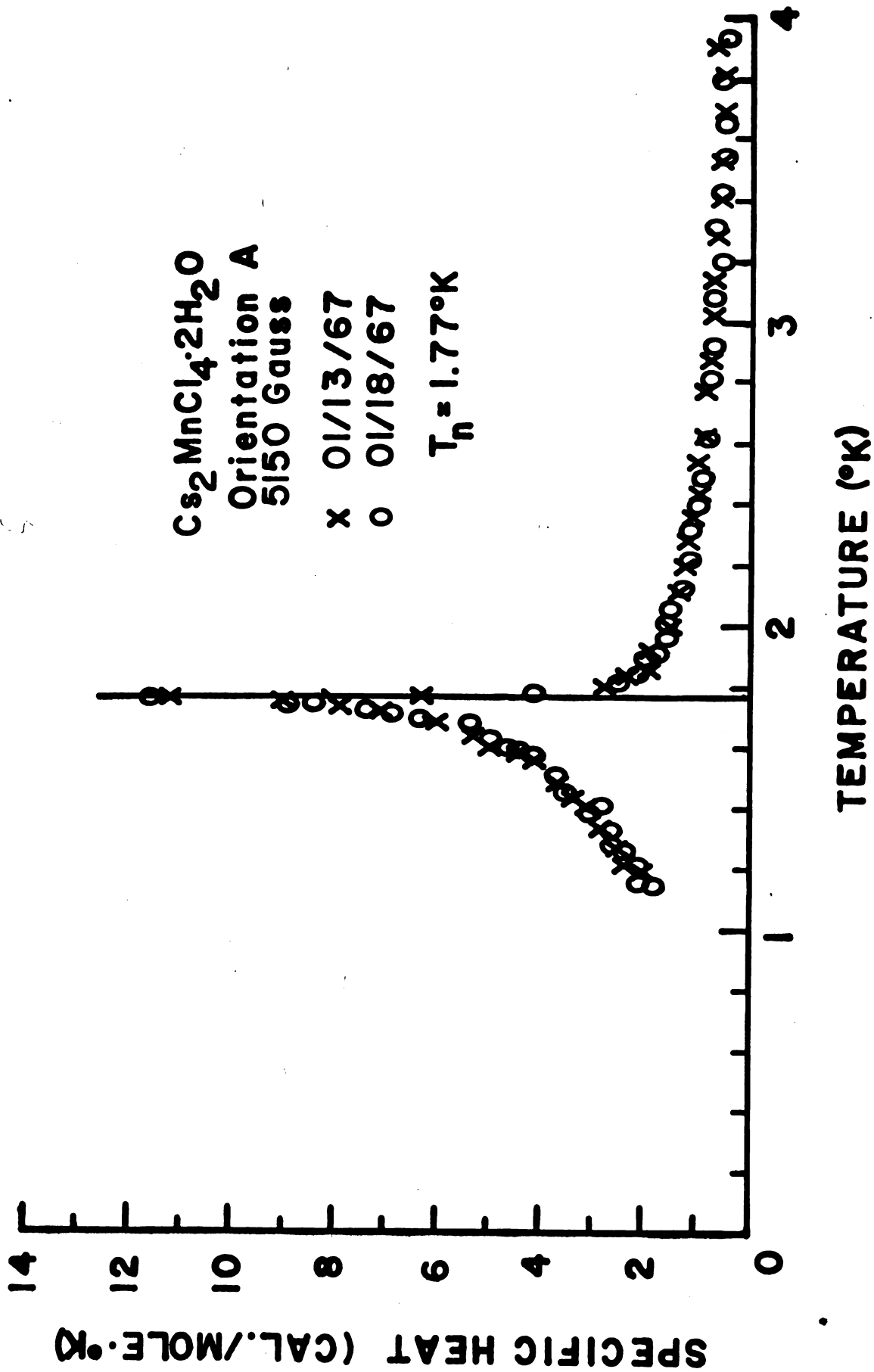


Fig. 17. Specific Heat Curve for Orientation A and 5150 Gauss.

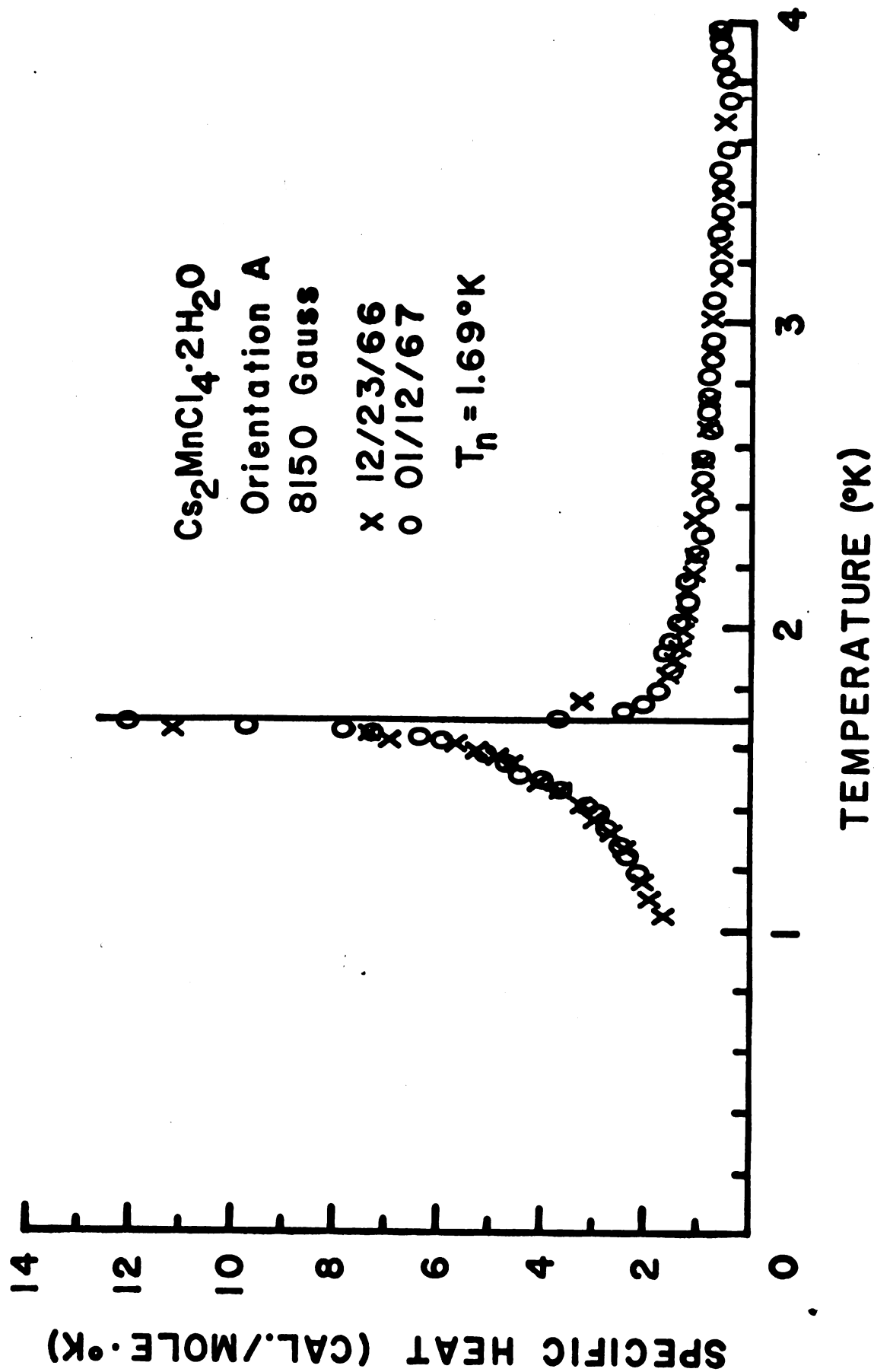


Fig. 18. Specific Heat Curve for Orientation A and 8150 Gauss.

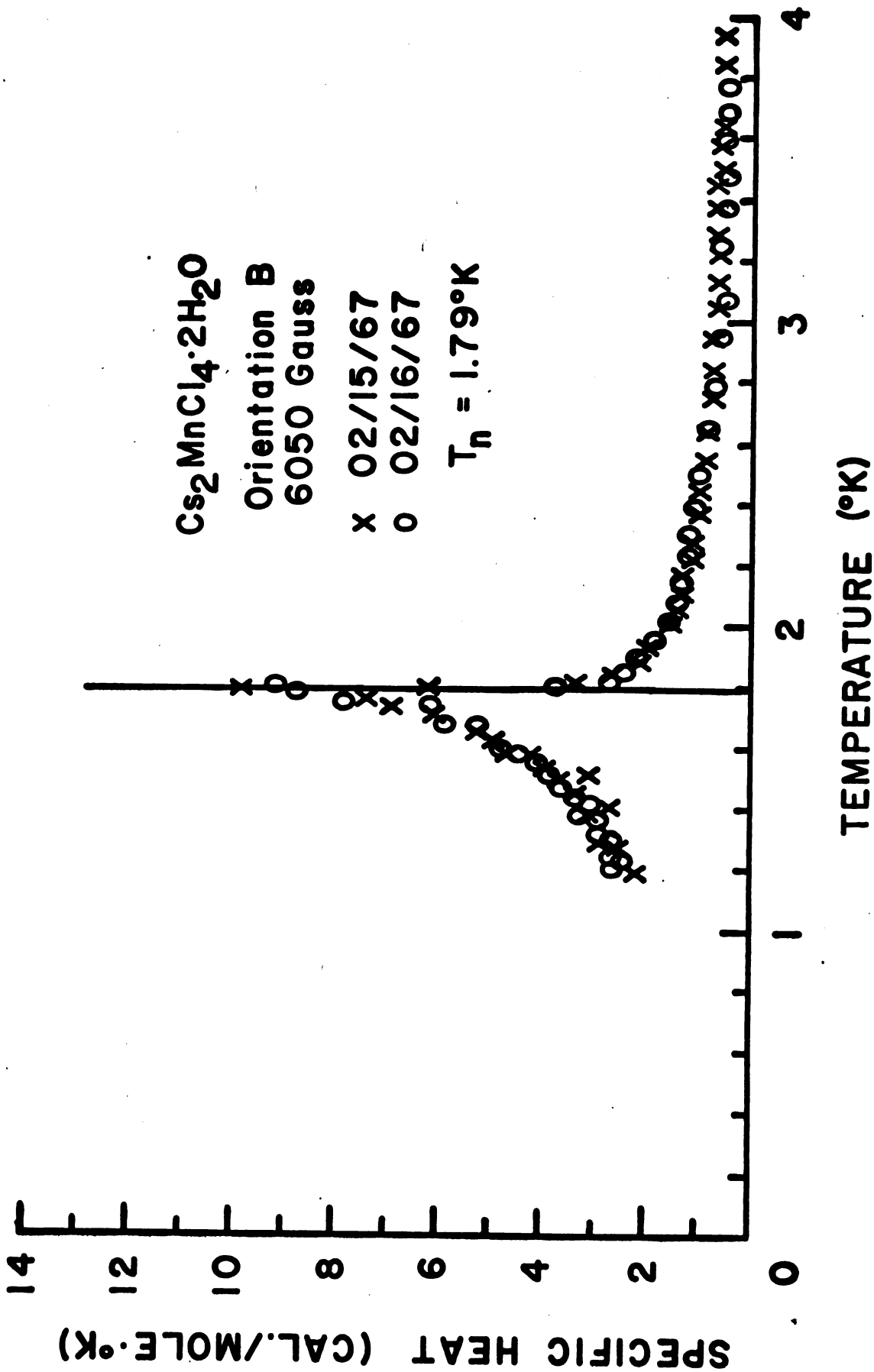


Fig. 19. Specific Heat Curve for Orientation B and 6050 Gauss.

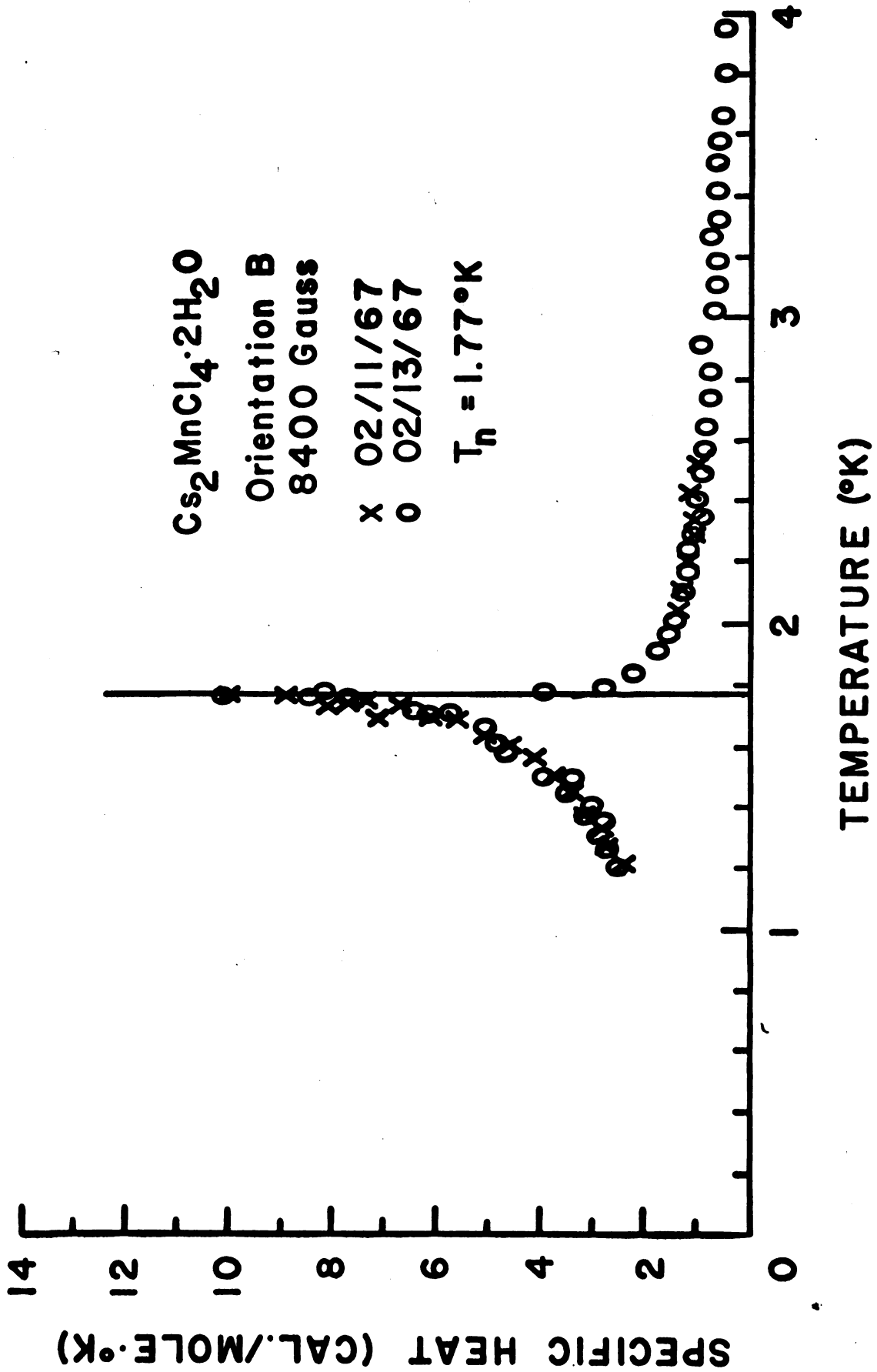


Fig. 20. Specific Heat Curve for Orientation B and 8400 Gauss.

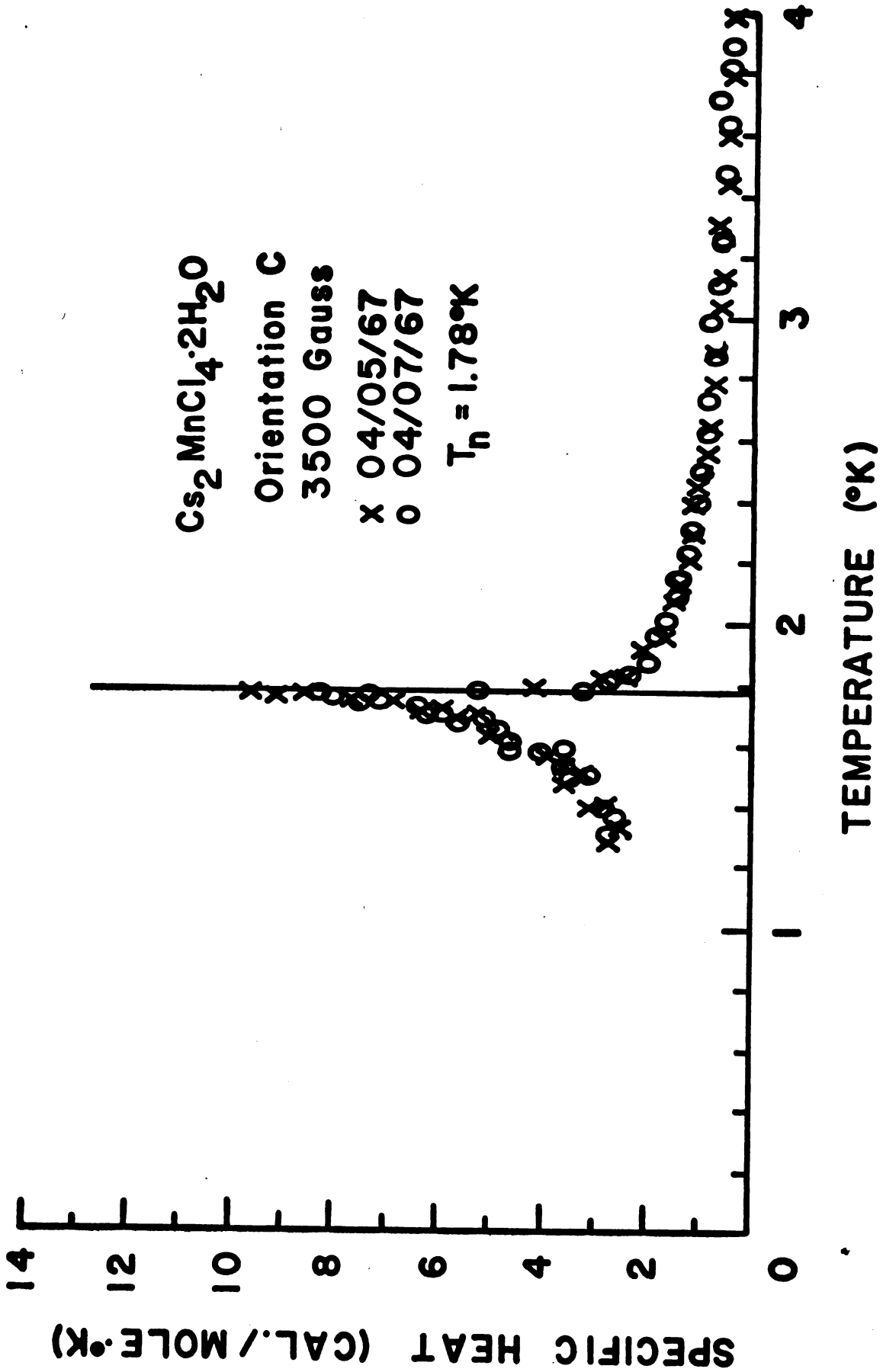


Fig. 21. Specific Heat Curve for Orientation C and 3500 Gauss.

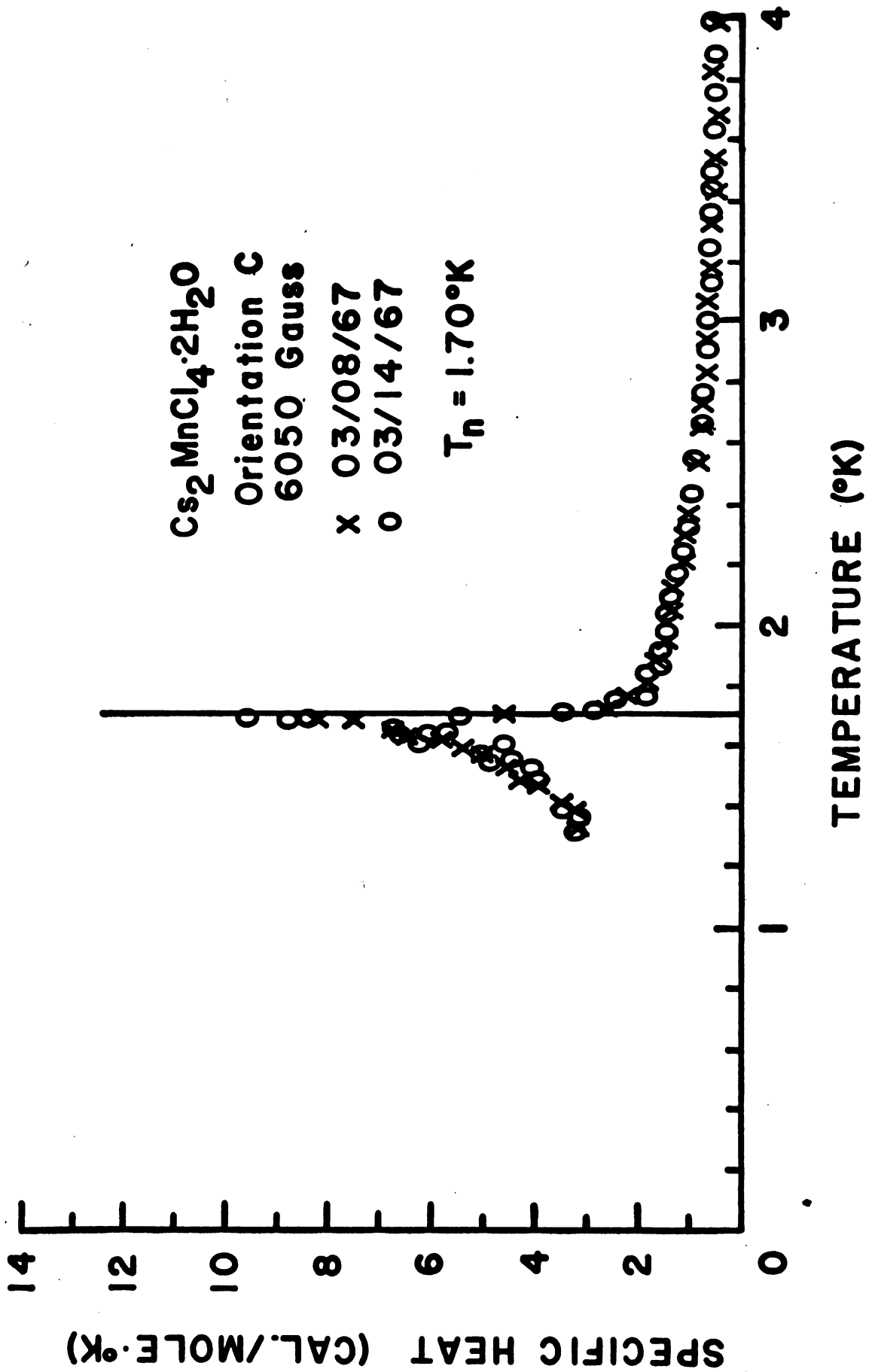


Fig. 22, Specific Heat Curve for Orientation C and 6050 Gauss.

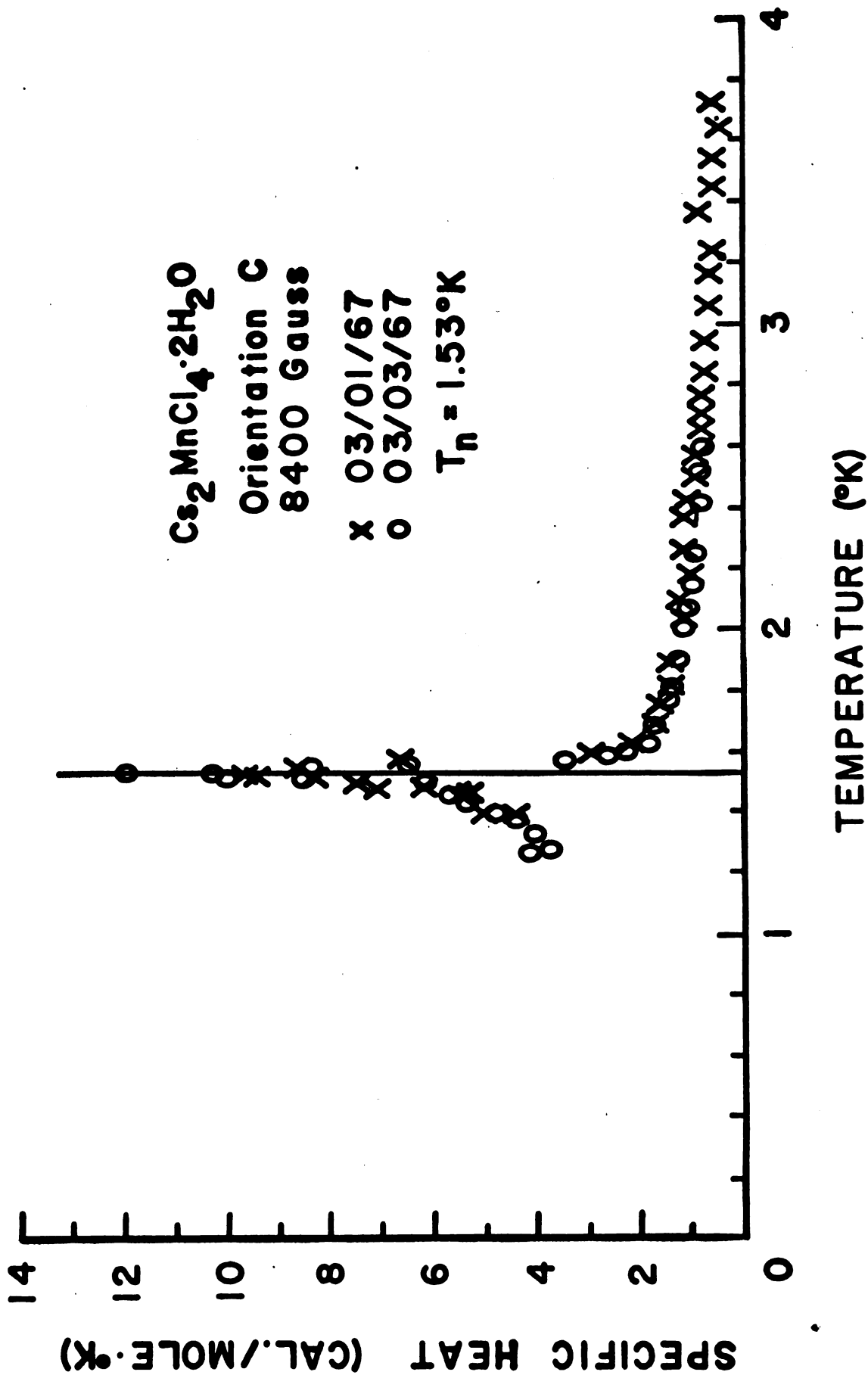


Fig. 23. Specific Heat Curve for Orientation C and 8400 Gauss.

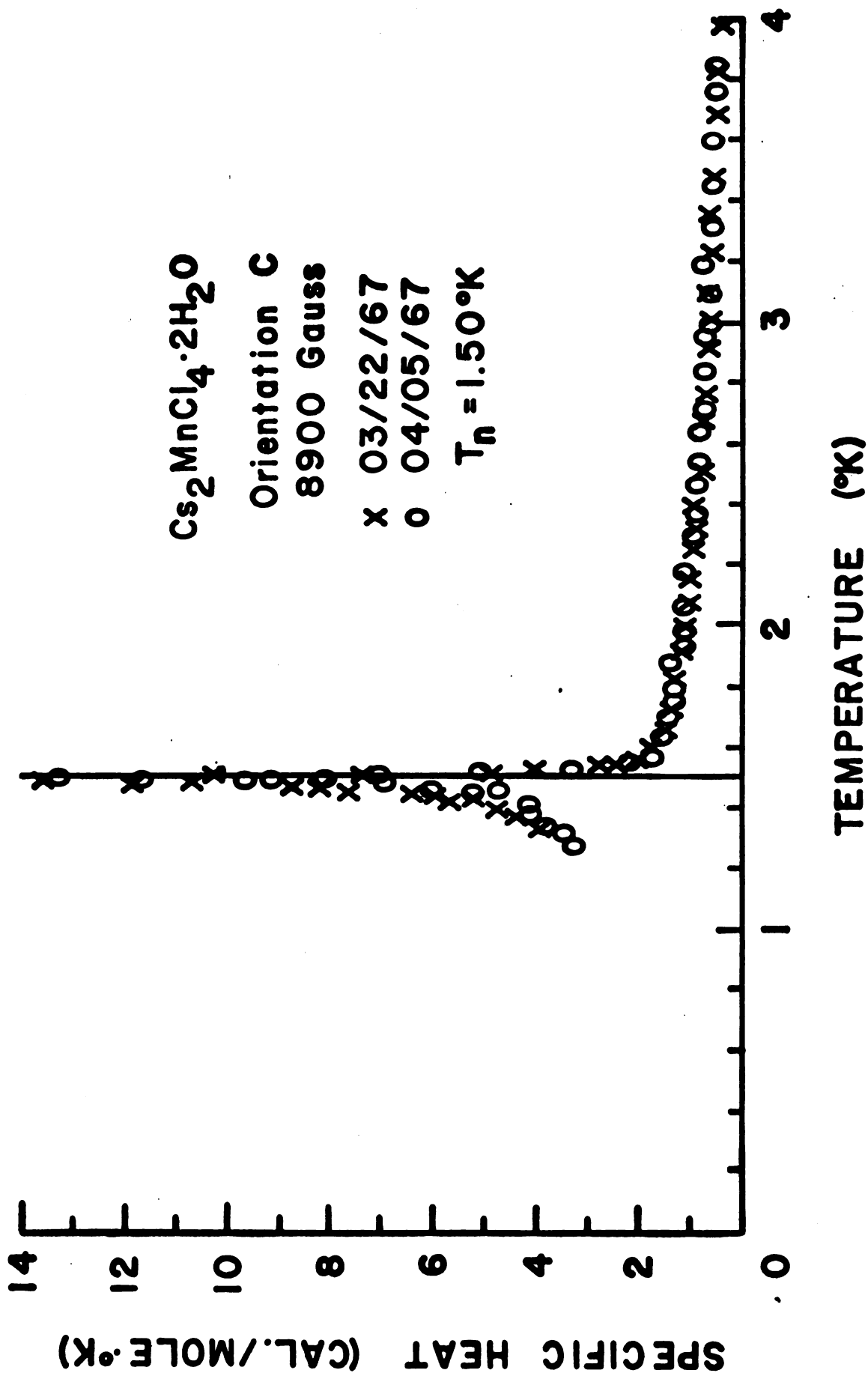


Fig. 24. Specific Heat Curve for Orientation C and 8900 Gauss.

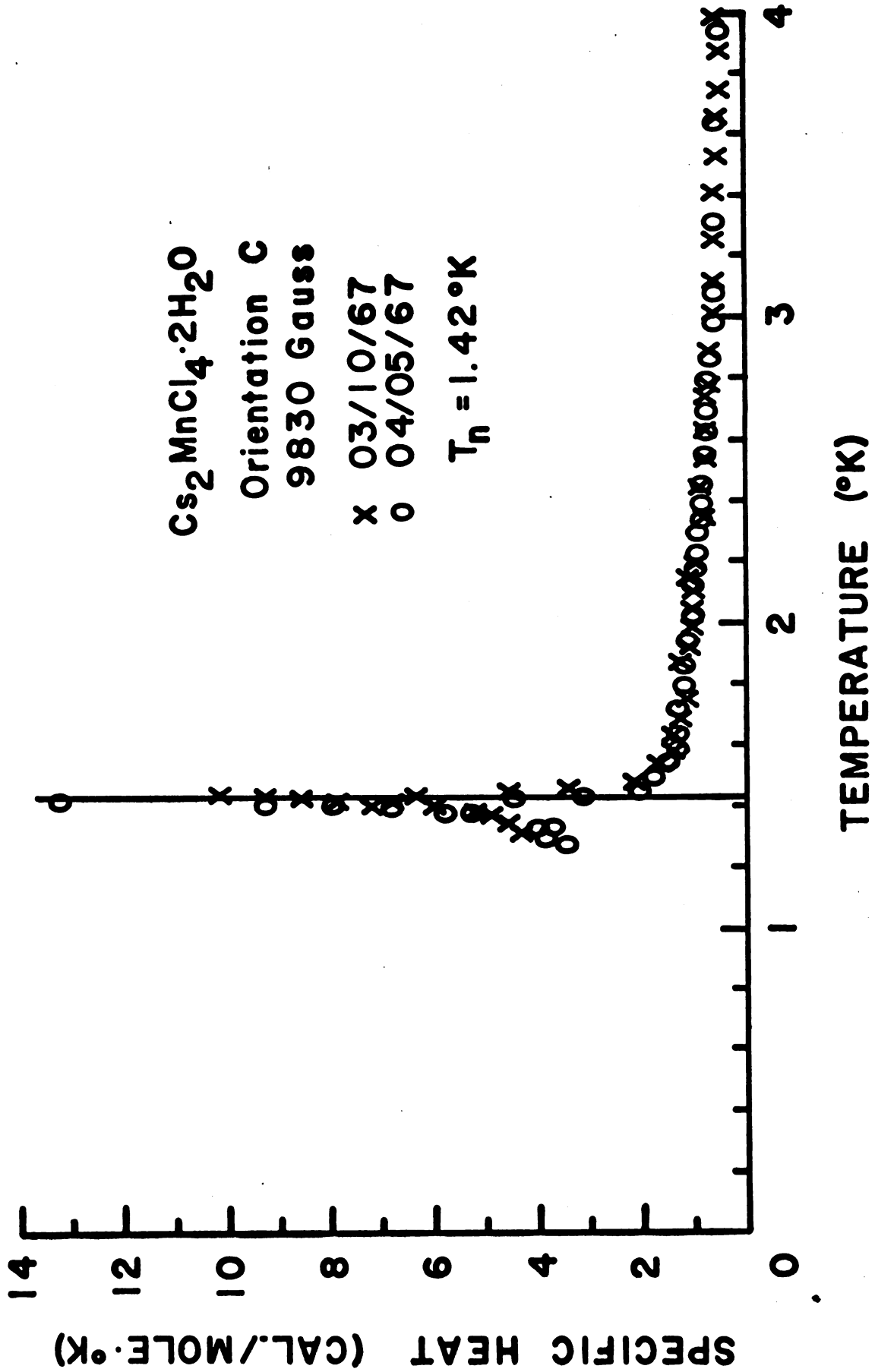


Fig. 25. Specific Heat Curve for Orientation C and 9830 Gauss.

Figures 26, 27, and 28 show the entropy as calculated from the specific heats. The curves in Figure 26 and 27 are normalized by extrapolating the C_m/T curves to 0°K . The curves in Figure 28 are normalized to the zero field entropy curve by an adiabatic magnetization experiment. This experiment was performed in the following way. The sample was thermally isolated and the temperatures were measured as the field was increased to a maximum and then decreased to zero. Table 27 in Appendix II list these temperatures. The entropy remains constant and its value for each magnetization is found from the zero field entropy curve. The points shown in Figure 28 are the results of this experiment.

Figures 29, 30, and 31 are three-dimensional plots of entropy, magnetic field, and temperature. These results indicate that at low temperatures, adiabatic magnetization may produce cooling by as much as 0.3°K , when the field is increased from zero to 8900 gauss.

D. Phase Diagram

Figure 32 is a plot of the applied magnetic field against the transition temperature, called the H-T phase diagram. All points to the right and above the curves are in the paramagnetic state and all points to the left and below the curves are in the antiferromagnetic state. The smooth curves were plotted assuming the points of each orientation follow the H^2 dependence as given by equation (101). Orientation C is the direction closest to the easy

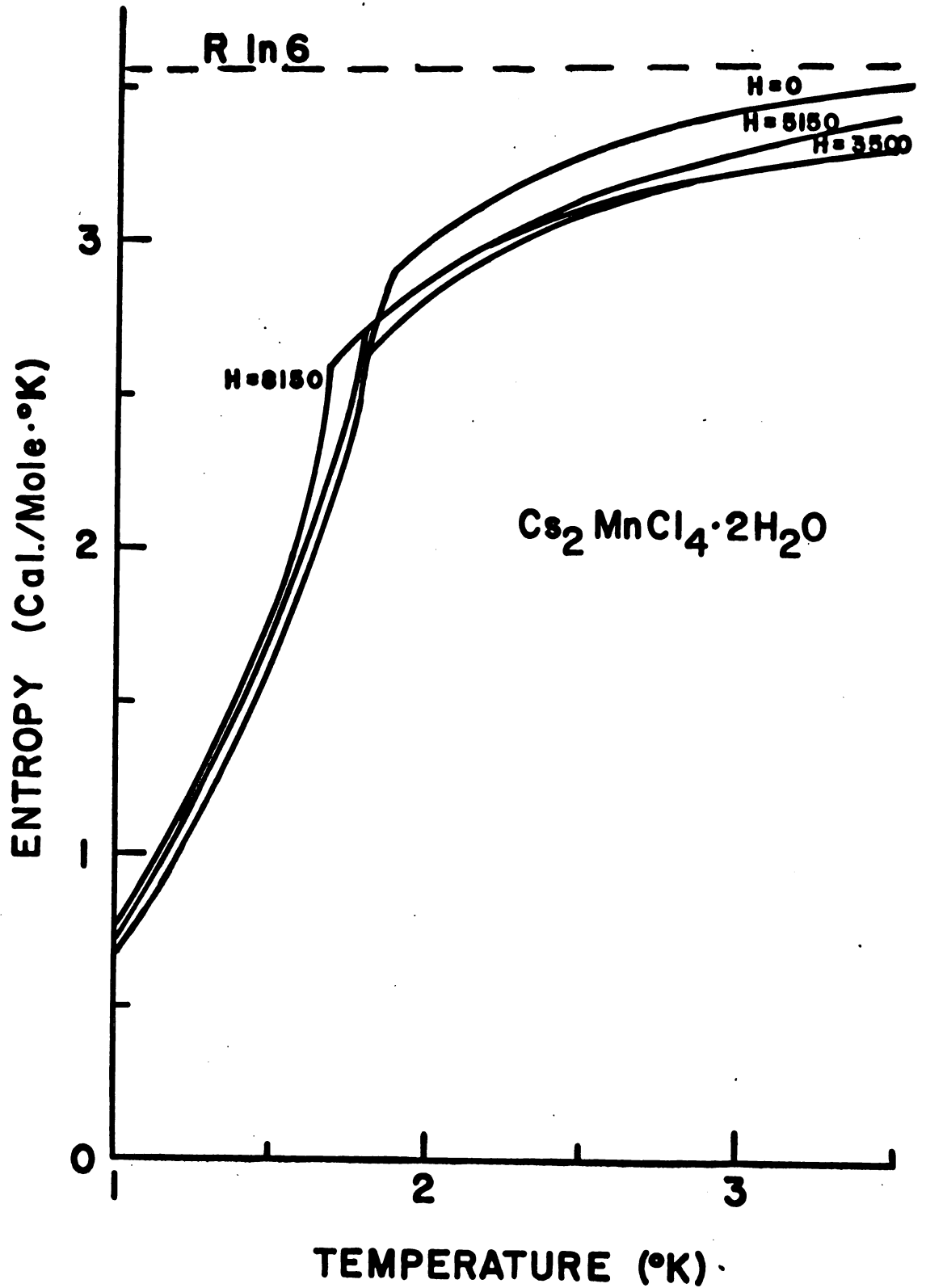


Fig. 26. Entropy Curves for Orientation A.

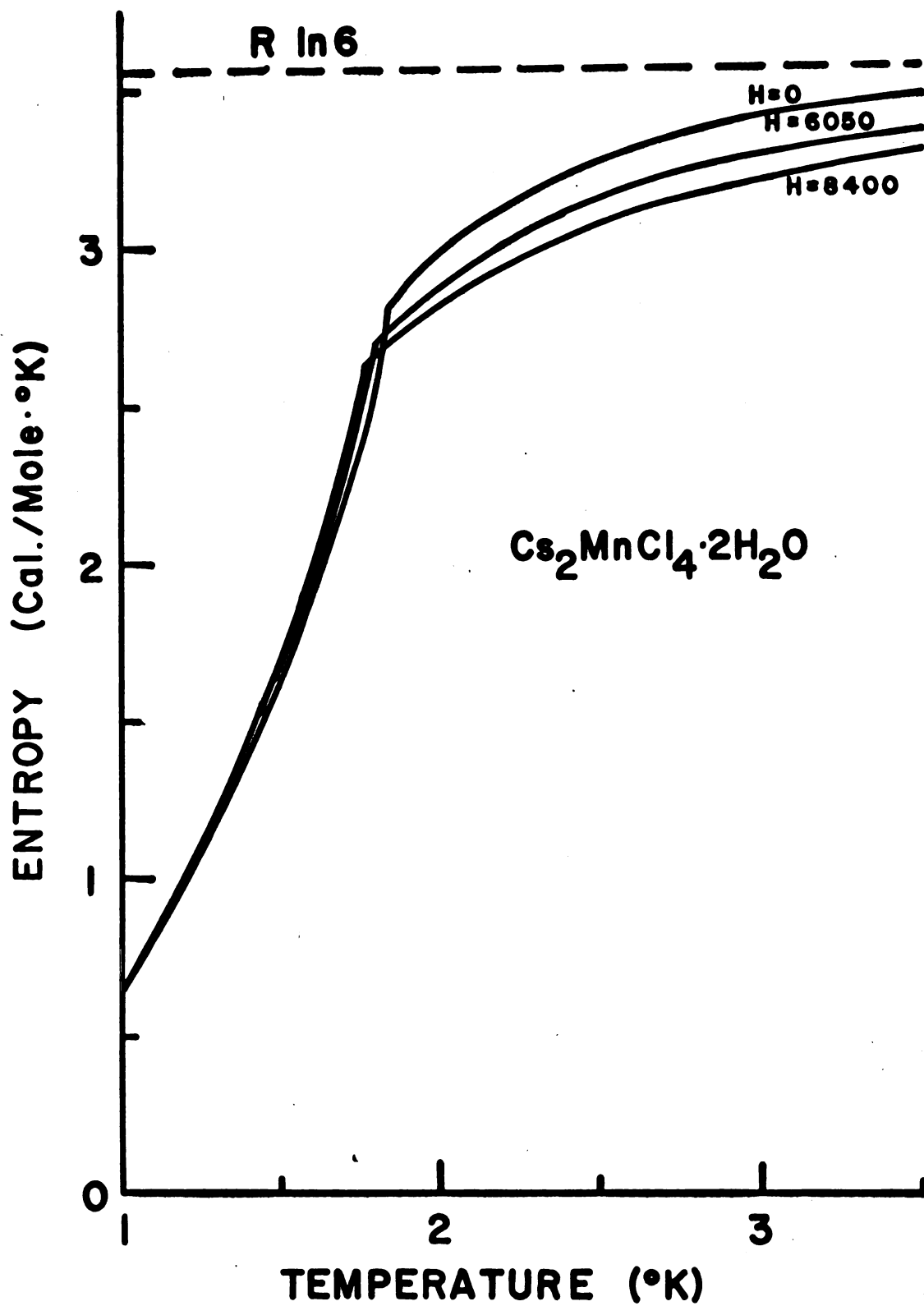


Fig. 27. Entropy Curves for Orientation B.

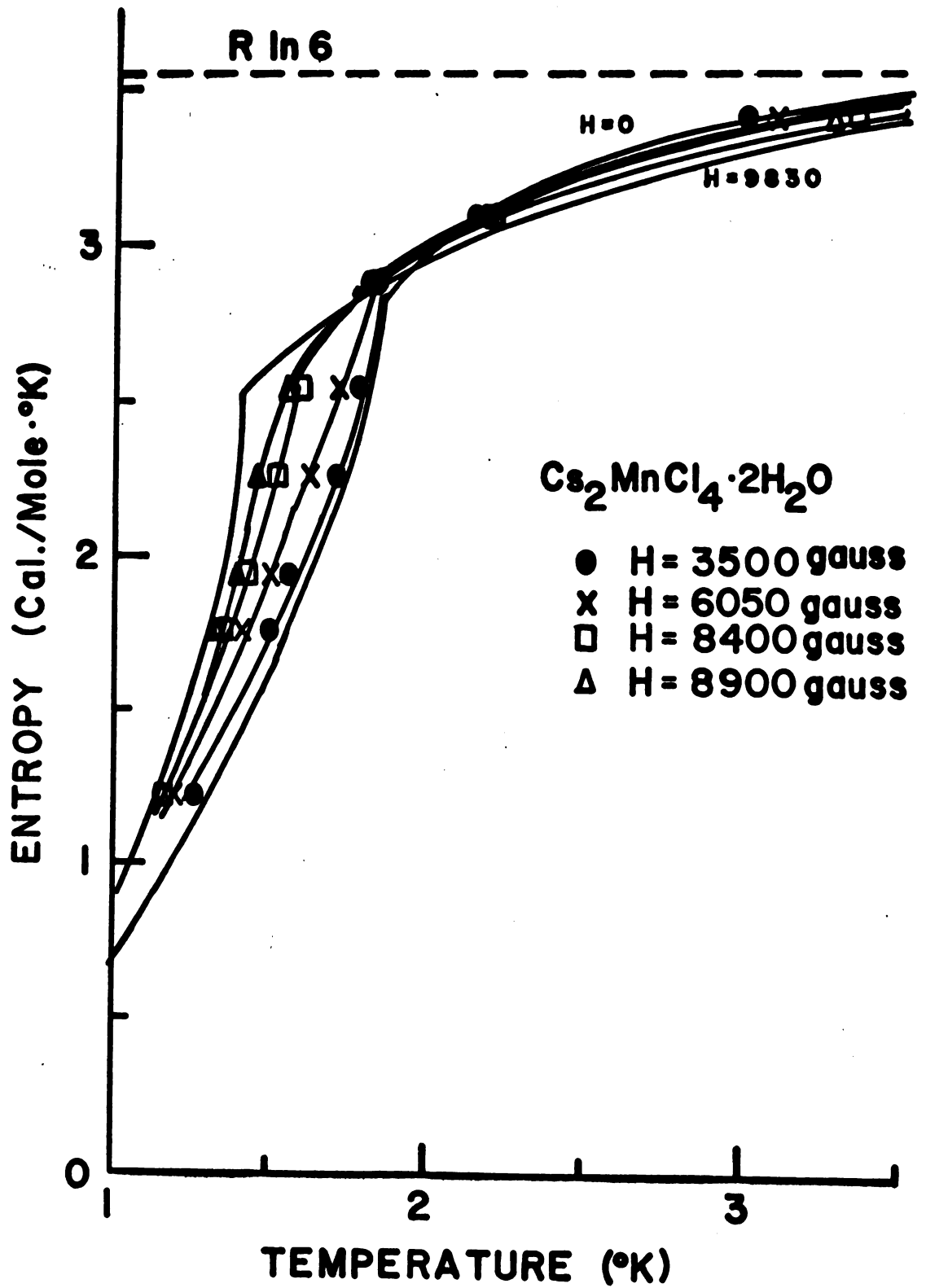


Fig. 28. Entropy Curves for Orientation C.

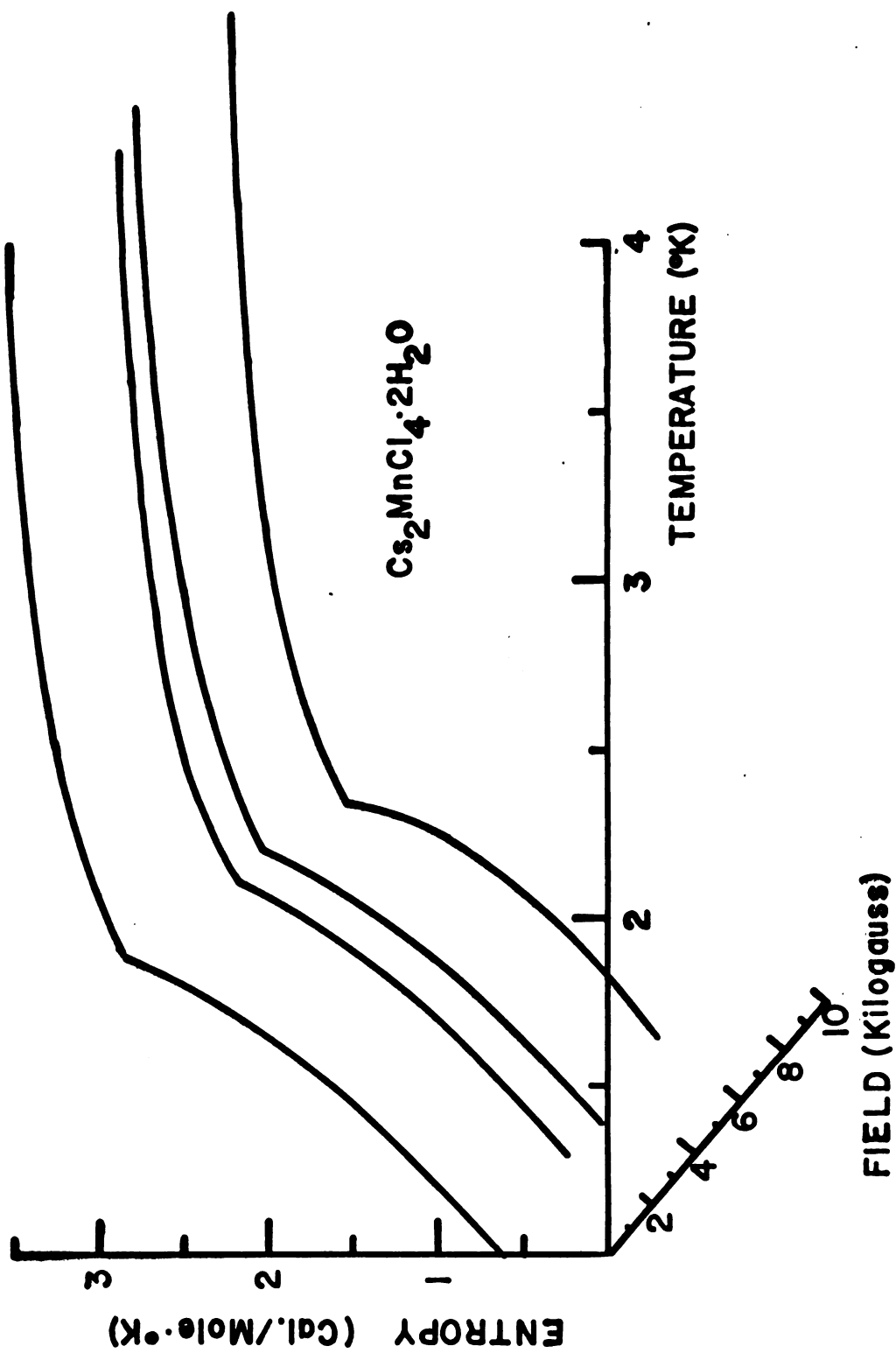


Fig. 29. Entropy, Field, and Temperature Surface for Orientation A.

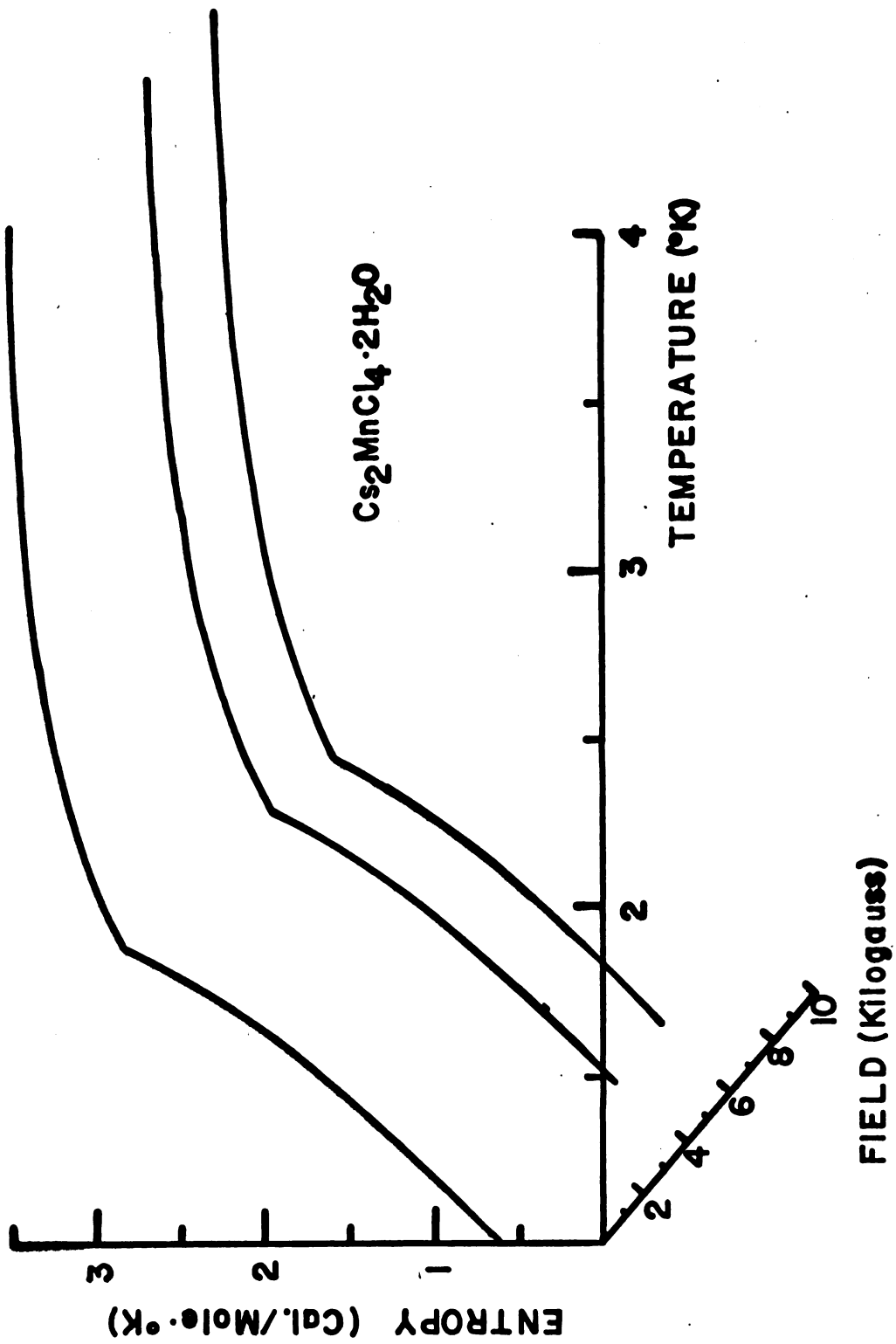


Fig. 30. Entropy, Field, and Temperature Surface for Orientation B.

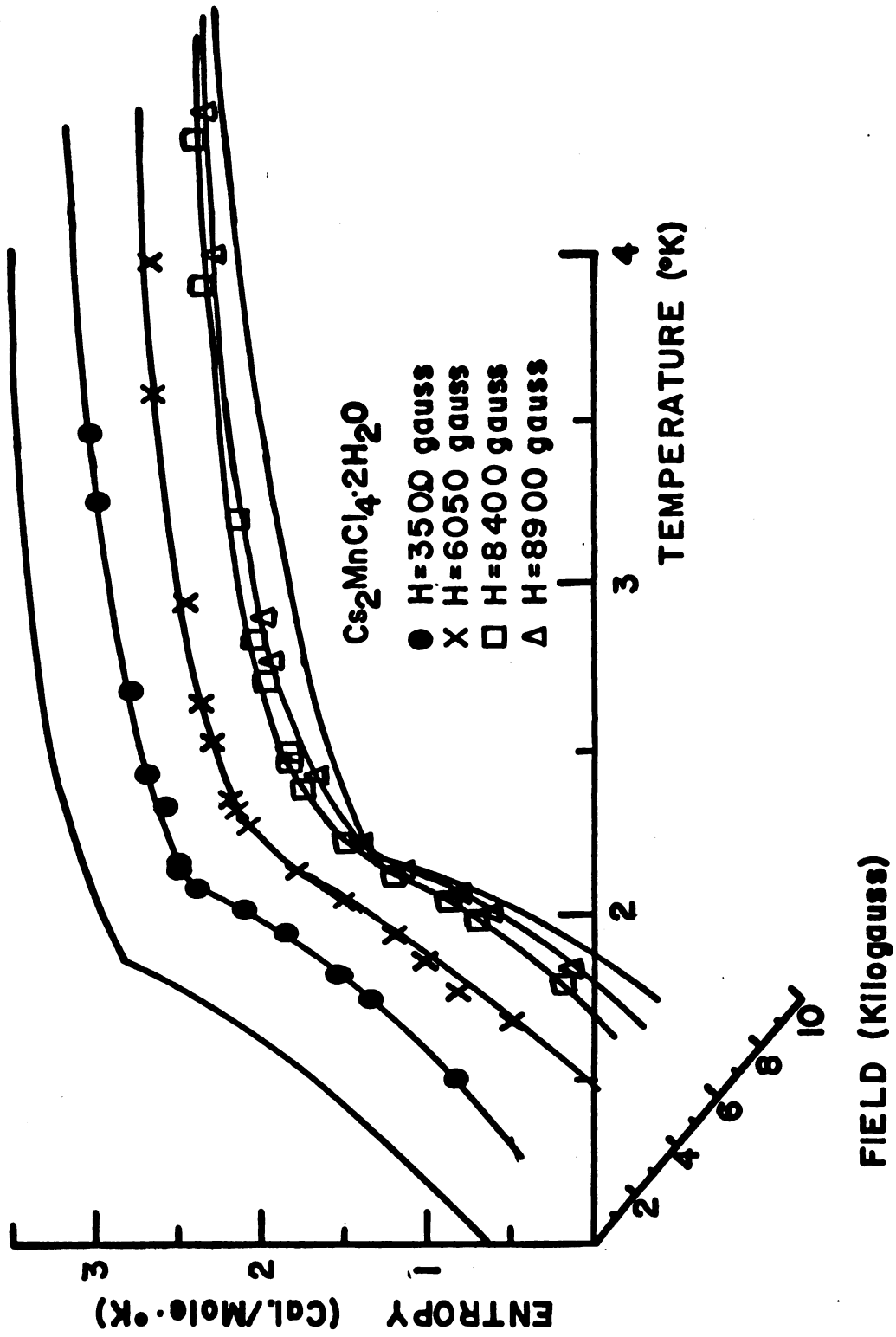


Fig. 31. Entropy, Field, Temperature Surface for Orientation C.

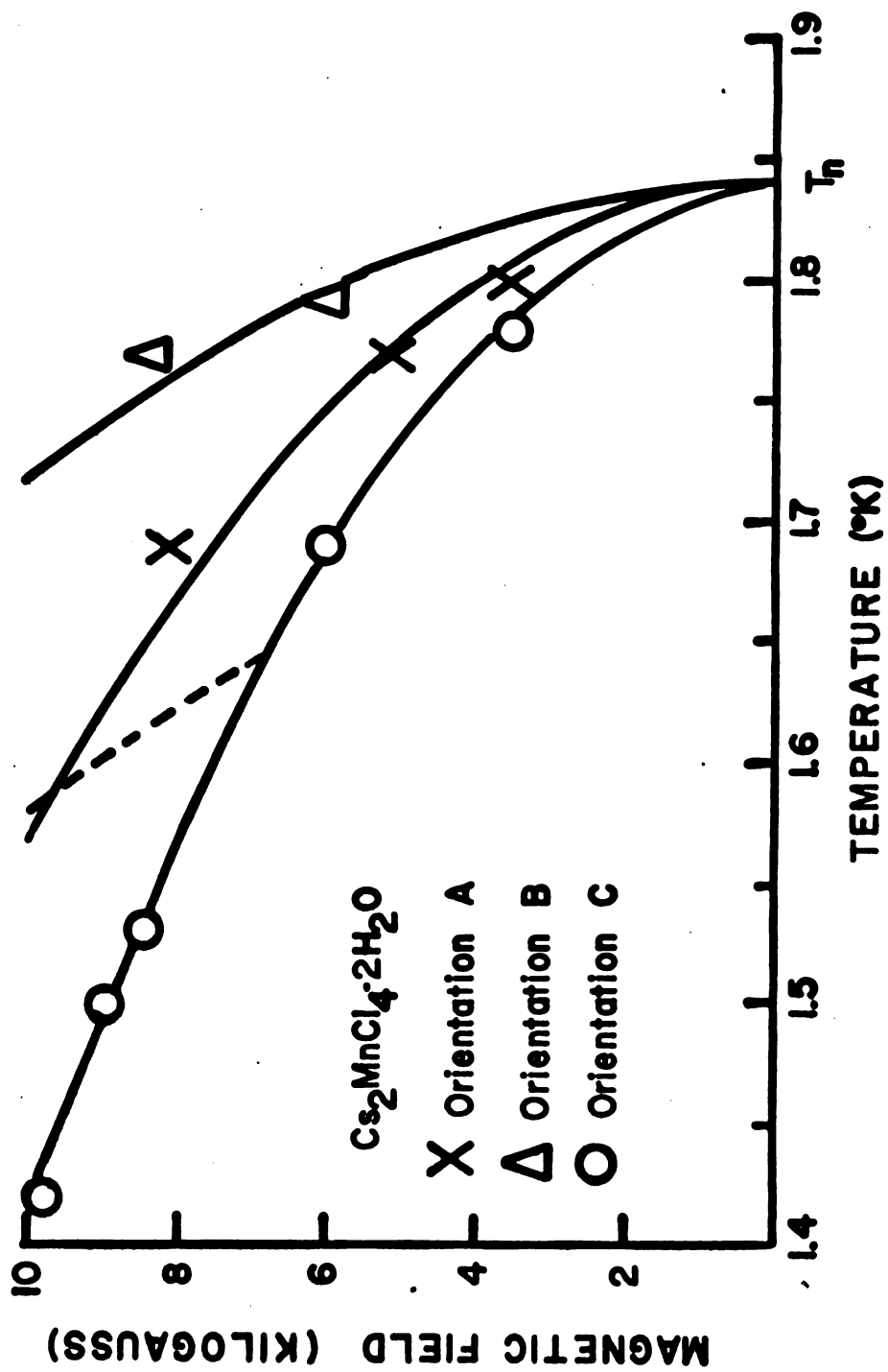


Fig. 32: Phase Diagram for Orientations A, B, and C.

direction of magnetization since it has the greatest curvature. This agrees with the nmr and susceptibility results.

Using the slope of the straight line fit to the T vs H^2 plot and $S = 5/2$, χ_{\perp} is calculated using equation (101). χ_{\perp} is found to be 0.58 cc/mole compared to the maximum of the parallel susceptibility curve which is 0.64 cc/mole. This is a reasonably good check on the reliability of equation (101).

Comparing the curvatures of the three curves on the phase diagram gives: $C/B = 3.6$, $C/A = 1.6$, and $A/B = 2.2$. The errors in these ratios may be as large as 45 percent because of the insufficient data in the A and B directions.

If spin-flop had occurred then the curvature of C would approximate that of B below the spin-flop transition temperature as indicated on Figure 32 by the dashed curve. Since this did not happen, it is believed that no spin-flop took place under the present experimental conditions. This does not preclude the possibility that such a spin-flop transition may occur at lower temperatures using higher fields. This suggestion is prompted by the fact that there may be large anisotropy in this crystal. Such anisotropy is also revealed in the magnetic susceptibility results.

E. Conclusions

In this specific heat study of single crystals of $\text{Cs}_2\text{MnCl}_4 \cdot 2\text{H}_2\text{O}$, the following conclusions may be drawn:

1. The zero-field experimental data cannot be fitted, in detail, by the molecular-field theory, although the general qualitative features may be seen.

2. The specific heat curve in zero-field agrees quite well with the curve predicted by Fisher using the magnetic susceptibility results.

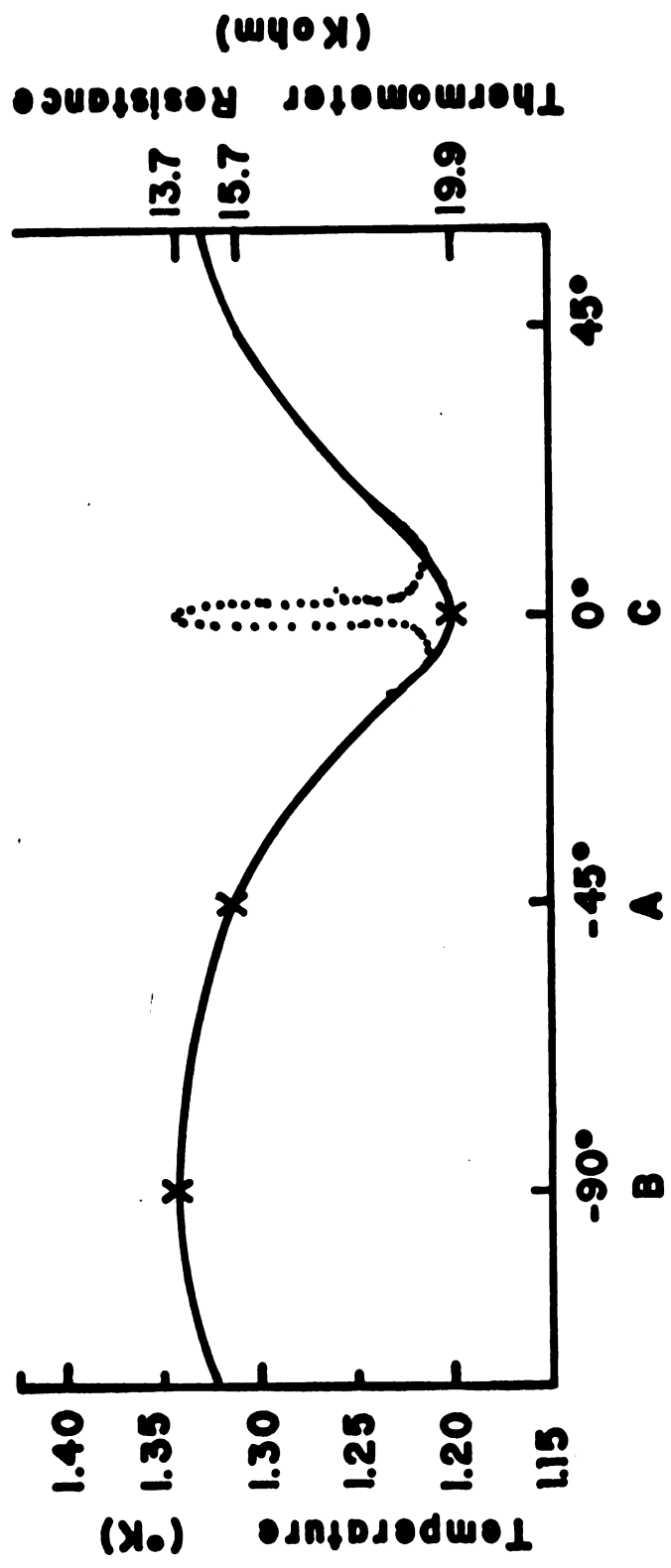
3. The non-zero-field results are in agreement with the modified form of the molecular-field theory. It was possible to predict $T_n(H)$ as a function of H , as well as verifying the value of χ_{\perp} .

4. The entropy curves predict the possibility of cooling by adiabatic magnetization in the low temperature region.

5. A spin-flop transition was not observed.

In connection with the failure to observe a spin-flop transition, several additional comments may be added. Since large anisotropy is indicated, higher-field measurements at lower temperatures are necessary before any definite statement can be made concerning the existence of a spin-flop transition in $\text{Cs}_2\text{MnCl}_4 \cdot 2\text{H}_2\text{O}$. Furthermore, it has been observed in $\text{CuCl}_2 \cdot 2\text{H}_2\text{O}$ ³⁴ that a misalignment of the applied field from the axis of easy magnetization by as little as 5° could explain the non-observation of the spin-flop transition. This is on the very edge of the uncertainty in the alignment in the present experiment. A possible method for improved alignment is suggested in Figure 33.

Figure 33 is a plot of the temperature change caused by rotating the magnet, at a constant field, under adiabatic conditions. The three points are from the approximate 8000 gauss entropy curves (for entropy = 1.35 cal./mole \cdot °K) of



Angles Measured from Direction of Easy Magnetization.

Fig. 33. Temperature vs. Angle from Easy Direction for a Adiabatic Rotation of a Constant External Magnetic Field of 8000 Gauss

the three different orientations. The curve is drawn assuming 2-fold symmetry, although the present crystal has only an inversion axis and the angles between A, B, and C are approximate. This method, however, will still be useful. On the right of Figure 33 are the resistances of the thermometer for the three plotted points. Therefore enough sensitivity exists so that by simply rotating the magnet and watching the thermometer, the crystal can be aligned so that the external field will be parallel to the direction of magnetization. This is achieved when maximum resistance is attained on the thermometer.

Neutron-diffraction studies would also be useful to help confirm the axis of easy magnetization.

Referring again to Figure 33, if a spin-flop transition did occur for a field of 8000 gauss at orientation C the spins would now be ordered in the same configuration as they would be in orientation B. It would appear that the temperatures for these two configurations should be identical for the same entropy value. Then if the crystal is adiabatically rotated in constant magnetic field from orientation B to orientation C, the temperatures would change as shown in Figure 33 until within approximately 5° of orientation C. Since spin-flop can only occur within approximately 5° of the easy direction, the temperature in Figure 33 will rise from about 1.20° to 1.34°K , the value of the temperature for orientation B. This is indicated by the dashed curve in Figure 33, and may be another method for detecting

the spin-flop transition. Justification for this technique would be evident from the fact that the three-dimensional S-H-T curves would show a depression in their surface.

In the above discussion it has been tacitly assumed that the shape of the crystal does not affect the results. To test the affect of the shape of the sample it would be necessary to grow larger crystals and grind them into spheres, etc. and repeat the experiment. In this way it may be possible to determine whether the field is uniform over the entire length of the crystal.

The effect of the external magnetic field on the nuclear-spin specific heat has, of course, been neglected, just as it was for the zero-field measurements. Such effects will not appear much before very low temperatures, and in external fields, probably greater than 50,000 gauss, since it would involve the further splitting of the nuclear-spin levels.

REFERENCES

1. R. D. Spence (Private communication)
2. J. A. Cowen (Private communication)
3. W. P. Allis and M. A. Herlin, Thermodynamics and Statistical Mechanics, McGraw-Hill, New York (1952).
4. F. W. Sears, Thermodynamics, the Kinetic Theory of Gases, and Statistical Mechanics, Addison-Wesley, Reading, Mass. (1953)
5. C. Kittel, Elementary Statistical Physics, John Wiley & Sons, New York (1958)
6. C. Kittel, Introduction to Solid State Physics, John Wiley & Sons, New York (1956)
7. W. Heisenberg, Z. Physik 49, 619 (1928)
8. E. Merzbacher, Quantum Mechanics, John Wiley & Sons, New York (1963)
9. L. Néel, Ann. Phys. (Paris) 5, 232 (1936)
10. J. H. Van Vleck, J. Chem. Phys. 9, 85 (1941)
11. A. B. Lidiard, Rept. Prog. Phys. 25, 441 (1962)
12. T. Nagamiya, K. Yosida, and R. Kubo, Advan. Phys. 4, 1 (1955)
13. P. R. Weiss, Phys. Rev. 74, 1493 (1948)
14. Y. Li, Phys. Rev. 84, 721 (1951)
15. T. Oguchi and Y. Ubata, Prog. Theoretical Phys. 9, 359 (1953)
16. E. Ising, Z. Physik 31, 253 (1925)
17. G. F. Newell and E. W. Montroll, Rev. Mod. Phys. 25, 353 (1953)
18. L. Onsager, Phys. Rev. 65, 117 (1944)

19. P. Weiss, *J. Phys.* 6, 667 (1907)
20. A. H. Morrish, *The Physical Principles of Magnetism*, John Wiley & Sons, New York (1965)
21. M. E. Fisher, *Phil. Mag.* 7, 1731 (1962)
22. C. J. Gorter and T. van Peski-Tinbergen, *Physica* 22, 273 (1956)
23. C. G. B. Garrett, *J. Chem. Phys.* 19, 1154 (1951)
24. J. A. Sauer and H. N. V. Temperley, *Proc. Roy. Soc. (London)* 176A, 203 (1940)
25. F. B. Anderson and H. B. Callen, *Phys. Rev.* 136, A1068 (1964)
26. I. S. Jacobs, *Bull. Am. Phys. Soc.* 12, 285 (1967)
27. N. J. Poulis, J. van den Handel, J. Ubbink, J. A. Poulis, and C. J. Gorter, *Phys. Rev.* 82, 552 (1951)
28. W. R. Roach and J. C. Wheatley, *Rev. Sci. Instr.* 35, 634 (1964)
29. F. G. Brickwedde, H. van Dijk, M. Durieux, J. R. Clement, and J. K. Logan, *J. Research* 64A, 1 (1960)
30. S. J. Jensen, *Acta Chem. Scand.* 18, 2085 (1964)
31. A. E. Cooke and D. T. Edmond, *Proc. Phys. Soc. (London)* 71, 517 (1958)
32. P. Debye, *Ann. Physik* 39, 780 (1912)
33. D. M. Burley, *Phil. Mag.* 5, 909 (1960)
34. J. van den Handel, H. M. Gijnsman, and N. J. Poulis, *Physica* 18, 862 (1952)



APPENDIX I

Using Kirchoff's Circuit Law for the current loop I_e in Figure 34 one can write,

$$(I_e - I_p)R_p + I_e R + (I_e + I_t)R_t = 0 \quad (1)$$

where I_p is the potentiometer current, R_p is the potentiometer resistance, R_t is the thermometer resistance, I_t is the thermometer current, R is the lead resistance, and I_e is the unbalance current. When $I_e = 0$ then $I_p R_p = I_t R_t$. Thus $I_p R_p = V_o$, where V_o is the voltage read from the potentiometer. Rewriting (1) using V_o one gets,

$$(1 - I_e/I_p)V_o = I_e R + (1 + I_e/I_t)I_t R_t. \quad (2)$$

I_e has been measured and found to be proportional to the recorder-pen deflection from zero, positive when deflected to the right and negative when deflected to the left. Let D be the deflections measured in chart divisions. I_e has never exceeded 0.1 microampere in any of the experiments to date. I_p is never less than 200 microamperes, therefore, I_e/I_p is always less than 0.0005 which can be neglected compared to 1. So that (2) may be written as,

$$V_o = \alpha DR + (1 + \alpha D/I_t)I_t R \quad (3)$$

where $I_e = \alpha D$ and α is a proportionality constant depending

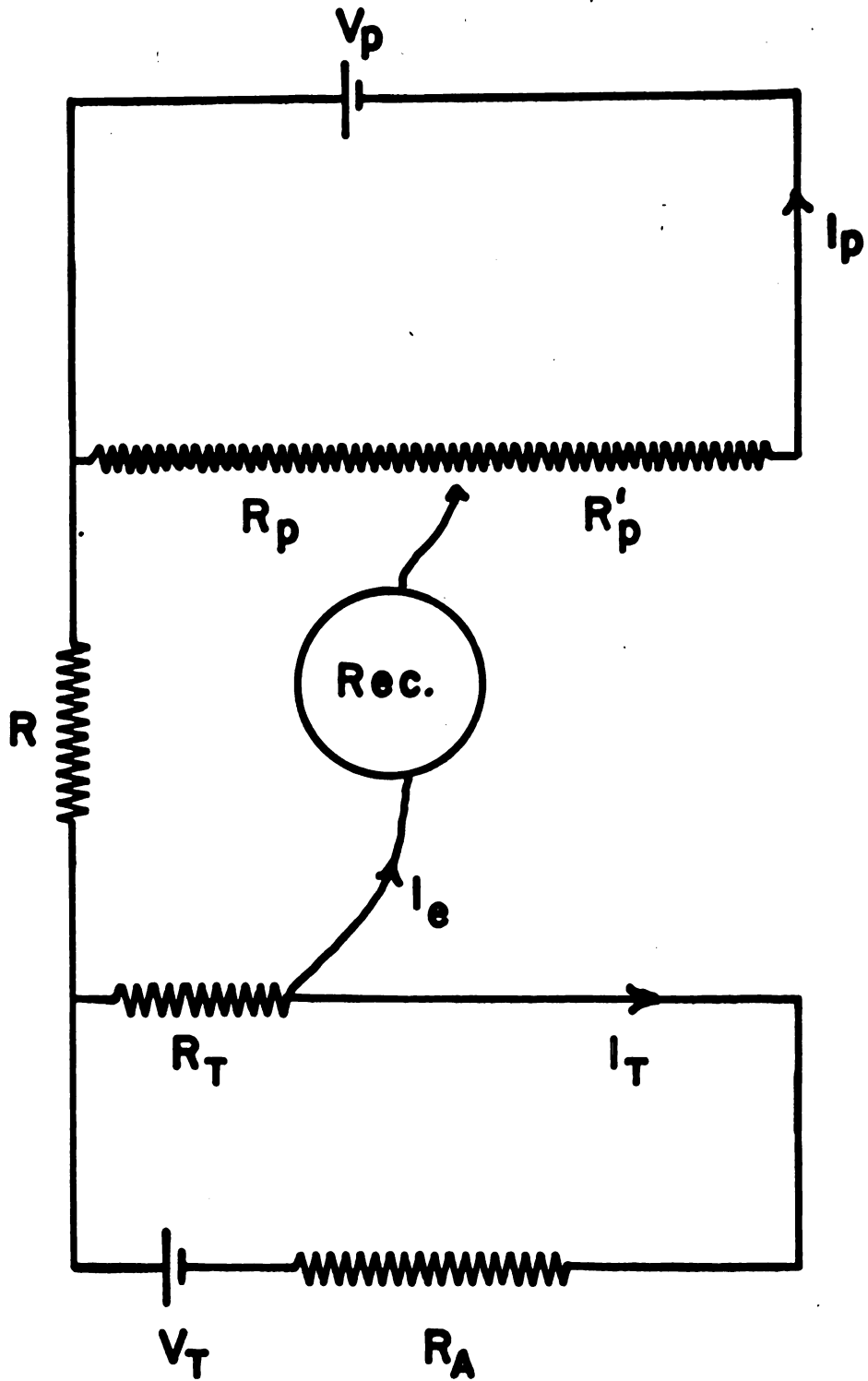


Fig. 34. Circuit Diagram for a Simple Potentiometer.

upon the range card and the D. C. amplifier scale factor. The α 's of different scales differ by an integral multiplying factor.

Since I_t is held constant, let $R_0 = V_0/I_t$ then (3) becomes,

$$R_0 = (\alpha/I_t)RD + [1 + (\alpha/I_t)D]R_t \quad (4)$$

Keeping R_t and R constant change the voltage setting on the potentiometer, and obtain,

$$R_{01} = (\alpha/I_t)RD_1 + [1 + (\alpha/I_t)D_1]R_t \quad (5)$$

$$R_{02} = (\alpha/I_t)RD_2 + [1 + (\alpha/I_t)D_2]R_t \quad (6)$$

Subtracting (6) from (5), gives,

$$R_{01} - R_{02} = (\alpha/I_t)(R + R_t)(D_1 - D_2) \quad (7)$$

or

$$\Delta R_0/\Delta D = C_1 + C_2 R_t \quad (8)$$

where $C_1 = (\alpha/I_t)R$ and $C_2 = \alpha/I_t$. Solving equation (4) for R_t gives,

$$R_t = [R_0 - (\alpha/I_t)RD]/[1 + (\alpha/I_t)D] \quad (9)$$

or finally,

$$R_t = \frac{R_0 - C_1 D}{1 + C_2 D}. \quad (10)$$

APPENDIX II

Table 3. The Specific Heat of $\text{Cs}_2\text{MnCl}_4 \cdot 2\text{H}_2\text{O}$ for Sample 1, Run 2, September 16, 1966, Zero Field.

C_m	dT	T	C_m	dT	T	C_m	dT	T
2.959	0.001	1.408	3.719	0.002	1.548	4.573	0.003	1.664
3.032	0.003	1.414	3.831	0.002	1.556	4.495	0.003	1.669
3.026	0.003	1.423	3.664	0.002	1.560	4.506	0.003	1.674
2.904	0.003	1.428	3.550	0.002	1.564	4.706	0.003	1.680
2.947	0.003	1.434	3.804	0.002	1.568	4.982	0.002	1.689
3.147	0.002	1.443	4.045	0.002	1.572	4.885	0.003	1.694
3.118	0.003	1.449	3.789	0.002	1.576	4.845	0.003	1.698
3.091	0.003	1.455	3.848	0.003	1.580	4.909	0.002	1.703
3.299	0.002	1.463	3.856	0.003	1.585	4.825	0.003	1.709
3.239	0.002	1.468	4.052	0.003	1.590	4.890	0.002	1.713
3.269	0.002	1.474	4.094	0.003	1.594	5.188	0.002	1.717
3.322	0.002	1.482	4.053	0.003	1.600	5.200	0.002	1.721
3.293	0.002	1.487	3.929	0.003	1.604	5.212	0.002	1.725
3.265	0.002	1.492	3.936	0.003	1.608	5.766	0.002	1.729
3.383	0.002	1.499	4.179	0.003	1.611	5.301	0.002	1.735
3.321	0.002	1.504	4.297	0.003	1.615	5.246	0.002	1.738
3.324	0.002	1.509	4.250	0.003	1.620	5.748	0.002	1.742
3.500	0.002	1.516	4.113	0.003	1.625	5.333	0.002	1.746
3.468	0.002	1.521	4.088	0.003	1.630	5.663	0.005	1.751
3.508	0.002	1.525	4.134	0.003	1.636	6.091	0.005	1.760
3.664	0.002	1.530	4.537	0.003	1.643	6.230	0.005	1.767
3.401	0.002	1.535	4.505	0.003	1.648	6.293	0.004	1.774
3.441	0.002	1.540	4.309	0.003	1.653	6.764	0.004	1.782
3.633	0.002	1.544	4.320	0.003	1.658	6.786	0.004	1.789

Table 3 (Continued)

C_m	dT	T	C_m	dT	T	C_m	dT	T
7.165	0.004	1.795	1.362	0.014	2.091	0.573	0.033	3.214
7.525	0.004	1.801	1.399	0.013	2.119	0.542	0.035	3.258
7.832	0.004	1.810	1.289	0.015	2.147	0.521	0.036	3.311
7.917	0.004	1.815	1.242	0.015	2.182	0.502	0.037	3.356
8.440	0.003	1.820	1.122	0.017	2.217	0.498	0.038	3.429
9.034	0.003	1.826	1.124	0.017	2.256	0.489	0.039	3.485
9.906	0.003	1.832	1.077	0.017	2.294	0.472	0.040	3.554
7.022	0.004	1.837	1.041	0.018	2.332	0.462	0.041	3.612
3.787	0.007	1.846	0.999	0.019	2.369	0.449	0.042	3.691
2.798	0.010	1.860	0.960	0.020	2.409	0.429	0.044	3.757
2.502	0.011	1.873	0.944	0.020	2.450	0.421	0.045	3.837
2.277	0.012	1.890	0.898	0.021	2.496	0.412	0.046	3.906
2.151	0.013	1.905	0.872	0.022	2.546	0.396	0.048	4.002
1.988	0.014	1.922	0.856	0.022	2.591	0.391	0.048	4.078
1.882	0.015	1.938	0.826	0.023	2.641	0.377	0.050	4.194
1.809	0.016	1.955	0.763	0.025	2.695	0.363	0.052	4.279
1.740	0.016	1.972	0.759	0.025	2.744	0.358	0.053	4.391
1.648	0.011	1.986	0.734	0.026	2.795	0.342	0.055	4.480
1.603	0.012	1.997	0.701	0.027	2.846	0.339	0.055	4.621
1.624	0.012	2.009	0.670	0.028	2.897	0.329	0.057	4.716
1.561	0.012	2.020	0.650	0.029	2.949	0.325	0.058	4.832
1.606	0.012	2.032	0.629	0.030	3.005	0.322	0.058	4.913
1.563	0.012	2.044	0.601	0.031	3.066	0.318	0.059	4.986
1.608	0.012	2.056	0.558	0.034	3.119	0.315	0.063	5.077
1.481	0.013	2.068	0.573	0.033	3.160	0.309	0.064	5.158

Table 4. The Specific Heat of $\text{Cs}_2\text{MnCl}_4 \cdot 2\text{H}_2\text{O}$ for Sample 1, Run 3, September 21, 1966, Zero Field

C_m	dT	T	C_m	dT	T	C_m	dT	T
3.019	0.004	1.365	4.348	0.004	1.594	7.128	0.004	1.794
2.774	0.003	1.381	4.492	0.004	1.600	7.462	0.004	1.802
2.953	0.003	1.399	4.454	0.004	1.610	7.613	0.004	1.808
3.089	0.004	1.411	4.535	0.004	1.616	7.948	0.004	1.814
3.093	0.004	1.423	4.048	0.005	1.623	8.060	0.004	1.819
3.252	0.004	1.438	4.998	0.004	1.630	8.594	0.003	1.826
3.414	0.004	1.452	4.932	0.004	1.636	9.289	0.003	1.832
3.390	0.004	1.459	4.951	0.004	1.646	10.010	0.003	1.838
3.501	0.004	1.468	5.028	0.004	1.652	10.410	0.003	1.843
3.473	0.004	1.475	5.063	0.006	1.663	11.057	0.003	1.849
3.597	0.003	1.484	5.217	0.005	1.673	10.347	0.003	1.853
3.621	0.003	1.491	5.292	0.005	1.684	4.981	0.006	1.860
3.594	0.003	1.501	5.442	0.005	1.693	3.399	0.008	1.872
3.655	0.003	1.506	5.569	0.005	1.704	3.036	0.006	1.883
3.724	0.003	1.515	5.857	0.005	1.712	2.598	0.007	1.896
3.766	0.003	1.521	5.811	0.005	1.724	2.478	0.008	1.906
3.820	0.003	1.529	5.916	0.005	1.731	2.313	0.008	1.920
3.911	0.003	1.535	6.080	0.005	1.742	2.198	0.009	1.931
4.015	0.005	1.544	6.166	0.005	1.749	2.058	0.009	1.947
4.062	0.005	1.551	6.216	0.005	1.758	1.976	0.010	1.962
4.165	0.005	1.561	6.382	0.004	1.765	1.899	0.010	1.974
4.123	0.005	1.568	6.718	0.004	1.772	1.864	0.010	1.992
4.252	0.004	1.578	6.834	0.004	1.781	1.788	0.011	2.005
4.325	0.004	1.585	6.736	0.004	1.787	1.703	0.011	2.023

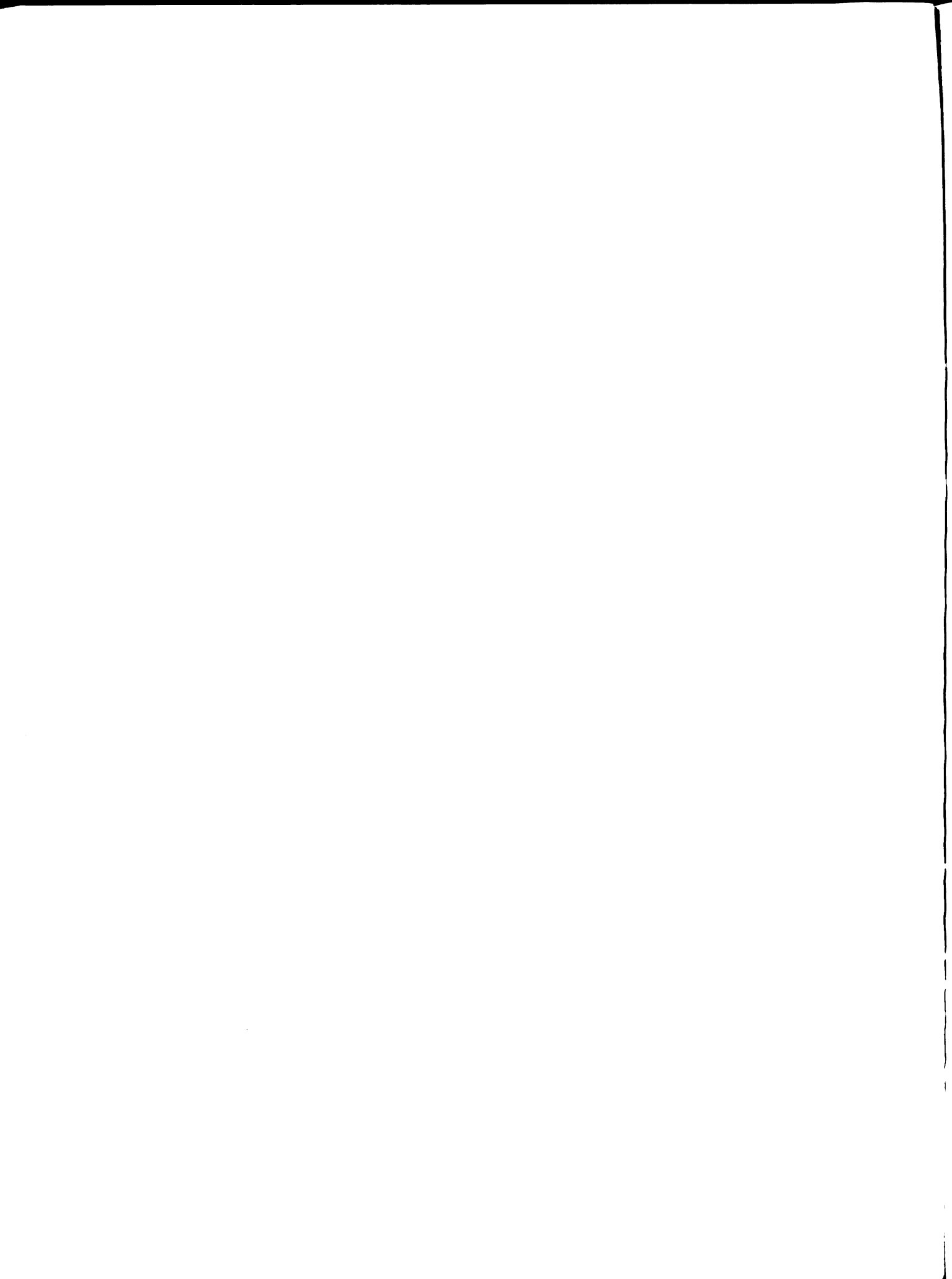


Table 4 (Continued)

C_m	dT	T	C_m	dT	T	C_m	dT	T
1.667	0.011	2.037	1.071	0.018	2.371	0.621	0.030	3.140
1.606	0.012	2.055	1.044	0.018	2.416	0.597	0.032	3.214
1.583	0.012	2.070	0.958	0.020	2.463	0.597	0.032	3.300
1.494	0.013	2.088	0.924	0.020	2.505	0.554	0.034	3.382
1.473	0.013	2.104	0.915	0.021	2.552	0.559	0.034	3.474
1.412	0.013	2.126	0.832	0.023	2.602	0.533	0.036	3.570
1.381	0.014	2.144	0.861	0.022	2.653	0.521	0.036	3.682
1.347	0.014	2.161	0.819	0.023	2.707	0.498	0.038	3.782
1.413	0.013	2.178	0.768	0.025	2.762	0.537	0.035	3.849
1.306	0.015	2.195	0.727	0.026	2.818	0.486	0.039	3.955
1.273	0.015	2.223	0.725	0.026	2.877	0.475	0.040	4.063
1.222	0.015	2.253	0.711	0.027	2.935	0.493	0.038	4.127
1.153	0.016	2.293	0.694	0.027	3.005	0.401	0.047	5.015
1.068	0.018	2.329	0.659	0.029	3.072	0.497	0.038	5.207
						0.496	0.057	5.281

Table 5. The Specific Heat of $\text{Cs}_2\text{MnCl}_4 \cdot 2\text{H}_2\text{O}$ for Sample 2, Run 1, October 5, 1966, Zero Field.

C_m	dT	T	C_m	dT	T	C_m	dT	T
3.322	0.006	1.417	4.670	0.009	1.635	10.292	0.004	1.835
3.294	0.006	1.430	4.775	0.009	1.650	10.233	0.004	1.840
3.245	0.006	1.442	4.959	0.008	1.665	4.624	0.009	1.848
3.418	0.005	1.450	5.120	0.008	1.679	3.216	0.009	1.861
3.291	0.006	1.461	5.230	0.008	1.692	2.917	0.009	1.872
3.362	0.005	1.475	5.520	0.007	1.703	2.529	0.011	1.887
3.477	0.005	1.484	5.657	0.007	1.718	2.363	0.012	1.900
3.460	0.005	1.494	5.823	0.007	1.727	2.192	0.013	1.917
3.566	0.005	1.509	5.902	0.007	1.740	2.065	0.013	1.935
3.658	0.005	1.516	6.285	0.007	1.749	1.948	0.014	1.954
3.713	0.005	1.526	6.424	0.006	1.762	1.872	0.015	1.972
3.817	0.005	1.535	6.280	0.007	1.770	1.772	0.016	1.991
3.679	0.005	1.545	6.901	0.006	1.780	1.708	0.016	2.011
3.873	0.005	1.553	7.086	0.006	1.788	1.649	0.017	2.032
3.912	0.005	1.563	7.351	0.006	1.796	1.596	0.017	2.052
3.994	0.005	1.571	7.542	0.005	1.804	1.527	0.018	2.075
4.095	0.004	1.581	7.979	0.005	1.811	1.475	0.019	2.098
4.188	0.004	1.588	8.271	0.005	1.817	1.430	0.019	2.121
4.170	0.010	1.601	8.902	0.005	1.823	1.426	0.019	2.140
4.355	0.009	1.618	9.637	0.004	1.830	1.404	0.020	2.159

Table 5 (Continued)

C_m	dT	T	C_m	dT	T	C_m	dT	T
1.359	0.020	2.190	0.853	0.032	2.659	0.559	0.049	3.421
1.373	0.020	2.221	0.826	0.033	2.723	0.587	0.047	3.506
1.288	0.021	2.257	0.814	0.034	2.781	0.624	0.044	3.595
1.216	0.023	2.300	0.746	0.037	2.848	0.655	0.021	3.665
1.178	0.023	2.343	0.727	0.038	2.910	0.492	0.056	3.820
1.101	0.025	2.388	0.684	0.040	2.982	0.607	0.023	3.904
1.057	0.026	2.437	0.646	0.043	3.069	0.576	0.048	4.006
1.020	0.027	2.487	0.603	0.046	3.147	0.413	0.033	4.233
0.972	0.028	2.541	0.578	0.048	3.237	0.552	0.025	4.290
0.886	0.031	2.601	0.563	0.049	3.331	0.587	0.023	4.395
						0.519	0.026	4.506

Table 6. The Specific Heat of $\text{Cs}_2\text{MnCl}_4 \cdot 2\text{H}_2\text{O}$ for Sample 2, Run 2, October 17, 1966, Zero Field.

C_m	dT	T	C_m	dT	T	C_m	dT	T
0.856	0.012	0.673	1.473	0.014	0.844	2.533	0.036	1.215
0.838	0.013	0.686	1.453	0.015	0.855	2.644	0.035	1.227
0.818	0.013	0.701	1.522	0.012	0.863	2.665	0.034	1.253
0.928	0.011	0.714	1.561	0.012	0.871	2.854	0.073	1.292
0.965	0.011	0.722	1.585	0.011	0.880	3.146	0.067	1.350
1.025	0.010	0.732	1.609	0.011	0.888	3.494	0.060	1.403
1.061	0.010	0.740	1.620	0.025	0.899	3.771	0.056	1.445
1.147	0.009	0.747	1.663	0.024	0.916	4.022	0.052	1.483
1.111	0.010	0.752	1.734	0.023	0.928	4.142	0.051	1.515
1.151	0.009	0.759	1.751	0.023	0.945	4.371	0.048	1.545
1.112	0.010	0.764	1.767	0.023	0.961	4.565	0.046	1.569
1.181	0.009	0.768	1.819	0.022	0.978	4.497	0.047	1.585
1.216	0.009	0.772	1.846	0.022	0.994	5.074	0.093	1.633
1.263	0.015	0.782	1.832	0.022	1.007	6.218	0.076	1.700
1.293	0.015	0.793	1.898	0.021	1.019	7.800	0.061	1.749
1.340	0.014	0.802	1.924	0.021	1.034	5.328	0.089	1.814
1.332	0.014	0.810	1.920	0.021	1.038	2.044	0.232	1.933
1.336	0.014	0.820	2.043	0.049	1.064	1.428	0.331	2.143
1.398	0.013	0.827	2.159	0.045	1.103	1.185	0.400	2.333
1.425	0.015	0.833	2.234	0.041	1.132	0.917	0.516	2.608
1.420	0.009	0.836	2.319	0.039	1.162	0.763	0.620	2.926
			2.428	0.038	1.190	0.639	0.741	3.255

Table 7. The Specific Heat of $\text{Cs}_2\text{MnCl}_4 \cdot 2\text{H}_2\text{O}$ for Sample 1, Run 5, December 23, 1966, 8150 Gauss, Orientation A.

C_m	dT	T	C_m	dT	T	C_m	dT	T
1.655	0.004	1.040	2.689	0.018	1.324	1.231	0.059	2.035
1.707	0.007	1.045	2.861	0.017	1.343	1.180	0.062	2.080
1.635	0.008	1.052	2.995	0.026	1.363	1.312	0.055	2.113
1.766	0.028	1.069	3.145	0.024	1.388	1.199	0.061	2.057
1.722	0.016	1.086	3.225	0.024	1.410	1.174	0.062	2.118
1.909	0.014	1.099	3.475	0.022	1.432	1.121	0.065	2.175
1.924	0.014	1.111	3.618	0.021	1.453	1.063	0.068	2.232
1.934	0.014	1.123	4.054	0.019	1.485	1.007	0.072	2.288
1.884	0.014	1.134	4.567	0.024	1.546	1.028	0.071	2.352
1.923	0.014	1.145	4.887	0.022	1.573	0.927	0.078	2.453
2.024	0.013	1.156	5.271	0.021	1.596	0.909	0.080	2.547
2.027	0.020	1.160	5.606	0.019	1.617	0.810	0.090	2.647
2.094	0.019	1.178	6.913	0.016	1.635	0.775	0.094	2.743
2.102	0.019	1.195	7.320	0.015	1.650	0.759	0.096	2.900
2.315	0.017	1.211	11.166	0.019	1.667	0.716	0.102	3.013
2.168	0.018	1.227	15.555	0.014	1.683	0.604	0.121	3.140
2.289	0.017	1.243	3.157	0.129	1.754	0.605	0.120	3.238
2.346	0.017	1.257	1.565	0.053	1.840	0.542	0.134	3.333
2.442	0.016	1.273	1.465	0.050	1.887	0.542	0.134	3.428
2.470	0.016	1.287	1.339	0.054	1.936	0.506	0.216	3.661
2.588	0.019	1.303	1.288	0.056	1.985	0.611	0.179	3.972
						0.446	0.245	4.297

Table 8. The Specific Heat of $\text{Cs}_2\text{MnCl}_4 \cdot 2\text{H}_2\text{O}$ for Sample 1, Run 6, January 12, 1967, 8150 Gauss, Orientation A.

C_m	dT	T	C_m	dT	T	C_m	dT	T
2.178	0.004	1.186	3.124	0.016	1.412	12.112	0.008	1.685
2.166	0.004	1.190	3.114	0.016	1.429	3.634	0.027	1.708
2.270	0.005	1.193	3.161	0.016	1.445	2.427	0.023	1.731
2.149	0.014	1.200	3.654	0.014	1.460	2.059	0.029	1.752
2.289	0.013	1.213	3.769	0.013	1.474	1.886	0.032	1.779
2.294	0.015	1.225	3.859	0.013	1.487	1.722	0.034	1.799
2.326	0.012	1.237	3.976	0.013	1.500	1.761	0.023	1.830
2.417	0.012	1.247	4.363	0.007	1.510	1.500	0.028	1.863
2.497	0.010	1.256	4.418	0.026	1.527	1.551	0.019	1.886
2.455	0.010	1.265	4.656	0.025	1.553	1.531	0.019	1.905
2.520	0.011	1.274	4.997	0.023	1.576	1.602	0.018	1.923
2.437	0.020	1.290	4.891	0.023	1.598	1.507	0.019	1.942
2.527	0.019	1.309	5.860	0.020	1.618	1.508	0.019	1.958
2.802	0.018	1.327	6.371	0.018	1.637	1.485	0.019	1.977
2.849	0.018	1.344	7.249	0.016	1.653	1.421	0.020	1.997
2.873	0.018	1.383	7.807	0.015	1.667	1.475	0.019	2.016
2.887	0.012	1.398	9.706	0.010	1.678	1.372	0.021	2.037

Table 8 (Continued)

C_m	dT	T	C_m	dT	T	C_m	dT	T
1.431	0.020	2.057	0.762	0.038	2.654	0.512	0.056	3.444
1.388	0.021	2.069	0.790	0.040	2.719	0.506	0.057	3.556
1.150	0.025	2.102	0.765	0.041	2.776	0.466	0.061	3.636
1.153	0.025	2.139	0.748	0.038	2.832	0.489	0.058	3.706
1.176	0.024	2.172	0.727	0.039	2.900	0.478	0.060	3.770
1.067	0.027	2.212	0.684	0.042	2.956	0.508	0.056	3.828
1.035	0.028	2.262	0.635	0.045	3.029	0.523	0.055	3.883
0.935	0.031	2.315	0.638	0.045	3.095	0.580	0.049	3.935
0.839	0.034	2.418	0.595	0.048	3.200	0.656	0.044	3.982
0.889	0.032	2.490	0.685	0.042	3.284	0.634	0.045	4.026
0.875	0.032	2.560	0.545	0.052	3.369	0.505	0.057	4.066

Table 9. The Specific Heat of $\text{Cs}_2\text{MnCl}_4 \cdot 2\text{H}_2\text{O}$ for Sample 1, Run 7, January 13, 1967, 5150 Gauss, Orientation A.

C_m	dT	T	C_m	dT	T	C_m	dT	T
2.083	0.009	1.190	3.916	0.013	1.496	1.681	0.020	1.954
2.231	0.009	1.198	3.774	0.013	1.509	1.517	0.034	2.005
2.429	0.012	1.206	4.154	0.012	1.522	1.428	0.035	2.053
2.269	0.013	1.215	3.961	0.013	1.534	1.320	0.040	2.105
2.298	0.012	1.227	4.081	0.029	1.554	1.254	0.042	2.151
2.431	0.012	1.238	4.424	0.021	1.580	1.202	0.043	2.195
2.519	0.011	1.246	4.938	0.019	1.600	1.155	0.045	2.239
2.421	0.012	1.256	4.477	0.021	1.618	1.196	0.044	2.284
2.536	0.011	1.266	5.252	0.018	1.637	1.063	0.049	2.321
2.492	0.011	1.277	5.188	0.018	1.655	1.059	0.049	2.363
2.561	0.011	1.289	5.766	0.016	1.673	0.929	0.056	2.434
2.594	0.011	1.300	6.070	0.016	1.689	0.905	0.058	2.537
2.729	0.010	1.309	5.801	0.016	1.704	0.861	0.061	2.632
2.801	0.010	1.319	7.037	0.017	1.720	0.821	0.064	2.770
2.841	0.018	1.333	7.881	0.015	1.736	0.754	0.069	2.876
2.820	0.018	1.350	8.986	0.013	1.750	0.676	0.077	3.019
2.833	0.018	1.366	11.160	0.011	1.761	0.692	0.073	3.130
2.784	0.018	1.379	6.262	0.019	1.777	0.607	0.086	3.280
3.040	0.017	1.395	2.763	0.034	1.803	0.576	0.091	3.405
3.125	0.016	1.421	2.297	0.033	1.834	0.544	0.096	3.523
3.410	0.015	1.435	2.023	0.017	1.857	0.495	0.105	3.695
3.518	0.014	1.454	2.018	0.026	1.869	0.484	0.108	3.809
3.518	0.014	1.468	1.897	0.028	1.895	0.588	0.089	3.907
3.628	0.014	1.482	1.823	0.029	1.920	0.463	0.113	4.026

Table 10. The Specific Heat of $\text{Cs}_2\text{MnCl}_4 \cdot 2\text{H}_2\text{O}$ for Sample 1, Run 8, January 18, 1967, 5150 Gauss, Orientation A.

C_m	dT	T	C_m	dT	T	C_m	dT	T
1.796	0.008	1.138	3.465	0.015	1.506	1.480	0.034	2.070
1.824	0.008	1.146	3.461	0.015	1.521	1.257	0.040	2.144
2.121	0.007	1.153	3.500	0.015	1.535	1.224	0.041	2.192
2.153	0.014	1.164	3.493	0.015	1.550	1.132	0.045	2.242
2.144	0.013	1.177	4.075	0.012	1.563	1.097	0.046	2.287
2.134	0.013	1.189	3.809	0.013	1.576	1.095	0.046	2.333
2.172	0.013	1.201	4.368	0.012	1.590	0.981	0.051	2.416
2.257	0.013	1.210	4.639	0.025	1.608	0.868	0.058	2.507
2.277	0.013	1.221	4.949	0.023	1.632	0.788	0.064	2.630
2.297	0.012	1.231	5.185	0.022	1.654	0.709	0.071	2.819
2.316	0.012	1.241	5.313	0.022	1.675	0.682	0.074	2.934
2.398	0.012	1.252	6.233	0.018	1.695	0.628	0.080	3.085
2.666	0.011	1.271	6.847	0.017	1.712	0.537	0.094	3.209
2.806	0.010	1.288	7.355	0.016	1.728	0.626	0.080	3.308
2.853	0.010	1.306	8.341	0.014	1.743	0.533	0.095	3.432
2.646	0.011	1.327	8.864	0.013	1.756	0.489	0.103	3.552
2.860	0.010	1.342	11.579	0.010	1.767	0.488	0.103	3.673
2.851	0.010	1.359	3.957	0.029	1.787	0.514	0.098	3.797
3.033	0.009	1.377	2.482	0.033	1.816	0.449	0.112	3.942
3.239	0.016	1.397	2.112	0.035	1.848	0.423	0.119	4.088
2.795	0.018	1.421	1.919	0.040	1.884			
3.490	0.015	1.448	1.719	0.044	1.923			
3.674	0.014	1.467	1.520	0.050	1.967			
3.718	0.014	1.486	1.563	0.032	2.021			

Table 11. The Specific Heat of $\text{Cs}_2\text{MnCl}_4 \cdot 2\text{H}_2\text{O}$ for Sample 1, Run 9, January 20, 1967, 3500 Gauss, Orientation A.

C_m	dT	T	C_m	dT	T	C_m	dT	T
1.757	0.011	1.007	2.534	0.011	1.286	3.897	0.013	1.589
1.962	0.010	1.016	2.556	0.011	1.296	4.034	0.013	1.602
1.920	0.010	1.024	2.640	0.011	1.306	4.722	0.011	1.616
1.630	0.012	1.032	2.613	0.011	1.316	4.763	0.024	1.633
1.897	0.010	1.056	2.623	0.011	1.326	5.062	0.023	1.656
2.051	0.009	1.071	2.647	0.011	1.336	5.280	0.022	1.678
2.021	0.009	1.084	2.536	0.011	1.345	6.179	0.018	1.720
1.776	0.011	1.099	3.096	0.009	1.354	6.783	0.017	1.738
1.950	0.010	1.109	2.804	0.010	1.362	6.868	0.017	1.754
2.046	0.009	1.119	2.885	0.010	1.370	7.625	0.015	1.770
1.987	0.009	1.128	2.857	0.010	1.379	10.244	0.011	1.798
2.049	0.009	1.144	2.976	0.017	1.391	6.231	0.018	1.812
2.015	0.009	1.152	2.949	0.017	1.404	3.032	0.022	1.832
2.033	0.009	1.160	3.084	0.017	1.421	2.548	0.022	1.853
2.026	0.009	1.168	3.153	0.016	1.438	2.321	0.025	1.877
2.123	0.009	1.176	3.230	0.016	1.454	1.866	0.031	1.902
2.089	0.013	1.190	3.326	0.015	1.472	1.913	0.030	1.929
2.122	0.013	1.206	3.263	0.016	1.487	2.026	0.017	1.949
2.186	0.013	1.219	3.463	0.015	1.503	1.975	0.017	1.966
2.281	0.012	1.232	3.300	0.015	1.518	1.898	0.018	1.983
2.074	0.014	1.242	3.717	0.014	1.535	1.789	0.019	2.002
2.366	0.012	1.255	3.603	0.014	1.549	1.789	0.019	2.020
2.400	0.012	1.265	3.813	0.013	1.563	1.687	0.020	2.039
2.376	0.012	1.276	4.007	0.013	1.576	1.486	0.023	2.052

Table 11 (Continued)

C_m	dT	T	C_m	dT	T	C_m	dT	T
1.417	0.024	2.079	1.008	0.034	2.400	0.675	0.075	2.879
1.329	0.025	2.105	0.964	0.035	2.441	0.624	0.082	3.033
1.349	0.025	2.131	0.974	0.035	2.494	0.597	0.085	3.186
1.268	0.027	2.158	0.875	0.039	2.534	0.534	0.095	3.374
1.182	0.029	2.186	0.890	0.038	2.575	0.498	0.102	3.529
1.280	0.026	2.217	0.856	0.040	2.616	0.478	0.106	3.674
1.198	0.028	2.249	0.840	0.040	2.655	0.461	0.110	3.843
1.145	0.030	2.281	0.853	0.040	2.696	0.508	0.100	3.996
1.125	0.030	2.322	0.965	0.035	2.734	0.403	0.126	4.165
1.047	0.032	2.360	0.801	0.063	2.783			

Table 12. The Specific Heat of $\text{Cs}_2\text{MnCl}_4 \cdot 2\text{H}_2\text{O}$ for Sample 1, Run 10, January 23, 1967, 3500 Gauss, Orientation A.

C_m	dT	T	C_m	dT	T	C_m	dT	T
1.542	0.012	0.979	2.301	0.008	1.238	3.628	0.014	1.514
1.542	0.012	0.990	2.375	0.008	1.246	4.533	0.011	1.526
1.516	0.013	1.000	2.464	0.014	1.257	4.229	0.012	1.546
1.533	0.012	1.011	2.432	0.014	1.270	4.386	0.012	1.572
1.587	0.012	1.020	2.427	0.014	1.283	4.400	0.017	1.594
1.485	0.013	1.050	2.532	0.013	1.295	4.735	0.016	1.616
1.862	0.010	1.077	2.486	0.014	1.308	4.967	0.015	1.639
1.825	0.010	1.107	2.948	0.011	1.336	5.167	0.015	1.660
2.078	0.009	1.128	2.920	0.012	1.354	5.406	0.014	1.680
2.207	0.009	1.152	3.076	0.016	1.379	5.935	0.013	1.709
1.959	0.010	1.167	3.072	0.017	1.401	6.351	0.018	1.730
2.143	0.009	1.179	2.874	0.018	1.420	7.016	0.016	1.752
1.913	0.010	1.192	2.870	0.018	1.439	7.264	0.016	1.772
1.893	0.010	1.203	3.269	0.016	1.456	7.325	0.016	1.791
2.223	0.009	1.213	3.336	0.015	1.471	9.397	0.009	1.804
2.226	0.009	1.221	3.514	0.014	1.486	5.077	0.014	1.815
2.300	0.008	1.230	3.476	0.015	1.500	2.683	0.013	1.828

Table 12 (Continued)

C_m	dT	T	C_m	dT	T	C_m	dT	T
2.365	0.024	1.847	1.262	0.040	2.163	0.765	0.066	2.836
2.421	0.011	1.867	1.238	0.041	2.204	0.762	0.067	2.952
2.067	0.021	1.892	1.176	0.043	2.245	0.673	0.076	3.112
1.622	0.021	1.921	1.169	0.044	2.288	0.625	0.081	3.228
1.813	0.019	1.945	1.166	0.044	2.332	0.611	0.083	3.332
1.780	0.019	1.970	1.118	0.045	2.374	0.522	0.097	3.541
1.605	0.021	1.998	0.960	0.053	2.419	0.594	0.086	3.659
1.583	0.021	2.023	0.942	0.054	2.457	0.530	0.096	3.791
1.471	0.023	2.051	0.932	0.055	2.495	0.535	0.095	3.961
1.362	0.037	2.084	0.880	0.058	2.597	0.493	0.103	4.103
1.280	0.040	2.123	0.856	0.059	2.702			

Table 13. The Specific Heat of $\text{Cs}_2\text{MnCl}_4 \cdot 2\text{H}_2\text{O}$ for Sample 1, Run 12, February 11, 1967, 8400 Gauss, Orientation B.

C_m	dT	T	C_m	dT	T	C_m	dT	T
2.421	0.011	1.206	3.320	0.016	1.404	4.476	0.012	1.599
2.762	0.014	1.218	3.152	0.017	1.416	4.595	0.011	1.609
2.719	0.012	1.230	3.401	0.015	1.429	4.799	0.007	1.618
2.700	0.012	1.239	3.366	0.016	1.442	5.096	0.007	1.624
2.710	0.012	1.250	3.428	0.015	1.455	4.807	0.007	1.630
2.730	0.012	1.255	3.492	0.015	1.468	5.143	0.007	1.636
2.700	0.012	1.264	3.639	0.014	1.480	4.926	0.007	1.641
2.719	0.012	1.273	3.532	0.015	1.493	5.362	0.006	1.647
2.736	0.012	1.283	3.692	0.014	1.503	4.890	0.004	1.651
2.741	0.012	1.294	3.924	0.013	1.515	5.149	0.007	1.654
2.688	0.013	1.305	3.852	0.014	1.527	5.968	0.006	1.664
3.099	0.011	1.312	3.949	0.013	1.539	5.620	0.006	1.669
2.936	0.018	1.325	4.013	0.013	1.549	5.642	0.006	1.674
2.843	0.018	1.342	4.176	0.013	1.561	5.374	0.007	1.678
2.907	0.018	1.358	4.184	0.013	1.572	5.627	0.006	1.682
3.073	0.017	1.373	4.329	0.012	1.580	6.127	0.006	1.686
3.093	0.017	1.388	4.289	0.012	1.591	5.614	0.006	1.691

Table 13 (Continued)

C_m	dT	T	C_m	dT	T	C_m	dT	T
6.819	0.005	1.695	7.710	0.005	1.735	1.162	0.045	2.152
5.737	0.006	1.700	7.196	0.007	1.740	1.188	0.044	2.196
7.195	0.005	1.705	8.032	0.007	1.745	1.224	0.043	2.241
8.083	0.004	1.709	8.131	0.006	1.750	1.075	0.049	2.287
6.610	0.005	1.714	8.312	0.006	1.754	1.081	0.048	2.336
7.093	0.005	1.718	8.934	0.006	1.758	1.063	0.049	2.384
6.953	0.005	1.723	9.990	0.005	1.763	1.085	0.048	2.432
6.525	0.005	1.726	1.313	0.028	2.035	1.000	0.052	2.482
7.320	0.005	1.730	1.299	0.040	2.069	0.722	0.072	2.536
6.700	0.005	1.733	1.288	0.041	2.109			

Table 14. The Specific Heat of $\text{Cs}_2\text{MnCl}_4 \cdot 2\text{H}_2\text{O}$ for Sample 1, Run 13, February 13, 1967, 8400 Gauss, Orientation B.

C_m	dT	T	C_m	dT	T	C_m	dT	T
2.634	0.013	1.196	3.332	0.010	1.377	4.635	0.011	1.598
2.889	0.012	1.207	3.230	0.015	1.390	4.607	0.011	1.608
2.832	0.012	1.217	3.134	0.016	1.403	4.849	0.010	1.618
2.765	0.012	1.227	3.005	0.017	1.423	5.032	0.010	1.627
2.657	0.013	1.234	3.499	0.014	1.439	5.069	0.010	1.637
2.687	0.012	1.243	3.612	0.014	1.453	5.050	0.010	1.646
2.746	0.012	1.253	3.571	0.014	1.467	5.030	0.010	1.656
2.730	0.012	1.263	3.553	0.014	1.481	4.986	0.010	1.665
2.673	0.012	1.273	3.397	0.015	1.491	5.056	0.010	1.674
2.745	0.012	1.283	4.021	0.012	1.505	5.622	0.009	1.687
2.733	0.012	1.300	3.944	0.013	1.517	6.177	0.008	1.697
2.927	0.011	1.312	4.079	0.012	1.530	5.709	0.009	1.708
2.906	0.011	1.324	4.029	0.012	1.542	5.608	0.009	1.719
2.903	0.011	1.335	4.010	0.012	1.553	6.408	0.008	1.727
2.918	0.011	1.346	4.691	0.011	1.565	6.642	0.008	1.735
2.780	0.012	1.356	4.468	0.011	1.576	7.002	0.007	1.742
3.173	0.011	1.367	4.594	0.011	1.587	7.397	0.007	1.749

Table 14 (Continued)

C_m	dT	T	C_m	dT	T	C_m	dT	T
8.447	0.006	1.755	1.329	0.038	2.066	0.654	0.077	3.018
7.723	0.006	1.761	1.248	0.040	2.124	0.624	0.080	3.104
10.091	0.005	1.767	1.201	0.042	2.176	0.628	0.080	3.184
8.163	0.006	1.772	1.143	0.044	2.235	0.662	0.076	3.262
3.906	0.013	1.782	1.060	0.047	2.299	0.573	0.087	3.329
2.772	0.012	1.795	0.948	0.053	2.360	0.591	0.085	3.421
2.509	0.013	1.807	0.944	0.053	2.423	0.589	0.085	3.506
2.733	0.012	1.823	0.892	0.056	2.503	0.564	0.089	3.572
2.212	0.015	1.845	0.840	0.060	2.571	0.487	0.103	3.656
2.037	0.025	1.876	0.801	0.062	2.645	0.446	0.112	3.799
1.729	0.029	1.921	0.747	0.067	2.742	0.456	0.110	3.959
1.537	0.033	1.974	0.714	0.070	2.827	0.544	0.092	4.124
1.425	0.035	2.022	0.903	0.055	2.910	0.482	0.104	4.312

Table 15. The Specific Heat of $\text{Cs}_2\text{MnCl}_4 \cdot 2\text{H}_2\text{O}$ for Sample 1, Run 14, February 16, 1967, 6050 Gauss, Orientation B.

C_m	dT	T	C_m	dT	T	C_m	dT	T
2.221	0.015	1.193	3.133	0.011	1.415	5.105	0.010	1.641
2.487	0.014	1.207	3.159	0.011	1.425	5.248	0.010	1.651
2.484	0.014	1.218	3.173	0.011	1.451	5.510	0.009	1.660
2.448	0.014	1.230	3.340	0.010	1.465	5.431	0.009	1.670
2.436	0.014	1.241	3.453	0.010	1.478	6.072	0.019	1.706
2.551	0.013	1.251	3.037	0.011	1.490	6.690	0.017	1.724
2.620	0.013	1.262	3.609	0.009	1.500	6.979	0.016	1.741
2.686	0.013	1.272	3.586	0.009	1.510	7.383	0.015	1.756
2.624	0.013	1.283	3.116	0.016	1.523	9.825	0.012	1.785
2.634	0.013	1.293	3.934	0.013	1.537	6.116	0.019	1.800
2.506	0.014	1.308	4.102	0.012	1.550	3.318	0.015	1.817
2.981	0.011	1.321	4.093	0.012	1.562	2.710	0.019	1.835
3.002	0.011	1.332	4.202	0.012	1.575	2.473	0.020	1.854
2.930	0.012	1.343	4.620	0.011	1.586	2.088	0.024	1.875
2.876	0.012	1.354	4.698	0.011	1.610	2.046	0.025	1.899
2.758	0.012	1.392	4.925	0.010	1.621	1.973	0.026	1.925
3.019	0.011	1.404	5.065	0.010	1.631	2.042	0.025	1.946

Table 15 (Continued)

C_m	dT	T	C_m	dT	T	C_m	dT	T
1.523	0.033	2.004	0.763	0.066	2.843	0.544	0.093	3.705
1.403	0.036	2.055	0.744	0.068	2.935	0.582	0.087	3.739
1.354	0.037	2.103	0.666	0.076	3.046	0.581	0.087	3.826
1.293	0.039	2.162	0.641	0.079	3.134	0.548	0.092	3.886
1.164	0.044	2.217	0.636	0.080	3.213	0.531	0.095	3.948
1.115	0.045	2.276	0.670	0.076	3.290	0.485	0.104	4.009
1.037	0.049	2.358	0.701	0.072	3.370	0.489	0.103	4.070
1.012	0.050	2.438	0.666	0.076	3.445	0.505	0.100	4.124
0.892	0.057	2.544	0.599	0.085	3.512	0.504	0.101	4.183
0.849	0.060	2.635	0.596	0.085	3.579	0.529	0.096	4.238
0.781	0.065	2.745	0.558	0.091	3.648			

Table 16. The Specific Heat of $\text{Cs}_2\text{MnCl}_4 \cdot 2\text{H}_2\text{O}$ for Sample 1, Run 15, February 16, 1967, 6050 Gauss, Orientation B.

C_m	dT	T	C_m	dT	T	C_m	dT	T
2.612	0.013	1.194	3.223	0.010	1.381	4.218	0.012	1.574
2.835	0.012	1.205	3.293	0.010	1.396	4.417	0.011	1.581
2.621	0.013	1.216	3.209	0.010	1.405	4.498	0.011	1.590
2.646	0.013	1.226	3.294	0.010	1.413	4.422	0.011	1.600
2.658	0.013	1.236	3.188	0.011	1.422	4.709	0.011	1.610
2.364	0.014	1.251	2.978	0.011	1.431	4.774	0.024	1.626
2.710	0.012	1.265	3.404	0.015	1.443	4.870	0.023	1.649
2.781	0.012	1.276	3.420	0.015	1.456	5.199	0.022	1.665
2.854	0.012	1.288	3.515	0.014	1.469	5.877	0.019	1.686
2.732	0.012	1.299	3.614	0.014	1.483	5.964	0.019	1.705
2.534	0.013	1.310	3.605	0.014	1.495	6.180	0.019	1.723
2.897	0.012	1.321	3.655	0.014	1.506	6.187	0.018	1.740
2.889	0.012	1.331	3.835	0.013	1.517	7.831	0.015	1.759
2.860	0.012	1.341	3.857	0.013	1.529	7.774	0.015	1.773
2.938	0.011	1.351	4.107	0.012	1.540	8.762	0.013	1.785
2.945	0.011	1.361	4.156	0.012	1.552	9.161	0.012	1.797
2.745	0.012	1.369	4.083	0.012	1.563	3.713	0.026	1.815

Table 16 (Continued)

C_m	dT	T	C_m	dT	T	C_m	dT	T
2.631	0.019	1.835	1.440	0.035	2.086	0.678	0.075	2.959
2.637	0.019	1.844	1.350	0.037	2.136	0.537	0.094	3.073
2.354	0.022	1.864	1.323	0.038	2.181	0.586	0.086	3.252
2.216	0.023	1.886	1.201	0.042	2.243	0.570	0.089	3.374
2.096	0.024	1.910	1.181	0.043	2.306	0.508	0.100	3.484
2.021	0.025	1.935	1.139	0.044	2.398	0.524	0.097	3.591
1.799	0.028	1.960	0.994	0.051	2.507	0.530	0.096	3.687
1.722	0.029	1.997	0.798	0.063	2.668	0.534	0.095	3.777
1.598	0.032	2.035	0.754	0.067	2.790			

Table 17. The Specific Heat of $\text{Cs}_2\text{MnCl}_4 \cdot 2\text{H}_2\text{O}$ for Sample 1, Run 16, March 1, 1967, 8400 Gauss, Orientation C.

C_m	dT	T	C_m	dT	T	C_m	dT	T
4.372	0.007	1.396	9.276	0.005	1.522	1.637	0.021	1.727
5.016	0.006	1.402	9.343	0.005	1.527	1.555	0.022	1.745
5.293	0.005	1.408	9.565	0.005	1.533	1.426	0.024	1.821
5.238	0.005	1.413	9.709	0.005	1.537	1.427	0.024	1.845
5.058	0.010	1.421	9.412	0.005	1.542	1.435	0.024	1.869
5.031	0.010	1.431	9.476	0.005	1.547	1.375	0.025	1.889
5.002	0.010	1.440	8.589	0.006	1.553	1.289	0.026	1.912
5.192	0.010	1.449	8.653	0.006	1.559	1.265	0.027	1.945
5.077	0.010	1.458	8.717	0.006	1.565	1.242	0.027	1.981
5.464	0.009	1.466	6.593	0.014	1.580	1.189	0.028	2.030
5.875	0.009	1.474	2.908	0.019	1.602	1.177	0.029	2.068
6.202	0.008	1.482	2.164	0.017	1.622	1.163	0.029	2.102
7.066	0.007	1.490	2.048	0.017	1.639	1.045	0.032	2.145
7.415	0.007	1.497	1.950	0.017	1.656	1.007	0.034	2.181
7.288	0.007	1.503	1.803	0.019	1.673	1.005	0.034	2.215
8.087	0.006	1.510	1.699	0.020	1.691	1.057	0.032	2.248
8.393	0.006	1.516	1.556	0.022	1.708	1.196	0.028	2.270

Table 17 (Continued)

C_m	dT	T	C_m	dT	T	C_m	dT	T
1.132	0.030	2.299	0.919	0.037	2.606	0.644	0.079	3.149
1.060	0.032	2.330	0.811	0.063	2.655	0.587	0.086	3.224
1.086	0.031	2.356	0.845	0.060	2.716	0.701	0.072	3.302
1.005	0.034	2.388	0.776	0.065	2.766	0.809	0.063	3.369
1.039	0.033	2.421	0.768	0.066	2.831	0.581	0.087	3.444
0.912	0.037	2.456	0.743	0.068	2.898	0.564	0.090	3.533
0.945	0.036	2.492	0.747	0.068	2.966	0.485	0.104	3.624
0.857	0.039	2.530	0.731	0.069	3.029	0.535	0.095	3.724
0.890	0.038	2.568	0.737	0.069	3.098			

Table 18. The Specific Heat of $\text{Cs}_2\text{MnCl}_4 \cdot 2\text{H}_2\text{O}$ for Sample 1, Run 17, March 3, 1967, 8400 Gauss, Orientation C.

C_m	dT	T	C_m	dT	T	C_m	dT	T
4.093	0.012	1.263	5.651	0.009	1.464	1.818	0.019	1.637
4.215	0.012	1.274	5.759	0.013	1.484	1.889	0.018	1.657
3.680	0.014	1.295	6.132	0.012	1.500	1.743	0.029	1.689
3.585	0.014	1.311	8.489	0.009	1.511	1.639	0.025	1.727
4.018	0.013	1.324	9.995	0.008	1.519	1.436	0.035	1.782
4.030	0.013	1.336	11.924	0.006	1.526	1.371	0.037	1.835
4.245	0.012	1.348	11.822	0.006	1.533	1.285	0.039	1.921
4.112	0.012	1.360	10.298	0.007	1.540	1.136	0.044	2.010
4.023	0.013	1.369	10.118	0.008	1.547	1.077	0.047	2.076
4.394	0.011	1.380	8.391	0.009	1.555	0.982	0.051	2.165
4.657	0.011	1.390	6.444	0.012	1.566	0.949	0.036	2.238
4.737	0.011	1.400	3.407	0.015	1.578	0.810	0.042	2.427
4.717	0.011	1.410	2.605	0.019	1.593	0.800	0.042	2.533
4.697	0.011	1.419	2.234	0.015	1.608	0.808	0.063	2.625
5.313	0.009	1.436	2.042	0.017	1.621			

Table 19. The Specific Heat of $\text{Cs}_2\text{MnCl}_4 \cdot 2\text{H}_2\text{O}$ for Sample 1, Run 18, March 8, 1967, 6050 Gauss, Orientation C.

C_m	dT	T	C_m	dT	T	C_m	dT	T
3.421	0.015	1.302	5.335	0.009	1.602	1.376	0.037	2.040
3.197	0.016	1.315	5.253	0.010	1.612	1.260	0.040	2.079
3.159	0.016	1.329	5.771	0.009	1.621	1.317	0.038	2.118
3.077	0.016	1.343	6.525	0.008	1.639	1.264	0.040	2.160
3.119	0.016	1.357	6.168	0.008	1.647	1.144	0.044	2.202
3.207	0.016	1.387	6.760	0.007	1.655	1.156	0.044	2.246
3.208	0.016	1.402	6.923	0.007	1.662	1.134	0.045	2.287
3.477	0.015	1.418	6.988	0.007	1.669	1.050	0.048	2.361
3.625	0.014	1.432	7.591	0.010	1.678	0.844	0.060	2.538
3.679	0.014	1.446	8.182	0.009	1.688	0.794	0.064	2.658
3.971	0.013	1.457	8.455	0.009	1.697	0.796	0.064	2.742
4.101	0.012	1.470	4.596	0.017	1.709	0.703	0.072	2.828
4.230	0.012	1.482	2.527	0.020	1.725	0.642	0.079	2.939
4.467	0.011	1.494	2.476	0.020	1.743	0.612	0.083	3.064
4.345	0.012	1.505	2.248	0.023	1.762	0.604	0.084	3.186
4.167	0.012	1.516	2.067	0.025	1.783	0.553	0.092	3.314
4.513	0.011	1.526	1.904	0.027	1.806	0.527	0.096	3.425
4.323	0.012	1.562	1.735	0.029	1.828	0.528	0.096	3.539
5.004	0.010	1.573	1.663	0.030	1.881	0.471	0.108	3.689
4.940	0.010	1.583	1.491	0.034	1.942	0.514	0.098	3.827
5.374	0.009	1.593	1.507	0.034	1.989	0.412	0.123	3.979

Table 20. The Specific Heat of $\text{Cs}_2\text{MnCl}_4 \cdot 2\text{H}_2\text{O}$ for Sample 1, Run 19, March 10, 1967, 9830 Gauss, Orientation C.

C_m	dT	T	C_m	dT	T	C_m	dT	T
4.279	0.012	1.314	1.638	0.021	1.536	0.806	0.042	2.348
4.441	0.011	1.335	1.532	0.022	1.561	0.850	0.040	2.438
4.557	0.011	1.345	1.422	0.024	1.587	0.795	0.042	2.540
4.673	0.011	1.355	1.351	0.025	1.611	0.759	0.044	2.617
4.789	0.011	1.365	1.394	0.024	1.636	0.746	0.045	2.677
4.941	0.010	1.374	1.352	0.025	1.659	0.748	0.045	2.743
5.225	0.010	1.382	1.274	0.027	1.682	0.677	0.050	2.791
5.967	0.008	1.399	1.280	0.026	1.702	0.715	0.047	2.821
6.863	0.007	1.405	1.266	0.027	1.725	0.703	0.072	2.890
7.214	0.007	1.413	1.162	0.029	1.750	0.590	0.086	3.008
7.800	0.006	1.419	1.233	0.027	1.775	0.595	0.085	3.130
8.593	0.006	1.426	1.250	0.027	1.872	0.601	0.084	3.250
9.230	0.005	1.431	1.102	0.031	1.916	0.598	0.085	3.406
10.123	0.005	1.437	1.039	0.033	1.954	0.545	0.093	3.523
10.010	0.005	1.440	1.030	0.033	1.986	0.508	0.099	3.644
14.591	0.003	1.444	1.066	0.032	2.012	0.501	0.101	3.744
6.324	0.008	1.442	0.993	0.034	2.045	0.513	0.099	3.876
4.500	0.011	1.450	0.982	0.034	2.073	0.568	0.089	3.977
3.402	0.015	1.462	0.970	0.035	2.100	0.568	0.089	4.057
2.115	0.016	1.476	1.074	0.031	2.148	0.521	0.097	4.089
1.972	0.017	1.509	0.982	0.034	2.202			

Table 21. The Specific Heat of $\text{Cs}_2\text{MnCl}_4 \cdot 2\text{H}_2\text{O}$ for Sample 1, Run 20, March 14, 1967, 6050 Gauss, Orientation C.

C_m	dT	T	C_m	dT	T	C_m	dT	T
3.201	0.016	1.308	5.019	0.010	1.568	3.467	0.012	1.714
3.370	0.015	1.321	5.233	0.010	1.578	2.810	0.012	1.726
3.249	0.016	1.334	4.890	0.010	1.588	2.590	0.012	1.738
3.193	0.016	1.347	4.583	0.011	1.599	2.368	0.012	1.750
3.117	0.016	1.360	6.201	0.008	1.608	2.294	0.015	1.762
3.346	0.015	1.378	6.039	0.008	1.616	1.808	0.019	1.777
3.427	0.015	1.393	5.629	0.009	1.625	1.997	0.017	1.794
3.398	0.015	1.407	6.645	0.008	1.633	1.922	0.018	1.810
3.406	0.015	1.420	6.009	0.008	1.642	1.772	0.019	1.825
3.488	0.015	1.432	6.285	0.008	1.650	1.759	0.019	1.833
3.942	0.013	1.476	5.653	0.009	1.657	1.655	0.020	1.851
3.924	0.013	1.493	6.704	0.008	1.664	1.572	0.021	1.870
4.018	0.013	1.507	6.427	0.008	1.671	1.607	0.021	1.891
4.029	0.013	1.524	9.584	0.005	1.685	1.581	0.021	1.911
4.456	0.011	1.536	8.727	0.006	1.690	1.546	0.022	1.932
4.819	0.011	1.547	8.307	0.006	1.696	1.470	0.023	1.953
4.490	0.011	1.557	5.449	0.009	1.704	1.458	0.023	1.960



Table 21 (Continued)

C_m	dT	T	C_m	dT	T	C_m	dT	T
1.449	0.023	1.981	1.025	0.049	2.330	0.579	0.087	3.341
1.457	0.023	2.002	0.941	0.054	2.449	0.585	0.087	3.428
1.353	0.025	2.024	0.883	0.057	2.542	0.583	0.087	3.514
1.347	0.025	2.005	0.802	0.063	2.669	0.529	0.096	3.639
1.432	0.024	2.040	0.793	0.064	2.770	0.502	0.101	3.771
1.369	0.025	2.099	0.692	0.073	2.922	0.461	0.110	3.894
1.295	0.026	2.141	0.659	0.077	3.022	0.511	0.099	3.998
1.226	0.028	2.180	0.616	0.082	3.114	0.561	0.090	4.079
1.094	0.046	2.252	0.608	0.083	3.244			

Table 22. The Specific Heat of $\text{Cs}_2\text{MnCl}_4 \cdot 2\text{H}_2\text{O}$ for Sample 1, Run 21, March 22, 1967, 8900 Gauss, Orientation C.

C_m	dT	T	C_m	dT	T	C_m	dT	T
3.835	0.013	1.318	13.579	0.004	1.494	1.083	0.031	2.039
4.144	0.012	1.331	7.342	0.007	1.502	1.064	0.032	2.070
4.422	0.011	1.341	6.827	0.007	1.508	1.106	0.030	2.101
4.100	0.012	1.352	4.828	0.010	1.515	1.076	0.031	2.128
4.374	0.012	1.363	3.986	0.013	1.525	1.050	0.032	2.164
4.367	0.012	1.373	2.800	0.012	1.536	1.106	0.030	2.205
4.428	0.011	1.383	2.490	0.014	1.539	0.987	0.034	2.251
4.755	0.011	1.393	2.074	0.016	1.558	0.922	0.037	2.321
4.901	0.010	1.402	1.856	0.018	1.575	0.969	0.035	2.388
5.764	0.009	1.412	1.827	0.018	1.593	0.865	0.039	2.515
5.219	0.010	1.421	1.712	0.020	1.612	0.751	0.045	2.673
5.654	0.009	1.428	1.718	0.020	1.631	0.738	0.046	2.761
5.969	0.008	1.437	1.528	0.022	1.651	0.681	0.050	2.907
6.372	0.008	1.444	1.445	0.023	1.690	0.670	0.050	3.011
6.592	0.008	1.452	1.407	0.024	1.721	0.652	0.052	3.102
7.636	0.007	1.459	1.375	0.025	1.766	0.626	0.081	3.236
8.269	0.006	1.466	1.389	0.024	1.824	0.655	0.077	3.346
8.774	0.006	1.472	1.422	0.024	1.868	0.595	0.085	3.482
10.751	0.005	1.479	1.197	0.028	1.922	0.501	0.101	3.680
11.812	0.004	1.483	1.219	0.028	1.962	0.496	0.102	3.828
14.589	0.003	1.487	1.155	0.029	1.998	0.409	0.124	3.978
10.271	0.005	1.491						

Table 23. The Specific Heat of $\text{Cs}_2\text{MnCl}_4 \cdot 2\text{H}_2\text{O}$ for Sample 1, Run 22, April 5, 1967, 9830 Gauss, Orientation C.

C_m	dT	T	C_m	dT	T	C_m	dT	T
3.429	0.015	1.271	6.781	0.007	1.415	1.048	0.032	2.084
3.850	0.013	1.284	4.430	0.011	1.422	1.011	0.033	2.128
3.865	0.013	1.296	3.104	0.016	1.434	0.962	0.035	2.185
3.880	0.013	1.308	2.028	0.025	1.452	0.916	0.037	2.245
3.922	0.013	1.319	1.768	0.019	1.498	0.921	0.037	2.294
3.965	0.013	1.330	1.615	0.021	1.526	0.882	0.038	2.346
3.656	0.014	1.340	1.508	0.022	1.553	0.859	0.039	2.407
3.757	0.013	1.350	1.420	0.024	1.580	0.819	0.041	2.457
4.560	0.011	1.360	1.401	0.024	1.603	0.819	0.041	2.501
4.758	0.011	1.369	1.336	0.025	1.627	0.747	0.045	2.546
5.220	0.010	1.377	1.290	0.026	1.651	0.774	0.044	2.627
5.400	0.009	1.385	1.253	0.027	1.673	0.739	0.069	2.709
5.771	0.009	1.392	1.304	0.026	1.697	0.738	0.069	2.795
6.818	0.007	1.399	1.259	0.027	1.720	0.676	0.075	2.886
6.801	0.007	1.405	1.223	0.028	1.807	0.570	0.089	2.971
7.876	0.006	1.411	1.155	0.029	1.865	0.570	0.089	3.092
7.969	0.006	1.409	1.253	0.027	1.904	0.567	0.089	3.316
9.274	0.005	1.414	1.135	0.030	1.950	0.563	0.090	3.646
13.220	0.004	1.418	1.069	0.032	1.995	0.464	0.109	3.953
13.474	0.004	1.426	0.976	0.035	2.038	0.511	0.099	4.171

Table 24. The Specific Heat of $\text{Cs}_2\text{MnCl}_4 \cdot 2\text{H}_2\text{O}$ for Sample 1, Run 23, April 5, 1967, 3500 Gauss, Orientation C.

C_m	dT	T	C_m	dT	T	C_m	dT	T
2.703	0.019	1.290	4.453	0.011	1.623	2.358	0.021	1.859
2.688	0.019	1.306	4.706	0.011	1.634	2.087	0.024	1.914
2.458	0.021	1.323	4.674	0.011	1.645	1.658	0.032	1.954
2.493	0.020	1.339	5.156	0.010	1.656	1.657	0.031	1.985
2.607	0.019	1.355	5.460	0.009	1.665	1.505	0.034	2.071
2.671	0.019	1.374	4.949	0.010	1.675	1.410	0.037	2.130
3.227	0.016	1.391	5.327	0.010	1.682	1.238	0.042	2.199
2.777	0.018	1.406	5.701	0.009	1.692	1.171	0.045	2.246
2.801	0.018	1.421	5.563	0.009	1.701	1.202	0.044	2.291
3.127	0.016	1.444	5.195	0.010	1.708	1.181	0.043	2.336
3.381	0.015	1.459	6.342	0.008	1.717	1.111	0.047	2.381
3.583	0.014	1.474	5.954	0.009	1.725	1.103	0.047	2.449
3.716	0.014	1.488	6.167	0.008	1.731	0.877	0.058	2.553
3.743	0.014	1.501	6.800	0.007	1.739	0.855	0.059	2.647
3.250	0.016	1.516	7.690	0.007	1.746	0.742	0.068	2.779
3.575	0.014	1.526	7.879	0.006	1.753	0.754	0.067	2.887
3.702	0.014	1.539	8.583	0.006	1.765	0.681	0.074	3.029
3.713	0.014	1.552	9.158	0.006	1.770	0.613	0.083	3.149
3.917	0.013	1.561	9.596	0.005	1.776	0.672	0.075	3.298
3.829	0.013	1.573	8.553	0.006	1.781	0.544	0.093	3.437
4.011	0.013	1.583	5.301	0.010	1.788	0.507	0.100	3.586
3.946	0.013	1.594	4.136	0.012	1.798	0.449	0.113	3.800
3.829	0.013	1.605	2.813	0.018	1.813	0.434	0.117	3.986
4.716	0.011	1.612	2.450	0.021	1.830	0.420	0.121	4.171

Table 25. The Specific Heat of $\text{Cs}_2\text{MnCl}_4 \cdot 2\text{H}_2\text{O}$ for Sample 1, Run 24, April 5, 1967, 8900 Gauss, Orientation C.

C_m	dT	T	C_m	dT	T	C_m	dT	T
3.381	0.015	1.266	6.995	0.007	1.514	1.063	0.033	2.024
3.449	0.015	1.279	5.112	0.010	1.522	1.136	0.031	2.074
3.501	0.015	1.293	3.324	0.016	1.535	1.119	0.032	2.119
3.491	0.015	1.305	2.170	0.024	1.555	1.097	0.032	2.178
3.525	0.015	1.318	1.779	0.020	1.576	1.045	0.034	2.224
3.497	0.015	1.331	1.780	0.020	1.596	0.941	0.038	2.310
3.859	0.014	1.343	1.682	0.021	1.615	0.856	0.041	2.376
3.787	0.014	1.356	1.573	0.023	1.635	0.882	0.040	2.472
3.913	0.013	1.368	1.529	0.023	1.655	0.832	0.043	2.546
4.091	0.013	1.378	1.516	0.023	1.677	0.809	0.044	2.654
4.203	0.012	1.389	1.444	0.025	1.699	0.754	0.047	2.735
4.126	0.013	1.428	1.398	0.025	1.721	0.766	0.046	2.851
4.796	0.011	1.440	1.458	0.024	1.741	0.720	0.049	2.933
5.246	0.010	1.450	1.311	0.027	1.763	0.645	0.055	3.000
6.005	0.009	1.460	1.310	0.027	1.787	0.619	0.057	3.094
6.089	0.009	1.468	1.259	0.028	1.811	0.750	0.047	3.196
6.985	0.007	1.476	1.372	0.026	1.853	0.603	0.059	3.320
8.141	0.006	1.483	1.366	0.026	1.894	0.532	0.098	3.468
9.105	0.006	1.489	1.157	0.031	1.940	0.571	0.092	3.608
9.629	0.005	1.495	1.195	0.030	1.970	0.494	0.106	3.751
11.642	0.004	1.498	1.154	0.031	1.997	0.507	0.103	3.851
13.337	0.004	1.508						

Table 26. The Specific Heat of $\text{Cs}_2\text{MnCl}_4 \cdot 2\text{H}_2\text{O}$ for Sample 1, Run 25, April 7, 1967, 3500 Gauss, Orientation C.

C_m	dT	T	C_m	dT	T	C_m	dT	T
2.713	0.019	1.309	5.155	0.010	1.660	1.966	0.026	1.878
2.620	0.019	1.326	5.667	0.009	1.670	1.991	0.025	1.905
2.661	0.019	1.342	5.091	0.010	1.679	1.794	0.028	1.964
2.625	0.019	1.358	6.253	0.008	1.688	1.616	0.031	2.024
2.736	0.018	1.374	5.765	0.009	1.697	1.439	0.035	2.098
2.878	0.018	1.392	6.367	0.008	1.705	1.411	0.036	2.150
3.025	0.017	1.409	5.867	0.009	1.713	1.217	0.042	2.231
3.036	0.017	1.426	7.531	0.007	1.721	1.125	0.045	2.300
3.511	0.014	1.481	6.377	0.008	1.727	1.018	0.050	2.401
3.097	0.016	1.502	7.101	0.007	1.735	0.968	0.052	2.513
3.153	0.016	1.518	7.278	0.007	1.742	0.866	0.058	2.640
3.706	0.014	1.534	6.515	0.008	1.749	0.830	0.061	2.743
3.575	0.014	1.548	6.378	0.008	1.756	0.717	0.071	2.883
3.851	0.013	1.562	6.596	0.008	1.762	0.771	0.066	2.983
4.050	0.012	1.575	8.035	0.006	1.768	0.639	0.079	3.128
4.618	0.011	1.586	7.365	0.007	1.774	0.599	0.084	3.266
3.580	0.014	1.599	8.273	0.006	1.779	0.549	0.092	3.470
4.597	0.011	1.611	5.239	0.010	1.786	0.544	0.093	3.623
4.518	0.011	1.621	3.222	0.016	1.797	0.699	0.072	3.722
4.756	0.011	1.630	2.746	0.018	1.812	0.487	0.104	3.821
4.870	0.010	1.641	2.321	0.022	1.832	0.479	0.106	3.904
4.722	0.011	1.651	2.315	0.022	1.854			

Table 27. The Temperature Changes from an Adiabatic Magnetization Experiment on Sample 1, Orientation C, April 21, 1967.

T(0)	T(3500)	T(6050)	T(8400)	T(8900)
1.282	1.244	1.196	1.161	1.154
1.311	1.256	1.202	1.164	1.156
1.298	1.263	1.209	1.166	1.156
1.514	1.471	1.402	1.345	1.330
1.519	1.474	1.406	1.346	1.331
1.516	1.473	1.402	1.345	1.330
1.519	1.477	1.405	1.345	1.330
1.607	1.565	1.485	1.412	1.393
1.607	1.566	1.488	1.413	1.393
1.607	1.561	1.486	1.412	1.392
1.607	1.565	1.489	1.412	1.392
1.729	1.685	1.601	1.485	1.449
1.728	1.687	1.602	1.486	1.449
1.727	1.671	1.602	1.485	1.447
1.726	1.671	1.603	1.485	1.447
1.798	1.757	1.672	1.573	1.550
1.798	1.756	1.669	1.572	1.550

Table 27 (Continued)

T(0)	T(3500)	T(6050)	T(8400)	T(8900)
1.857	1.833	1.792	1.755	1.747
1.852	1.828	1.788	1.753	1.747
1.903	1.884	1.853	1.830	1.827
1.894	1.877	1.848	1.828	1.827
1.920	1.902	1.873	1.855	1.853
1.913	1.896	1.870	1.853	1.853
2.068	2.063	2.061	2.076	2.086
2.066	2.059	2.058	2.074	2.086
2.165	2.165	2.176	2.208	2.221
2.156	2.157	2.168	2.203	2.221
2.432	2.449	2.490	2.570	2.595
2.417	2.434	2.478	2.560	2.595
3.028	3.081	3.182	3.313	3.333
2.960	2.993	3.083	3.255	3.333
3.322	3.386	3.531	3.717	3.762
3.224	3.284	3.424	3.660	3.762

MICHIGAN STATE UNIVERSITY LIBRARIES



3 1293 03062 3411